Co-movement of Yield Curves and International Macroeconomic Variables: A Wavelet Approach

Mustapha Olalekan Ojo

UMinho | 2020

Universidade do Minho
Escola de Economia e Gestão

Mustapha Olalekan Ojo

Co-movement of Yield Curves and International Macroeconomic Variables: A Wavelet Approach

Setembro de 2020

Universidade do Minho
Escola de Economia e Gestão

Mustapha Olalekan Ojo

Co-movement of Yield Curves and International Macroeconomic Variables: A Wavelet Approach

PhD. Thesis
PhD. Economics

A project supervised by
Prof. Luís Aguiar-Conraria
Prof. Maria Joana Soares

Setembro de 2020

Direitos De Autor E Condições De Utilização Do Trabalho Por Terceiros

Acknowledgement

I wish to express my profound gratitude to my two supervisors, Prof. Luís Aguiar-Conraria and Prof. Maria Joana Soares, for their incredible academic support. While your guidance was invaluable, your contributions were stimulating and productive. I am equally highly appreciative of Estela Vieira for her valuable support during my PhD journey. Your invaluable advice and guidance made my PhD experience and stay in Portugal worthwhile.

My appreciation goes to my mother for her incredible support, especially her sacrifice after my father's demise. Your constant encouragement and advice are highly instrumental during this journey. I equally thank my brother and sister for their support and assistance. My heartfelt appreciation goes to Mr Bamishebi Thompson for his support and encouragement.

My foremost gratitude goes to my supportive and encouraging wife. Your sacrifice during my PhD sojourn is highly appreciated. I am hugely indebted to you as my PhD would not have been completed without your encouragement, patience and support. I appreciate my children for their sacrifice and commitment to the family values during my absence.

Statement of Integrity

I hereby declare that I have acted with integrity during the conduct of this Doctoral Thesis. I confirm that I have not resorted to any form of plagiarism practices or other forms of misuse, falsification of information or results in any of the steps leading to the completion of this thesis. The thesis is an original work, except where duly indicated with references. I further declare that I have fully complied with the Code of Ethical Conduct of the University of Minho.

Resumo

Esta tese recorre à análise de *wavelets* para explorar a estrutura de prazo das taxas de juro. A tese sublinha as vantagens das *wavelets* e argumenta que o seu uso para estudar interações económicas complexas e séries não-estacionárias é muito vantajoso. Adicionalmente, justifica também o recurso à transformada contínua da wavelet. A tese recorre a diversos instrumentos associados à transformada contínua da *wavelet* — em especial o espetro de potência de *wavelet*, a coerência de *wavelet*, a diferença de fase da *wavelet* e a distância de espetros de wavelet — para explorar processos e fenómenos económicos em três artigos.

Enquanto dois dos artigos se focam na curva de rendimentos, o terceiro avalia a capacidade preditiva do indicador avançado da OCDE.

Um artigo usa as taxas de juro das dívidas soberanas para avaliar o contágio financeiro na Zona Euro, distinguindo entre contágio e interdependência. O artigo mostra que há contágio entre países periféricos e que a crise grega levou a uma fuga de capitais para países seguros.

O segundo artigo extrai três fatores latentes da curva de rendimentos do Canadá e explora os seus co-movimentos com quatro variáveis macroeconómicas.

O terceiro artigo investiga o poder preditivo do indicador compósito avançado da OCDE. O artigo mostra que o indicador avançado é um preditor útil dos índices de produção industrial, mas que tem uma performance pobre relativamente à taxa de crescimento do PIB. Relativamente à taxa de desemprego, os resultados são mistos.

Globalmente, a tese demonstra que a curva de rendimentos contém informação sobre vários eventos económicos e pode ser usada como preditor de várias variáveis económicas. Também se demonstra que a informação contida na curva de rendimentos oferece informação valiosa sobre política monetária e a dinâmica de variáveis económicas como a inflação ou o desemprego.

***Palavras-chave**: Indicado Ciclo de Negócios, Indicador Compósito Avançado, Contágio; Interdependência; Variáveis Macroeconómicas; estrutura de prazos; Curva de Rendimento; Wavelet*

Abstract

The thesis utilises wavelet analysis to explore the term structure of interest rates. It highlights the benefits of wavelet analysis and offers justification for its use in analysing complex economic interactions and non-stationary series. Similarly, the thesis provides a rationale for the adoption of Continuous Wavelet Transforms. The thesis utilises various wavelet tools – such as wavelet power spectrum, wavelet coherency, wavelet phase-difference and wavelet spectra distance – to explore economic phenomena and processes in three papers. While the first two papers focus on the yield curve, the third paper evaluates the forecasting ability of the composite leading indicator.

The first paper utilises the sovereign bond yield to evaluate financial contagion in the Eurozone and distinguish between contagion and interdependencies in the Eurozone. The paper found evidence of contagion among some periphery countries and established a flight-to-quality flow to core countries during the Greek crisis. The second paper extracts the three latent factors of the Canadian yield curve and explore their co-movement with four macroeconomic variables. The study established a bidirectional link between the yield curve and macroeconomic variables but found different relationships between the latent factors and macroeconomic variables.

The third paper investigates the forecasting power of OECD's composite leading indicator. The paper found that the composite leading indicator is a useful forecasting tool for Industrial Production Index but exhibit poor performance on GDP growth. However, its forecasting power on the unemployment rate is mixed. Overall, the thesis established that the yield curve is a crucial bellwether of economic events and could be used to forecast various economic variables. It also demonstrated that the information content of the yield curve could offer valuable information about monetary policy and the dynamics of economic variables, such as inflation and unemployment.

***Keywords**: Business Cycle Indicator, Composite Leading Indicator, Contagion; Interdependence; Macroeconomic variables; Term Structure; Yield Curve; Wavelet*

Table of Contents

Direitos De Autor E Condições De Utilização Do Trabalho Por Terceiros i

Acknowledgement ii

Statement of Integrity iii

Resumo iv

Abstract v

1 Introduction 1

1.1 Background 1
1.2 Continuous Wavelet Analysis 3
1.2.1 Basic Definitions and Notations 3
1.2.2 Short-Time Fourier Transform 4
1.3 Continuous Wavelet Transform 6
1.3.1 Definition of Continuous Wavelet Transform 6
1.3.2 Localisation Properties 7
1.3.3 Wavelet Choice 9
1.3.4 Wavelet Power and Wavelet Phase 10
1.4 Bivariate Wavelet Analysis 11
1.5 Multivariate Wavelet Analysis 12
1.6 Implementation Details 13
1.6.1 CWT for a Finite Time-Series 13
1.6.2 Significance Tests 14
1.7 Wavelet Spectra Dissimilarity Matrix 15
1.7.1 Leading Patterns and Leading Vectors 15
1.7.2 Dissimilarity between Two Spectra 17

2 A Time-Frequency Analysis of Financial Market Contagion in Europe 18

2.1 Introduction 19
2.2 Empirical Findings 23

2.2.1 Wavelet Power Spectrum . . . 24
2.2.2 Core Countries . . . 26
2.2.3 Wavelet Coherency and Phase-Differences between the Core Countries and the Peripheral Countries . . . 28
2.2.4 Wavelet Partial Coherency and contagion between Greece, Ireland and Portugal . . . 30
2.3 Conclusions . . . 32

3 A Time-Frequency Analysis of the Canadian Macroeconomy and the Yield Curve 33
3.1 Introduction . . . 34
3.2 Methodology and Data . . . 36
3.2.1 Yield Curve Model Specification and Estimation . . . 36
3.2.2 Data . . . 37
3.3 Empirical Results . . . 41
3.3.1 Bank Rate and the Yield Curve . . . 41
3.3.2 Inflation Rate and the Yield Curve . . . 43
3.3.3 Unemployment Rate and the Yield Curve . . . 44
3.3.4 Industrial Production and the Yield Curve . . . 45
3.4 Conclusion . . . 48

4 The Performance of OECD's Composite Leading Indicator 50
4.1 Introduction . . . 51
4.2 Data and Exploratory Analysis . . . 54
4.3 Results . . . 58
4.3.1 Industrial Production and Composite Leading Indicator . . . 59
4.3.2 Unemployment and Composite Leading Indicator . . . 64
4.3.3 GDP Growth and Composite Leading Indicator . . . 69
4.4 Conclusion . . . 74

5 Conclusion 75

Chapter 1

Introduction

1.1 Background

Fourier analysis is frequently relied upon to determine the most appropriate cyclical components of a time series[1]. The idea of Fourier transform hinges on 'capturing' series with different sinusoidal functions, each with varying frequency, and determining the best-matched sinusoids for the original series. Fourier spectral analysis has been used to identify some stylised business cycle facts (see, e.g. Granger, 1966; King and Watson, 1996), explore seasonal components (see, e.g. Nerlove, 1964; Wen, 2002) and evaluate relationships among economic variables at distinct frequencies (see, e.g. Wen, 2005).

However, Fourier transform has some limitations. With sinusoidal functions being waves of infinite duration, Fourier transform does not provide any localisation in time. That is, Fourier transforms do not allow us to determine when different frequencies occur, making it impossible to identify structural changes or differentiate transient relations. More importantly, spectral analysis is suitable for time series with stable statistical properties. However, most financial and economic time series are characterised by non-stationarity.

Wavelet analysis, an extension of Fourier analysis, addresses these limitations. It estimates spectral characteristics of a series as a function of time. Thus, it reveals the evolution of its varying periodic components. Although some of the ideas behind the wavelet transform had been in existence for many years[2], wavelet started as a coherent body of mathematics in the mid-1980s (Goupillaud et al., 1984; Grossmann and Morlet, 1984). It is now widely used in various fields, such as astronomy, epidemiology, geophysics, oceanography, physics and signal processing.

Ramsey and Lampart (1998) are precursors of wavelet in economics before its adoption by other authors, such as Gençay et al. (2001, 2005), Wong et al. (2003), Connor and

[1]There are various types of Fourier transforms (discrete, continuous and finite), depending on the nature of the series involved.

[2]We can trace the history of wavelets to at least 1909, when a Hungarian mathematician, Alfred Haar, used, in his doctoral thesis, what is now recognised as the prototype of an orthogonal wavelet.

Rossiter (2005), Fernandez (2005), Gallegati (2008) and Gallegati et al. (2011). The earliest studies utilised discrete versions of the wavelet transform - Discrete Wavelet Transform (DWT) and the Modified Discrete Wavelet Transform (MODWT). During the last decade, many authors have gravitated towards the continuous-time version of wavelet transform – Continuous Wavelet Transform (CWT) – to investigate economic issues.

The utilisation of CWT is increasingly becoming interminable with its adoption in various economics studies, such as Aguiar-Conraria et al. (2008), Crowley and Mayes (2009), Baubeau and Cazelles (2009), Rua and Nunes (2009), Aguiar-Conraria and Soares (2011); Aguiar-Conraria et al. (2013b), Rua and Nunes (2012), Aguiar-Conraria et al. (2012b); Aguiar-Conraria and Soares (2014), Alvarez-Ramirez et al. (2012), Caraiani (2012), Fernández-Macho (2012), Jammazi (2012), Vacha and Barunik (2012), Verona (2016), Bekiros et al. (2017), Flor and Klarl (2017), and Ko and Funashima (2019). This thesis deepens the utilisation of CWT in the economics literature. It uses continuous wavelet tools to address three crucial economic issues.

One, the increasing integration of global financial markets sometimes exposes the vulnerability of various markets to external shocks. While such vulnerability often sparks episodes of financial crises, the snowballing effects of such crises have galvanised interest in identifying channels through which the crises spread. The first objective of this thesis is to explore the spread of a financial crisis from one market to another. The thesis investigates the financial contagion in the Eurozone debt market, using wavelet tools to distil the cross-country co-movement of sovereign bond yields.

Two, the behaviour of the yield curve changes across the business cycle, and this has propelled a proliferation of literature exploring the information content of the yield curve. Notable studies - such as Smets (1997) and Diebold et al. (2006a) – established that the yield curve explains the dynamics of inflation, economic activity, monetary policy and unemployment. While Bonser-Neal and Morley (1997) established that the yield curve predicts the real economic activity in the US, they noted that such a result is not evident outside the US. This thesis evaluates the link between the Canadian yield curve and its macroeconomic variables.

Three, leading indicators are considered a useful tool for predicting future economic conditions. With such utility, policymakers and economists consider them as a bellwether of economic activities. However, leading indicators are criticised as 'measurement without theory' (Koopmans, 1947). The ensuing debate galvanised a vast body of literature on the predictive power of leading indicators and has resulted in a multiplicity of leading indicators at both national and supranational levels. While OECD's composite leading indicator is one of such, it is under constant scrutiny. This

thesis explores the predictive performance of the OECD's composite leading indicator on three macroeconomic indicators: industrial production index, unemployment and GDP growth.

The structure of the thesis is as follows: The rest of Chapter 1 focuses on the description of wavelet tools utilised in the thesis. Chapter 2 evaluates the financial market contagion in the Eurozone. Chapter 3 investigates the link between the latent factors of the Canadian yield curve and its macroeconomic variables. Chapter 4 explores the forecasting power of OECD's composite leading indicator, while Chapter 5 concludes.

1.2 Continuous Wavelet Analysis

This section describes the continuous wavelet tools utilised in the three subsequent chapters. The materials presented in this section were mostly adopted from Aguiar-Conraria et al. (2012a, 2013a) and Aguiar-Conraria and Soares (2014).

1.2.1 Basic Definitions and Notations

Hereafter, $L^2(\mathbb{R})$ represents square-integrable functions and denotes set of functions defined on the real line, satisfying $\int_{-\infty}^{\infty} |x(t)|^2 \, dt < \infty$. The inner product

$$\langle x, y \rangle := \int_{-\infty}^{\infty} x(t) \, \overline{y}(t) \, dt$$

and corresponding norm

$$\|x\| := \sqrt{\langle x, x \rangle}$$

The symbol := connotes 'by definition' while the overbar denotes complex conjugation. Unless otherwise stated, all functions are assumed to be in $L^2(\mathbb{R})$. With the influence of the signal processing literature, this space refers to the space of *finite energy functions*, with the energy of a function x being $\|x\|^2$.

The *Fourier Transform* (FT) of a function $x(t)$ is denoted by $\mathcal{F}_x(\omega)$ or simply $\hat{x}(\omega)$ and defined as:

$$\mathcal{F}_x(\omega) := \int_{-\infty}^{\infty} x(t) e^{-i\omega t} dt = \int_{-\infty}^{\infty} x(t) \big(\cos(\omega t) - i \sin(\omega t)\big) dt, \quad \omega \in \mathbb{R} \tag{1.1}$$

where Euler's identity, $e^{i\theta} = \cos\theta + i \sin\theta$, is utilised in the second equality.

Remark 1 *It is noteworthy that various definitions of Fourier transform of a function appear in the literature, with ω as the angular (or radian) frequency and has a relation, $\mathsf{f} = \frac{\omega}{2\pi}$, with the ordinary frequency f.*

Eq. 1.1 shows that the value of the Fourier transform of function x at the frequency ω utilises the information of $x(t)$ for all $t \in \mathbb{R}$. Hence, it has no localisation in time. Similarly, a function of the frequency ω is obtained, suggesting that time information is lost under the Fourier transform. In this case, we are either in time-domain without frequency information or frequency-domain without time information.

However, the representation of the function in the *time-frequency* domain is necessary to overcome this problem. That is, a representation in time and frequency domains. Denis Gabor proposed one such type of representations in his seminal paper on communication theory (Gabor, 1946), and this is obtained using the *Short-Time Fourier Transform* (STFT).

1.2.2 Short-Time Fourier Transform

The STFT is based on a simple idea: a function g, such as the Gaussian function, with a very fast decay towards zero as $t \to \pm\infty$[3] is multiplied by $x(t)$ to select a 'local section' of $x(t)$, and the Fourier transform of this is computed. Furthermore, g is shifted (translated) to obtain another 'section', and the Fourier transform of this new section is calculated. The continuous repetition of this process would result in a two-variable function of τ (translation parameter) and ω (angular frequency), with the function defined as:

$$\mathcal{F}_{g,x}(\tau,\omega) = \int_{-\infty}^{\infty} x(t)\overline{g}(t-\tau)e^{-i\omega t}dt \tag{1.2}$$

STFT could also be viewed from a different perspective: we can translate and modulate a basic function g by τ and ω, respectively, to obtain a two-parameter family of functions $g_{\tau,\omega}(t) := (t-\tau)e^{-i\omega t}$, and the computation of inner products of x and all family members is then carried out:

$$\mathcal{F}_{g,x}(\tau,\omega) = \langle x, g_{\tau,\omega}\rangle \tag{1.3}$$

Although a different representation using the continuous wavelet transform is intensively adopted in this thesis, some concepts would be defined before exploring this representation. The concepts would enable the comparison of time-frequency localisation properties of this representation with those of the STFT.

A *time-center* μ of a function $g(t)$ is defined by

$$\mu = \mu(g) := \frac{1}{\|g\|^2}\int_{-\infty}^{\infty} t|g(t)|^2\,dt.$$

[3]Gabor, in his original paper, used Gaussian functions; with this type of window functions; the STFT is more commonly known as the Gabor transform.

This implies that the centre of the wavelet is the mean of the probability distribution obtained from $\frac{|g(t)|^2}{\|g\|^2}$. As a measure of the concentration of g around its centre, the standard deviation is usually computed as:

$$\sigma = \sigma(g) := \sqrt{\frac{1}{\|g\|^2}\int_{-\infty}^{\infty}(t-\mu)^2|g(t)|^2dt},$$

This is referred to as the *time-radius* of g. The *frequency-center* $\hat{\mu}$ and the *frequency-radius* $\hat{\sigma}$ of g are defined in a similar manner, but applied to the Fourier transform of g:

$$\hat{\mu} = \hat{\mu}(g) := \frac{1}{\|\hat{g}\|^2}\int_{-\infty}^{\infty}\omega|\hat{g}(\omega)|^2\,d\omega \quad \text{and} \quad \hat{\sigma} = \hat{\sigma}(g) := \sqrt{\frac{1}{\|\hat{g}\|}^2\int_{-\infty}^{\infty}(\omega-\hat{\mu})^2|\hat{g}(\omega)|^2d\omega}$$

An assumption is made about function g when defining the above quantities. It is implicitly assumed that the function g is such that all these quantities are finite. This corresponds to assuming a sufficiently fast decay for g and its Fourier transform $\hat{g}$. In such cases, we refer to g as a *(time-frequency) window function.* Thus, we have $\langle x, g\rangle = \int_{-\infty}^{\infty} x(t)\overline{g}(t)dt \approx \int_{\mu-\sigma}^{\mu+\sigma} x(t)\overline{g}(t)dt$, with the Fourier Parseval formula,

$$\langle x, g\rangle = \frac{1}{2\pi}\langle \hat{x}, \hat{g}\rangle = \frac{1}{2\pi}\int_{-\infty}^{\infty}\hat{x}(\omega)\overline{\hat{g}}(\omega)d\omega \approx \frac{1}{2\pi}\int_{\hat{\mu}-\hat{\sigma}}^{\hat{\mu}+\hat{\sigma}}\hat{x}(\omega)\overline{\hat{g}}(\omega)d\omega$$

This indicates that the computation of the inner product of x and g provides information about $x(t)$ and $\hat{x}(\omega)$ for various values of t and ω in the undermentioned rectangular region in the time-frequency plane:

$$\mathcal{H}_g := [\mu-\sigma, \mu+\sigma] \times [\hat{\mu}-\hat{\sigma}, \hat{\mu}+\hat{\sigma}] \tag{1.4}$$

The rectangle, as shown in Figure 1.1, is known as the *Heisenberg box* for g, while the area of this box measures the joint time-frequency resolution of the window.

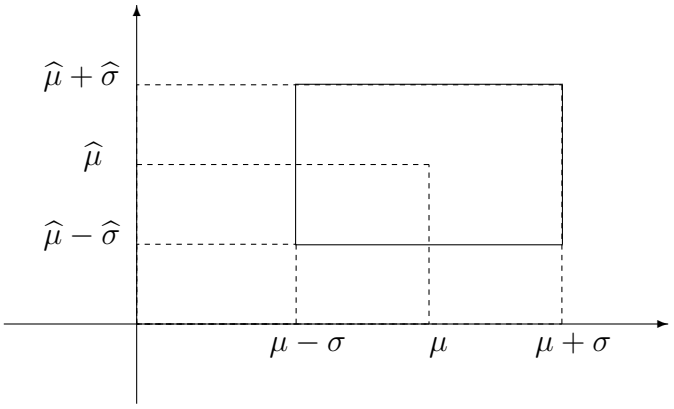

Figure 1.1: Heisenberg box

The Heisenberg uncertainty principle states that there is a minimum area for any Heisenberg box. That is, we always have for any window function g,

$$4\,\sigma(g)\hat{\sigma}(g) \geq 2 \tag{1.5}$$

Hence, a well-localised function in time (very small σ) cannot be well-localised in frequency and vice-versa. With the functions $g_{t,\omega}$ utilised in the STFT obtained by translations and modulations of the window function g, it can be easily shown that:

$$\sigma(g_{\tau,\omega}) = \sigma(g) \;\text{ and }\; \hat{\sigma}(g_{\tau,\omega}) = \hat{\sigma}(g), \qquad \forall \tau, \omega \in \mathbb{R}.$$

This shows that all the functions $g_{\tau,\omega}$ have Heisenberg boxes with the same height and width. Its main limitation is the rigidity of the windows utilised in the STFT, having the same width for both low- and high-frequency values.

1.3 Continuous Wavelet Transform

1.3.1 Definition of Continuous Wavelet Transform

The essence of the CWT is to calculate the inner products of the function x and family members of two-parameter functions $\psi_{\tau,s}$, generated from a given mother wavelet ψ by translation and scaling factors τ and s, respectively.

$$\psi_{\tau,s}(t) = \frac{1}{\sqrt{|s|}}\psi\left(\frac{t-\tau}{s}\right), \tau, s \in \mathbb{R}, s \neq 0 \tag{1.6}$$

The function ψ must satisfy the following minimum requirements to be considered a *(mother) wavelet*:

1. $0 \neq \psi \in L^2(\mathbb{R})$;

2. $C_\psi := \int_{-\infty}^{\infty} \frac{|\hat{\psi}(\omega)|^2}{|\omega|} d\omega < \infty$;

(see Daubechies, 1992, p. 24).

While the square integrability of ψ connotes a very mild decay condition, the wavelets utilised in practice have much faster decay. Typically, it exhibits exponential decay behaviour or even compact support. Although the second condition above is typically referred to as the *admissibility condition* (AC), it is equivalent to requiring the followings for functions with sufficient decay:

$$\hat{\psi}(0) = \int_{-\infty}^{\infty} \psi(t)\, dt = 0.$$

This implies that the function ψ must wiggle along the t-axis. That is, it must have a wavy behaviour, and in conjunction with the decaying property, justifies the term wavelet (originally *ondelette* in French).

The definition of the CWT is analogous to the STFT when the family of functions $g_{\tau,\omega}$ in (1.3) is replaced with wavelet daughters $\psi_{\tau,s}$ defined by (1.6). Thus, the CWT of a function $x(t)$ with respect to a certain wavelet ψ is a two-variable function given by

$$\mathcal{W}_{x,\psi}(\tau, s) := \langle x, \psi_{\tau,s} \rangle = \frac{1}{\sqrt{|s|}} \int_{-\infty}^{\infty} x(t) \overline{\psi}\left(\frac{t-\tau}{s}\right) dt \tag{1.7}$$

Remark 2 *With the lack of ambiguity with which wavelet ψ is used in the CWT, the notation is simplified and written as $\mathcal{W}_x$ for $\mathcal{W}_{x,\psi}$.*

In the definition of wavelet, the imposition of C_ψ as a finite quantity guarantees the possible recovery of $x(t)$ from the wavelet transform $\mathcal{W}_{\psi,x}(\tau, s)$. Moreover, for analytic wavelet ψ, i.e. it is such that $\hat{\psi}(\omega) = 0$ for $\omega < 0$, and $x(t)$ is real, a reconstruction formula involving only values of the real part of $\mathcal{W}_{\psi,x}(\tau, s)$, for $s > 0$, exists. This implies that we may restrict ourselves to the use of positive scales (see Daubechies, 1992, p. 27). In what follows, we assume we are working with an analytic wavelet and restrict the computation of the CWT to positive values of s.

1.3.2 Localisation Properties

Let the wavelet function ψ be a window function[4]. For simplicity, it is centred at zero (this is always achievable with the appropriate translation of ψ). Similarly, assume that $\hat{\mu} > 0$ is the frequency-centre of ψ. Suppose $\hat{\sigma}$ and σ denote the frequency-radius and

[4]The wavelet adopted in this thesis satisfies this requirement.

time-radius of the wavelet ψ. Then, we have for the wavelet daughter $\psi_{\tau,s}$ $(s > 0)$,

$$\mu(\psi_{\tau,s}) = t, \qquad \sigma(\psi_{\tau,s}) = s\sigma$$
$$\hat{\mu}(\psi_{\tau,s}) = \frac{\hat{\mu}}{s}, \qquad \hat{\sigma}(\psi_{\tau,s}) = \frac{\hat{\sigma}}{s}$$

Hence, the Heisenberg box related to the function $\psi_{\tau,s}$ is

$$\Big[t - s\sigma, t + s\sigma\Big] \times \Big[\frac{\hat{\mu}}{s} - \frac{\hat{\sigma}}{|s|}, \frac{\hat{\mu}}{s} + \frac{\hat{\sigma}}{s}\Big]$$

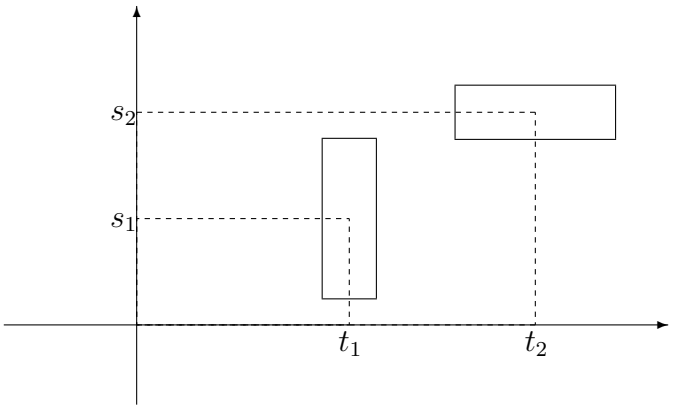

Figure 1.2: Heisenberg boxes with $0 < s_1 < s_2$

Despite all the windows having the same area $4\sigma\hat{\sigma}$, their dimensions vary with the scale. We have large windows (in time) centred, in frequency, around low frequencies $\omega = \frac{\hat{\mu}}{s}$ for large values of s and short windows (in time) centred, in frequency, around high frequencies $\omega = \frac{\hat{\mu}}{s}$ for small values of s. Thus, there is an automatic adjustment of window size to frequencies: short windows for high frequencies and large windows for low frequencies. Such window flexibility is a big challenge in the STFT.

Remark 3 *For technical clarity, the wavelet transform offers a time-scale representation of the function x rather than a time-frequency representation. The inverse relation between the angular frequency and the scale*

$$\omega(s) = \frac{\hat{\mu}}{s} \tag{1.8}$$

make sense only if the Fourier transform of the wavelet has a single prominent peak around the non-zero frequency $\hat{\mu}$ (see Meyers et al., 1993). This is precisely the case of the wavelet utilised in three subsequent chapters of this thesis.

1.3.3 Wavelet Choice

The required conditions for a function to be considered a wavelet are weak, and there are various wavelets. In practice, the choice of a wavelet is driven by its intended application. For instance, to study cycles, as this thesis focuses on, requires choosing a wavelet with wavelet transform containing information on both phase and amplitude. This requires the utilisation of a complex-valued wavelet. The phase provides vital information about the variable's position in the cycle.

The most popular complex wavelet belongs to the *Morlet wavelet family*, a family of wavelets indexed by a parameter ω_0, given by

$$\psi_{\omega_0}(t) = \pi^{-\frac{1}{4}} e^{-t^2/2} \left(e^{i\omega_0 t} - K_{\omega_0}\right), \quad K_{\omega_0} = e^{-\omega_0^2/2}.$$

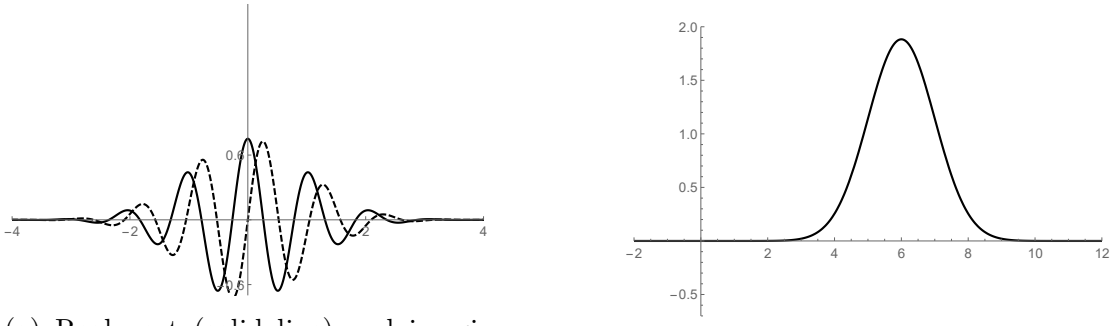

(a) Real part (solid line) and imaginary part (dashed line)

(b) Fourier transform

Figure 1.3: The simplified Morlet with parameter $\omega_0 = 6$ and its Fourier transform

The constant term K_{ω_0} is included in the definition of the Morlet family to guarantee that all its members satisfy the admissibility condition, i.e., we have $\int_{-\infty}^{\infty} \psi(t)dt = 0$. However, for reasonably large ω_0, this term becomes so small (for example, when $\omega_0 = 6$, we have $K_{\omega_0} \approx 1.5 \times 10^{-8}$) that it is usually neglected in practice. This thesis uses a simplified Morlet wavelet, corresponding to the choice $\omega_0 = 6$, i.e., it is the function:

$$\psi(t) = \pi^{-1/4} e^{-t^2/2} e^{6it} = \pi^{-1/4} e^{-t^2/2} \left(\cos(6t) - i \sin(6t)\right). \tag{1.9}$$

Observe that:

1. $\hat{\psi}(\omega) = \sqrt{2}\pi^{1/4} e^{-\frac{1}{2}(\omega-6)^2}$; hence, for $\omega < 0$, we have $\hat{\psi}(\omega) < 2.9 \times 10^{-8}$, so ψ can be seen, for all practical purposes, as an analytic wavelet.

2. $\hat{\mu}(\psi) = 6$ and $\hat{\psi}(\omega)$ has only one pronounced peak at $\hat{\mu} = 6$; hence, it is fair to use the relation (1.8), $\omega(s) = \frac{6}{s}$ to convert scales to (angular) frequencies (see Remark 3). If we relate this to the more common Fourier frequency, we obtain $\mathsf{f}(s) = \frac{1}{2\pi}\frac{6}{s} \approx \frac{1}{s}$.

For the Fourier periods, we have $\mathsf{p} = \frac{1}{\mathsf{f}} \approx s$. This is why, in the interpretation of our results, we often refer to frequencies or periods, instead of scales.

3. $\sigma(\psi) = \hat{\sigma}(\psi) = \frac{1}{\sqrt{2}}$; hence, this wavelet has a Heisenberg box of area $4\frac{1}{\sqrt{2}}\frac{1}{\sqrt{2}} = 2$, which is the minimum valued allowed by the Heisenberg principle. It is noteworthy that function ψ has an equilibrated time-frequency resolution since the spread in time and the spread in frequency are equal.

1.3.4 Wavelet Power and Wavelet Phase

A complex-valued wavelet function ψ equally has complex-valued wavelet transform $\mathcal{W}_x$. Therefore, it can be expressed in polar form, i.e. $\mathcal{W}_x(\tau, s)$ can be written in terms of its modulus $|\mathcal{W}_x(\tau, s)|$ and argument (angle) $\phi_{\mathcal{W}_x}(\tau, s)$ as follows:

$$\mathcal{W}_x(\tau, s) = |\mathcal{W}_x(\tau, s)|\, e^{i\phi_{\mathcal{W}_x(\tau,s)}}, \quad \phi_{\mathcal{W}_x(\tau,s)} \in (-\pi, \pi].$$

Recall that, given a complex number $z = \Re z + i\Im z$, the modulus of z is denoted by $|z|$ and expressed as:

$|z| = \sqrt{z\overline{z}} = \sqrt{(\Re z)^2 + (\Im z)^2}$ while the angle ϕ_z is expressed as:

$$\phi_z = \arctan\left(\frac{\Im z}{\Re z}\right),$$

where arctan represents the undermentioned extension of the typical principal component of the arctan function, with range $(-\pi/2, \pi/2)$:

$$\arctan\left(\frac{b}{a}\right) := \begin{cases} \arctan\,(\frac{b}{a}), & a > 0, \\ \arctan\,(\frac{b}{a}) + \pi, & a < 0, \quad b \geq 0, \\ \arctan\,(\frac{b}{a}) - \pi, & a < 0, \quad b < 0, \\ \pi/2, & a = 0, \quad b > 0, \\ -\pi/2, & a = 0, \quad b < 0. \end{cases}$$

The local *wavelet power spectrum* of x, denoted by WPS_x, follows the terminology adopted in the Fourier case, and it is expressed as the square of the modulus of $\mathcal{W}_x$, i.e.

$$WPS_x(\tau, s) := |\mathcal{W}_x(\tau, s)|^2 = \mathcal{W}_x(\tau, s)\overline{\mathcal{W}}_x(\tau, s).$$

The wavelet power spectrum measures the variance distribution of the time-series in the time-frequency plane. The angle of $\mathcal{W}_x(\tau, s)$ is called the *phase* of x and denoted by $\phi_x(\tau, s)$.

1.4 Bivariate Wavelet Analysis

This section focuses on the description of various wavelet tools that can be utilised to explore the link between series x and y in the time-frequency domain.

The *cross-wavelet transform* (XWT) of two series x and y is expressed as

$$\mathcal{W}_{xy}(\tau, s) = \mathcal{W}_x(\tau, s)\overline{\mathcal{W}_y(\tau, s)}. \tag{1.10}$$

Similarly, the *cross-wavelet power* of x and y is computed as the absolute value of the cross-wavelet transform, $|\mathcal{W}_{xy}(\tau, s)|$, and describes the local covariance between the series at each time and frequency.

Remark 4 *While all described wavelet measures are functions of variables s and t, we simplify the notation by omitting the argument (τ, s) in the formulas unless absolutely necessary.*

The *complex wavelet coherency* between x and y is given by

$$\varrho_{xy} := \frac{S\left(\mathcal{W}_{xy}\right)}{\sqrt{\left[S\left(|\mathcal{W}_y|^2\right) S\left(|\mathcal{W}_x|^2\right)\right]}}, \tag{1.11}$$

where S is a smoothing operator in both time and scale. Smoothing is essential to prevent coherency of one at all scales and time[5]. The smoothing across time and scale is attained through convolution with appropriate windows (see Cazelles et al., 2007; Grinsted et al., 2004, for details).

The *wavelet coherency*, denoted by R_{xy}, is the modulus of the complex wavelet coherency and expressed as:

$$R_{xy} := \frac{\left|S\left(\mathcal{W}_{xy}\right)\right|}{\sqrt{\left[S\left(|\mathcal{W}_y|^2\right) S\left(|\mathcal{W}_x|^2\right)\right]}} \tag{1.12}$$

The phase-difference ϕ_{xy} between x and y is the angle of the complex wavelet coherency, and expressed as:

$$\phi_{xy} := \arctan\left(\frac{\Im(\varrho_{xy})}{\Re(\varrho_{xy})}\right). \tag{1.13}$$

The wavelet coherency is viewed as the correlation between the two variables at each frequency and time.

The phase-difference between series x and y provides information on the possible oscillatory delays of two series as a function of scale (frequency) and time. A phase-difference

[5]The same applies to the Fourier coherency

ϕ_{xy} of zero implies that the two series move together at the specified frequency. The two series move in phase and series x leads y when ϕ_{xy} lies within $(0, \frac{\pi}{2})$. A phase relation still exists, but y leads when ϕ_{xy} lies within $(\frac{-\pi}{2}, 0)$. However, a phase difference of $\pi(-\pi)$ implies an anti-phase relation between x and y. An anti-phase relation exists and y leads when ϕ_{xy} lies within $(\frac{\pi}{2}, \pi)$ while x leads when ϕ_{xy} lies within $(-\pi, \frac{-\pi}{2})$. These relations are represented in Figure 1.4.

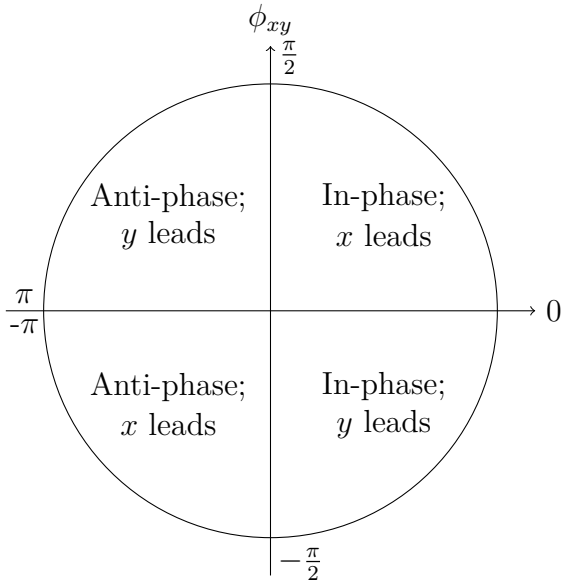

Figure 1.4: Phase Relations

Remark 5 *Some authors define the phase difference as the angle of the cross-wavelet transform. Comparing the formula* (1.11) *for the complex wavelet coherency with the formula* (1.10) *for the cross-wavelet transform, the two measures of the phase-difference show that they do not totally coincide due to the smoothing process involved in the coherency. Adopting the definition of the phase-difference as the angle of the cross wavelet transform, i.e. as the angle of* $\mathcal{W}_x\overline{\mathcal{W}}_y$ *and recalling the well-known results for the angle of the conjugate and product of complex numbers, we immediately see that* $\phi_{xy} = \phi_x - \phi_y$*, which better explains the name phase-difference. This seems to be a more natural definition. But the definition in terms of the complex wavelet coherency, which is adopted in this thesis, is more suitable for generalisation. However, the two measures are closely related.*

1.5 Multivariate Wavelet Analysis

With more than two series, the association between two series often requires accounting for the effect of their interaction with other series. Aguiar-Conraria and Soares (2014) introduced the concepts of multiple wavelet coherency, partial wavelet coherency and partial phase-difference for the general case of $m \geq 3$ series. This thesis is restricted to

the case of three series.

The concept of partial coherence focuses on the interdependence between two variables in the time-frequency domain after accounting for the effects of other variables. However, the notion of multiple coherency can be used when the interest is on the dependence of one variable on two other variables. If the (partial) coherency between two variables decreases in some regions after controlling for the effect of a third variable, the third variable can be assumed to be partly responsible for their interdependence. Otherwise, it could be concluded that the omission of the third variable is obscuring the relation.

The *multiple wavelet coherency* of series x, y and z, denoted by

$$R_{x(yz)} := \sqrt{\frac{R_{xy}^2 + R_{xz}^2 - 2\Re\big(\varrho_{xy}\,\varrho_{yz}\,\overline{\varrho_{xz}}\big)}{1 - R_{yz}^2}}. \tag{1.14}$$

The *complex partial wavelet coherency* $\varrho_{xy.z}$ between x and y after controlling for the effect of z is given by

$$\varrho_{xy.z} := \frac{\varrho_{xy} - \varrho_{xz}\overline{\varrho_{yz}}}{\sqrt{(1 - R_{xz}^2)(1 - R_{yz}^2)}}. \tag{1.15}$$

The *partial wavelet coherency* $R_{xy.z}$ between x and y, after controlling for z is defined as the absolute value of the complex partial-wavelet coherency while the *partial phase-difference* $\phi_{xy.z}$ of x over y, given z, is the angle of $\varrho_{xy.z}$.

1.6 Implementation Details

1.6.1 CWT for a Finite Time-Series

In practice, the computation of the CWT of a finite time series $x = \{x_t : t = 0, \ldots, T-1\}$, comprising T observations corresponding to a uniform time step δt, requires the discretisation of the integral in formula (1.7) and its replacement with a summation. For computational efficiency, it is suitable to compute the transform for T values of the parameter $t = n\delta_t; n = 0, \ldots, T-1$. Similarly, the wavelet transform is computed only for a chosen set of scale values $s = s_m$. Hence, the computed wavelet transform of the finite time-series x will simply be a $S \times T$ matrix $W_x = (w_{mn})$, with its (m, n) element given by

$$w_{mn} = \frac{\delta_t}{\sqrt{s_m}} \sum_{k=0}^{T-1} x_k \overline{\psi}\left(\frac{(k-n)\delta t}{s_m}\right); \quad m = 0, \ldots, S-1, n = 0, \ldots, T-1$$

Although the above formula can be used to compute the wavelet transform for each m and n, the simultaneous computation of all the T values of n can also be identified as a

convolution of two sequences. Thus, the standard computational procedure for convolutions (which involves the use of the FFT) can be used to perform the computation for each value of s and T values of n simultaneously (see Torrence and Compo, 1998, for details). This computational procedure is adopted in the Matlab package ASToolbox[6] for this thesis.

When the CWT is applied to a finite length time series, the values of the transform at the beginning and end of the series comprise missing values that must be prescribed in some way. Hence, the computed values near the borders are always 'incorrectly computed.' For instance, data periodisation is assumed when utilising the FFT approach. This implies that values from one end of the series are utilised for computing transform values at the other end. To avoid this wrapping, the series is usually padded with enough zeros (the number of zeros is generally chosen to obtain a series with several elements equal to a power of 2, to gain efficiency with the FFT), before using the FFT.

With the 'size' of the wavelets $\psi_{t,s}$ increasing with s, the edge-effects equally increase with s. The *cone-of-influence* (COI) represents the region where the transform suffers from these edge-effects. However, the result of this area of the time-frequency plane must be interpreted cautiously (see Torrence and Compo, 1998).

1.6.2 Significance Tests

The tests of significance for wavelet measures are carried out using Monte-Carlo simulations. This involves fitting an ARMA model to the series while new samples are constructed by drawing errors from a Gaussian distribution with the same variance as the estimated error terms. For each series, this exercise is performed severally (typically 5000 times), and critical values are extracted.

Alternatively, theoretical distributions could be utilised for significance testing. For instance, Torrence and Compo (1998) used large Monte Carlo simulations to establish that the wavelet power spectrum obtained with a Morlet wavelet of an AR(0) or AR(1) process is approximated by a Chi-squared distribution. But if computational speed is not an issue, the Monte Carlo simulations can simply be performed. Cohen and Walden (2010) and Ge (2008) established vital theoretical results on the test of significance for the wavelet coherency. These authors utilised Morlet wavelet, assumed a Gaussian white noise process, and analytically derived the sampling distributions. These results are obviously important. However, they are still restrictive, as they imply the use of Gaussian white noises. If one, for robustness, wants to consider the null a general ARMA(p,q), these tests are not appropriate.

[6]This package, developed by Luís Aguiar-Conraria and Maria Joana Soares, is available at `https://sites.google.com/site/aguiarconraria/joanasoares-wavelets/the-astoolbox`.

Presumably, there are no suitable statistical tests regarding the phase-difference due to the difficulty in defining the null hypothesis. In particular, Ge (2008) argued that significance tests should not be used for the phase-difference. Instead, the analysis should be complemented by inspecting the coherency and focusing on phase-differences with the corresponding statistical significance coherency. More so, there appears to be no viable existing study on the test of significance for the partial or multiple coherency.

1.7 Wavelet Spectra Dissimilarity Matrix

Aguiar-Conraria and Soares (2011) proposed a mechanism for evaluating the distance between a given pair of wavelet spectra[7]. This can be adopted to generate a dissimilarity matrix that is relevant for cluster analysis when studying synchronisation between several series. This approach utilises the singular value decomposition (SVD) of a matrix to explore typical common high-powered time-frequency regions. This technique is equivalent to the principal component analysis. But unlike the principal component analysis, this technique extracts components that maximise covariances, with the first extracted components corresponding to the essential common patterns between the wavelet spectra. Aguiar-Conraria and Soares (2011) proposed a technique for estimating the pairwise dissimilarity between various extracted components.

1.7.1 Leading Patterns and Leading Vectors

Let W_x and W_y be two $S \times T$ wavelet spectral matrices. Suppose $Q_{xy} := W_x W_y^H$ is their covariance matrix[8] and W_y^H represents the conjugate transpose of W_y. The execution of an SVD of this matrix yields

$$Q_{xy} = U \Sigma V^H \tag{1.16}$$

where U and V represent unitary matrices (i.e. $U^H U = V^H V = I$) while $\Sigma = \text{diag}(\sigma_i)$ is a diagonal matrix with non-negative sequential diagonal elements, which are ordered from highest to lowest, $\sigma_1 \geq \sigma_2 \geq \ldots \geq \sigma_S \geq 0$.

The column $\mathbf{u}_k$ of the matrix U is the singular vector for W_x, V is the singular vector for W_y, and σ_i represents the singular values. The number of non-zero singular values equal to the rank of the matrix Q_{xy}.

The singular vectors $\mathbf{u}_k$ and $\mathbf{v}_k$ satisfy a vital variational property. For each k,

$$\mathbf{u}_k^{\mathrm{H}} Q_{xy} \mathbf{v}_k = \max_{\mathbf{p}_k, \mathbf{q}_k \in \mathcal{S}} \left\{ \mathbf{p}_k^{\mathrm{H}} Q_{xy} \mathbf{q}_k \right\} \tag{1.17}$$

[7] For mathematical clarity, the measure introduced by Aguiar-Conraria and Soares (2011) is a dissimilarity measure and not a true distance since it does not necessarily satisfy $d(x, z) \leq d(x, y) + d(x, z)$.

[8] Q_{xy} is a square $S \times S$ matrix.

where S represents the set of vectors satisfying the following orthogonality conditions:

$$\mathbf{p}_k^{\mathrm{H}}\mathbf{p}_j = \mathbf{q}_k^{\mathrm{H}}\mathbf{q}_j = \delta_{k,j}, \quad \text{for} \quad j = 1, \ldots, k, \tag{1.18}$$

with $\delta_{k,j}$ denoting the Kronecker delta symbol, i.e. $\delta_{k,j} = 1$ if $j = k$ and $\delta_{k,j} = 0$, if $j \neq k$.

Suppose $\mathbf{l}_x^k$ and $\mathbf{l}_y^k$ denote the leading patterns, i.e. $1 \times T$ vectors obtained through the projection of each spectrum W_x and W_y onto the respective k^{th} singular vector (axis):

$$\mathbf{l}_x^k := \mathbf{u}_k^{\mathrm{H}} W_x \quad \text{and} \quad \mathbf{l}_y^k := \mathbf{v}_k^H W_y \tag{1.19}$$

Please note that $\mathbf{l}_x^k$ is a linear combination of the rows of W_x, with weights being the conjugates of the components of the k^{th} singular vector $\mathbf{u_k}$ (and similarly for $\mathbf{l}_y^k$). Since

$$\mathbf{u}_k^{\mathrm{H}} Q_{xy} \mathbf{v}_k = \mathbf{u}_k^{\mathrm{H}} W_x W_y^{\mathrm{H}} \mathbf{v}_k = \mathbf{u}_k^{\mathrm{H}} W_x (\mathbf{v}_k^{\mathrm{H}} W_y)^{\mathrm{H}} = \mathbf{l}_x^k \, (\mathbf{l}_y^k)^{\mathrm{H}} \tag{1.20}$$

it can be concluded that the leading patterns represent linear combinations of the rows of W_x and W_y, respectively, which maximise their mutual covariance (subject to the referred orthogonality constraints).

Equation (1.16) is equivalent to

$$U^H Q_{xy} V = \Sigma \tag{1.21}$$

One can obtain the covariance of the k^{th} leading patterns by equating the diagonal elements of the matrices on each side of this equation. This is given by

$$\left| \mathbf{l}_x^k \, (\mathbf{l}_y^k)^H \right|^2 = \left| \mathbf{u}_k^{\mathrm{H}} Q_{xy} \mathbf{v}_k \right|^2 = \sigma_k^2 \tag{1.22}$$

Similarly, the (squared) covariance of W_x and W_y is given by $\|Q_{xy}\|^2$, where $\|.\|$ represents the Frobenius matrix norm, defined by $\|A\| := \sqrt{\sum_{ij} |a_{ij}|^2}$. With this norm invariant under a unitary transformation, we obtain

$$\|Q_{xy}\|^2 = \|U^H Q_{xy} V\|^2 = \|\Sigma\|^2 = \sum_{i=1}^{F} \sigma_i^2.$$

The (squared) singular values σ_k^2 represent the weights attributed to each leading pattern and are equal to the (squared) covariance explained by each pair of singular vectors.

If L_x and L_y denote matrices with rows representing leading patterns $\mathbf{l}_x^k$ and $\mathbf{l}_y^k$, Equation(1.19) shows that $L_x = U^H W_x$ and $L_y = V^H W_y$. We then obtain

$$W_x = U L_x = \sum_{k=1}^{S} \mathbf{u}_k \mathbf{l}_x^k, \qquad W_y = V L_y = \sum_{k=1}^{S} \mathbf{v}_k \mathbf{l}_y^k$$

We typically select, in practice, a certain number $K < S$ (K is usually much smaller than S) of leading patterns, guaranteeing, for instance, that the fraction of covariance $\left(\sum_{k=1}^{K} \sigma_k^2\right) / \left(\sum_{k=1}^{S} \sigma_k^2\right)$ is above a certain threshold[9], and use

$$W_x \approx \sum_{k=1}^{K} \mathbf{u}_k \mathbf{l}_x^k, \quad W_y \approx \sum_{k=1}^{K} \mathbf{v}_k \mathbf{l}_y^k.$$

1.7.2 Dissimilarity between Two Spectra

The information in the two wavelet spectra has been reduced to a few components: K most appropriate leading vectors and patterns. The objective is to define a distance between two spectra, and this would be done by appropriate measurement of the distance from each pair of these vectors.

Consider the usual inner product in C^n, $\langle \mathbf{a}, \mathbf{b} \rangle = \sum_{i=1}^{n} \overline{a}_i b_i$ and the associated norm $\|\mathbf{a}\| := \sqrt{\langle \mathbf{a}, \mathbf{a} \rangle} = \sqrt{\sum_{i=1}^{n} |a_i|^2}$. Similarly, consider the so-called *Hermitian angle* between two vectors $\mathbf{a}, \mathbf{b} \in C^n$, $\Theta_H(\mathbf{a}, \mathbf{b})$, defined by the formula

$$\Theta_H(\mathbf{a}, \mathbf{b}) = \text{Arccos} \frac{|\langle \mathbf{a}, \mathbf{b} \rangle|}{\|\mathbf{a}\| \|\mathbf{b}\|}. \tag{1.23}$$

The dissimilarity between two vectors $\mathbf{p} = (p_1, \ldots, p_M)$ and $\mathbf{q} = (q_1, \ldots, q_M)$ with M components in $\mathbb{C}$ (applicable to the leading patterns and vectors), $d(\mathbf{p}, \mathbf{q})$, is defined by

$$d(\mathbf{p}, \mathbf{q}) = \frac{1}{M-1} \sum_{i=1}^{M-1} \Theta_H \left(\mathbf{s}_i^{\mathbf{p}}, \mathbf{s}_i^{\mathbf{q}}\right) \tag{1.24}$$

where the i^{th} segment $\mathbf{s}_i^{\mathbf{p}}$ is the two-vector $\mathbf{s}_i^{\mathbf{p}} := (i+1, p_{i+1}) - (i, p_i) = (1, p_{i+1} - p_i)$ and where $\mathbf{s}_i^{\mathbf{q}}$ is defined analogously. The dissimilarity measure $D\left(W_x, W_y\right)$ is computed to compare the wavelet spectra x and y:

$$D\left(W_x, W_y\right) = \frac{\sum_{k=1}^{K} \sigma_k^2 \left[d\left(\mathbf{l}_x^k, \mathbf{l}_y^k\right) + d\left(\mathbf{u}_k, \mathbf{v}_k\right)\right]}{\sum_{k=1}^{K} \sigma_k^2}, \tag{1.25}$$

where σ_k^2 are weights equal to the squared covariance explained by each axis. The dissimilarity measure could be computed for each pair of wavelet spectra and the information extracted from this to fill a dissimilarity matrix.

[9] K = 3 is adopted in this thesis: three leading patterns are sufficient for the attainment of a fraction above 90%. The use of larger K values yields almost identical results.

Chapter 2

A Time-Frequency Analysis of Financial Market Contagion in Europe

Abstract

This paper adopted a wavelet approach to investigate the financial contagion in the Eurozone debt market during various crisis-ridden periods in the zone. We used weekly 10-year bond yield data and showed that until the onset of the financial crisis of 2007/2008, bond yields were highly synchronised among all countries. However, the bond yields in Greece, Ireland, Italy, Spain, and Portugal became non-synchronised with core countries after 2008. Similarly, there was no synchronisation among the periphery countries during this period, except for Italy and Spain.

We found evidence of contagion emanating from Ireland during the first part of the sovereign debt crisis until around 2010, and from Greece afterwards. We also established that contagion spread to Portugal, Greece and Ireland, and can be observed at high frequencies. However, Italy and Spain were not affected. At business cycle frequencies, we found that the Greek crisis propelled a flight-to-quality flow to Belgium, Finland, France and Germany.

Keywords*: Contagion; Interdependence; Fundamental-based Contagion; Pure Contagion; Spillovers; Cross-market Co-movements; Wavelet Power Spectrum; Wavelet Coherency; Wavelet Phase-Difference; Wavelet Distance*

2.1 Introduction

The increasing interconnectedness of the global economy and the rapid integration of global financial markets propel global economic growth, increase volume and velocity of international financial transactions, and improve capital flows to many countries (Gereffi, 2005; Kenc and Dibooglu, 2010; Rajan, 2006). On the flip side, it poses challenges to global economy and financial architecture. For instance, global financial markets have witnessed various financial and currency crises in the last four decades. One feature of these crises is their snowballing effect from one market or geographical location to another. While this undesired domino effect of financial market crises is generally called contagion, there is no consensus on the definition or measurements of contagion.

Some prominent definitions include a substantial increase in the conditional probability of a crisis in one country relative to another country; volatility asset-price spillover from a crisis-ridden country to another; cross-country co-movement of asset prices that is unexplained by fundamentals; substantial increases in co-movements of prices and quantities across markets conditioned on the occurrence of a crisis in at least one market; intensified shock transmissions or changes after a shock in a market; substantial increases in the cross-market correlation during turmoil (see Dungey* et al., 2005; Forbes and Rigobon, 2002; Pericoli and Sbracia, 2003, for details).

Overall, there are four fundamental considerations in these definitions: significant cross-market correlation; measures of shock transmission across markets; differences between contagion and interdependence; distinguish between normal and excessive co-movements across financial markets. Numerous studies incorporated these features in their definitions of contagion. For example, Dornbusch et al. (2000) defined contagion as a significant increase in cross-market linkages after a shock to at least one market. Forbes and Rigobon (2002) deepened this definition and posited that contagion implies a fundamental difference in the cross-market link after a shock to one market; similarly, interdependence emphasises no significance change in cross-market relationships.

Although there is a proliferation of studies on contagion, some studies were driven by definitions ascribed to contagion. With contagion defined as a substantial increase in cross-market linkages after a shock to at least one market (Forbes and Rigobon, 2002), some studies evaluated evidence of contagion based on the notion of correlation breakdown. Such studies emphasised the statistically significant increase in correlation during the crisis period (Rodriguez, 2007). For instance, Edwards and Susmel (2001) utilised switching volatility models to analyse the evolutionary volatility in Latin America and found short-lived high-volatility episodes, lasting between two and twelve weeks and accompanied by volatility co-movements across countries in the sample.

Similarly, Bertero and Mayer (1990) and King and Wadhwani (1990) found an increase in the correlation of stock returns during the 1987 stock market crash while Calvo (1999) established correlation shifts during the Mexican Tequila crisis. Chiang et al. (2007) adopted a dynamic conditional correlation model and found evidence of contagion, as shown by increases in correlation.

However, some studies are critical about linking contagion to the structural shift in correlation. For instance, Boyer et al. (1997) argued that evaluating correlation changes without accounting for conditional heteroskedasticity might result in a severely biased result. Rodriguez (2007) corroborated this and argued that the correlation between two random variables, conditioning on extreme realisations of one variable would likely suggest correlation breakdown, even if the true data generation process has a constant correlation. Forbes and Rigobon (2002) deepened this argument by utilising the generalised approach of Boyer et al. (1997) and found no evidence of correlation breakdown after adjusting for heteroscedasticity.

The criticism of the correlation framework for measuring contagion galvanised a shift of focus in another strand of literature and propelled varying methodologies in those studies. For instance, Bae et al. (2003) utilised the multinomial logistic regression model for stock markets and established that contagion is dependent on changes in exchange rates, interest rate and stock return volatility. Similarly, Masih and Masih (1999) examined the short- and long-term dynamic linkages among stock markets in OECD countries and Asia using a VAR model. The study found that regional markets, rather than OECD markets, explained stock market fluctuations in Asia. Also, Schwert (1990) found a dramatic jump in stock return volatility during and after the crash, while Forbes and Rigobon (2002) argued that such market-return volatility can bias correlation coefficients and induce heteroscedasticity.

Furthermore, Bekaert et al. (2014) analysed the crisis transmission to 415 country-industry equity portfolios using a factor model in 55 countries and found limited evidence of contagion from both the US market and the global financial sector. However, the study found substantial evidence of contagion from domestic equity markets to individual domestic equity portfolios. But its severity is inversely related to the quality of economic policies and fundamentals of the countries. Additionally, a strand of literature explored the recent sovereign debt crisis in Europe. For example, Missio and Watzka (2011) used dynamic conditional correlation models to assess contagion during the European debt crisis and found that yield returns in Belgium, Italy, Portugal, and Spain increased as Greece experienced increasing yield spread with Germany.

Similarly, Arghyrou and Kontonikas (2012) explored the European sovereign debt crisis and found a shift in market pricing behaviour from a convergence-trade model to one

propelled by macro-fundamentals and international risk. Specifically, the study found that other Economic and Monetary Union (EMU) countries experienced contagion from Greece but established no significant speculation effects from CDS markets. Giordano et al. (2013) investigated the link between a sharp increase in the sovereign spread of Eurozone countries and deterioration of macroeconomic and fiscal fundamentals or financial contagion after the Greek crisis and found evidence of wake-up contagion, but not pure contagion. Martins and Amado (2018) found long-run contagion effects across periphery countries while Broto and Perez-Quiros (2015) and Mink and De Haan (2013) established Greece, Portugal and Ireland as sources of contagion.

While most studies on contagion utilised time-domain analysis, there is increasing adoption of spectral analysis and wavelet analysis in evaluating the spread of financial crisis from one market to another. These techniques are adopted to provide insight on contagion that is hidden in the traditional time-domain framework. Orlov (2009) adopted spectral analysis to evaluate the co-movement of exchange rates during the Asian financial crisis. The study found greater co-movement among high-frequency components. Similarly, Gray (2014) utilised cross-spectral methods to investigate co-movement between currency market in Eurozone and selected markets outside Eurozone and found evidence of contagion in at least three markets.

On the other hand, Gallegati (2012) utilised the wavelet approach to distinguish between contagion and interdependence in stock markets during the US subprime crisis and found that the crisis affected all stock markets in the sample. However, Brazil and Japan are two countries showing evidence of contagion at all scales. Rua and Nunes (2009) utilised the wavelet analysis to assess the co-movement among international stock markets. The study found that the extent of co-movement of international stock market return is dependent on the frequency. Specifically, the study found stronger co-movement between markets at the lower frequencies. However, the study established stronger co-movement at higher frequencies between the UK and the US markets around the 1987 crash and the dotcom era towards the end of the century, with the dotcom bubble associated with contagion.

Similarly, Madaleno and Pinho (2012) adopted the continuous wavelet approach to explore the stock market linkages and found a strong but heterogeneous relationship among four stock market indices - Brazil, Japan, UK and the US. Additionally, the study showed the impact of geography in the co-movement between markets by establishing that geographically and economically closer markets show higher correlation and exhibit deepening short-run co-movement. However, the study found that strong co-movement is mostly experienced with long-run fluctuations. In evaluating the evidence of contagion and interdependence among OECD countries, Ftiti et al. (2015)

combined spectral and wavelet analysis. While the study found evidence of contagion and interdependence at different periods, it demonstrated that long-term co-movement is related to the interdependence of stock market indexes. In contrast, short-term co-movement is linked to the evidence of contagion.

Despite the proliferation of definitions of contagion in the existing literature, the definition provided by Forbes and Rigobon (2002) is mostly adopted. One major takeaway from this definition is contagion is driven by shock transmission that is unexplained by fundamentals. With the inability of fundamentals to explain contagion, some authors viewed it as a short-run phenomenon due to the typical rigidity of fundamentals in this time horizon. This view galvanised a strand of literature utilising either spectral analysis or wavelet analysis to explore contagion. This literature considers contagion as a temporary and significant shift in cross-market linkages and interdependence as a permanent shift in cross-market linkages after a shock (Bodart and Candelon, 2009). The established link between period (time horizon) and frequency prompted several authors - such as Bodart and Candelon (2009), Madaleno and Pinho (2012), Gallegati (2012) and Orlov (2009) – to associate contagion with high frequencies and interdependence with low frequencies.

While our work builds on the papers mentioned in the previous paragraph, we propose a different way of distinguishing between contagion and interdependence. As stressed by Martins and Amado (2018), an increase in the correlation between financial series during times of turmoil is not enough evidence of contagion. It may be merely the result of higher volatility accompanied by stable and substantial interdependence. Contagion is the change in market interdependence during periods of high volatility. Similarly, our paper contrasts with most of the existing literature and relates to Martins and Amado (2018) in two ways. One, we do not impose a pre-defined date for the turmoil; instead, we allow the dynamics of bond-yield data to speak for itself. Two, our wavelet approach allows us to work in different timescales simultaneously, and this enables us to distinguish between the short- and the long-run.

Our approach relies mainly on the concept of partial wavelet coherence proposed by Aguiar-Conraria and Soares (2014), with Aguiar-Conraria et al. (2017), Ko and Funashima (2019) and Verona (2019) applying this concept to the financial time series. In this paper, we used a set of countries, called the core countries, to control for structural interdependence. To identify these countries, we rely on a wavelet dissimilarity measure proposed by Aguiar-Conraria and Soares (2011) and applied by Aguiar-Conraria et al. (2013a), Aguiar-Conraria et al. (2013b), and Flor and Klarl (2017). The core countries are mostly immune to the turmoil that affected the sovereign yields. The coherency between core countries and each of the periphery countries

captured ordinary market interdependence and synchronisation between countries across frequencies. This allowed us to identify precise time and frequencies that the highly affected countries cease to anchor to core countries.

Furthermore, we explored the highly affected countries for evidence of contagion and the source of such contagion. We identified contagion as the leftover coherence - partial coherency - between these countries. Therefore, when studying the contagion between two countries, say Portugal and Greece, we estimated the interdependence, in the time-frequency domain, between their yields after eliminating the effect of yield returns of other countries. We relied on the concept of partial coherency to achieve. However, if there is a significant region of the (partial) coherency between Portugal and Greece after controlling for effects for other countries, we will conclude that there is evidence of contagion. The Partial Phase-difference identifies the originating country of such contagion.

The paper proceeds as follows. Section 2.2 presents the empirical findings by identifying core countries and the peripheral countries, analyses the time-frequency relationship between these two categories of countries, and tests for evidence of contagion between peripheral countries. Similarly, Section 2.3 concludes the study.

2.2 Empirical Findings

We utilised weekly data from January 2001 to June 2019. We extracted daily data of 10-year sovereign bond yields from Eurostat for nine European countries: Belgium, Finland, France, Germany, Greece, Ireland, Italy, Portugal, and Spain. However, the data were converted to weekly data to reduce the computational burden.

We present the empirical results in this section. We estimated the wavelet power spectrum of weekly returns for each country. This is akin to presenting the descriptive statistics. We then identified the core countries by exploring the wavelet spectra dissimilarity of yields for countries in our sample. Subsequently, we estimated the wavelet coherency between core countries and each of the periphery countries. Finally, we used partial coherency and phase-difference to evaluate evidence of contagion between selected countries.

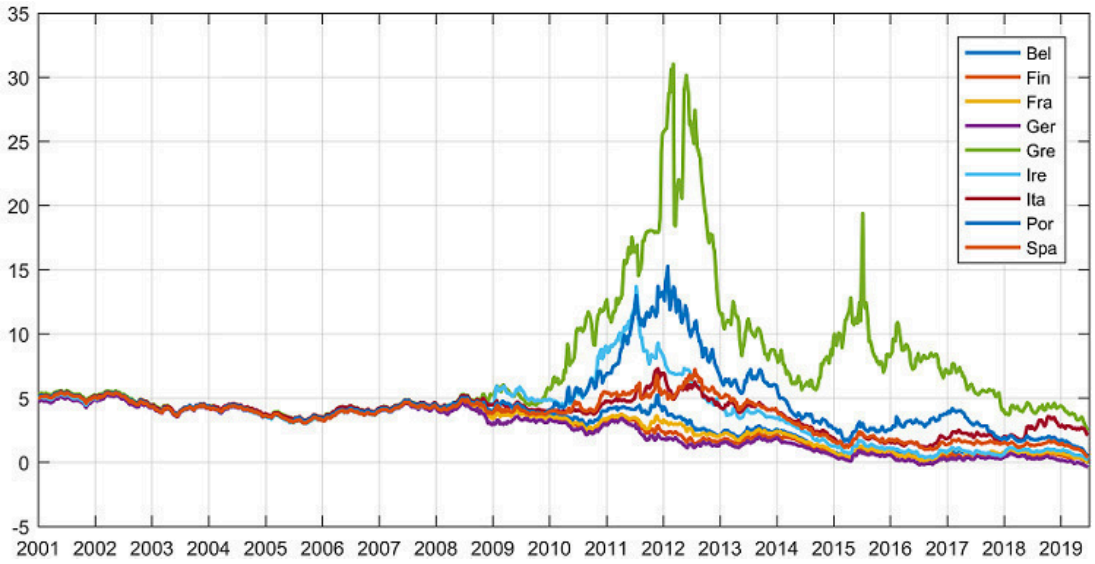

Figure 2.1: Weekly data on 10-year government bond yields for nine Eurozone countries

2.2.1 Wavelet Power Spectrum

Figure 2.1 shows the weekly 10-year government benchmark bond yields for the nine countries in our sample. It should be noted that the turmoil in the sovereign debt started in late 2008 or early 2009. Greek bonds spiked the most, followed by Portugal and Ireland. With these dynamics, the leading country is not completely obvious. While it is also apparent that Italy and Spain have similar dynamics, the turmoil did not affect Belgium, Finland, France, and Germany. However, it is unclear if Italy and Spain are closer to the former or the latter group.

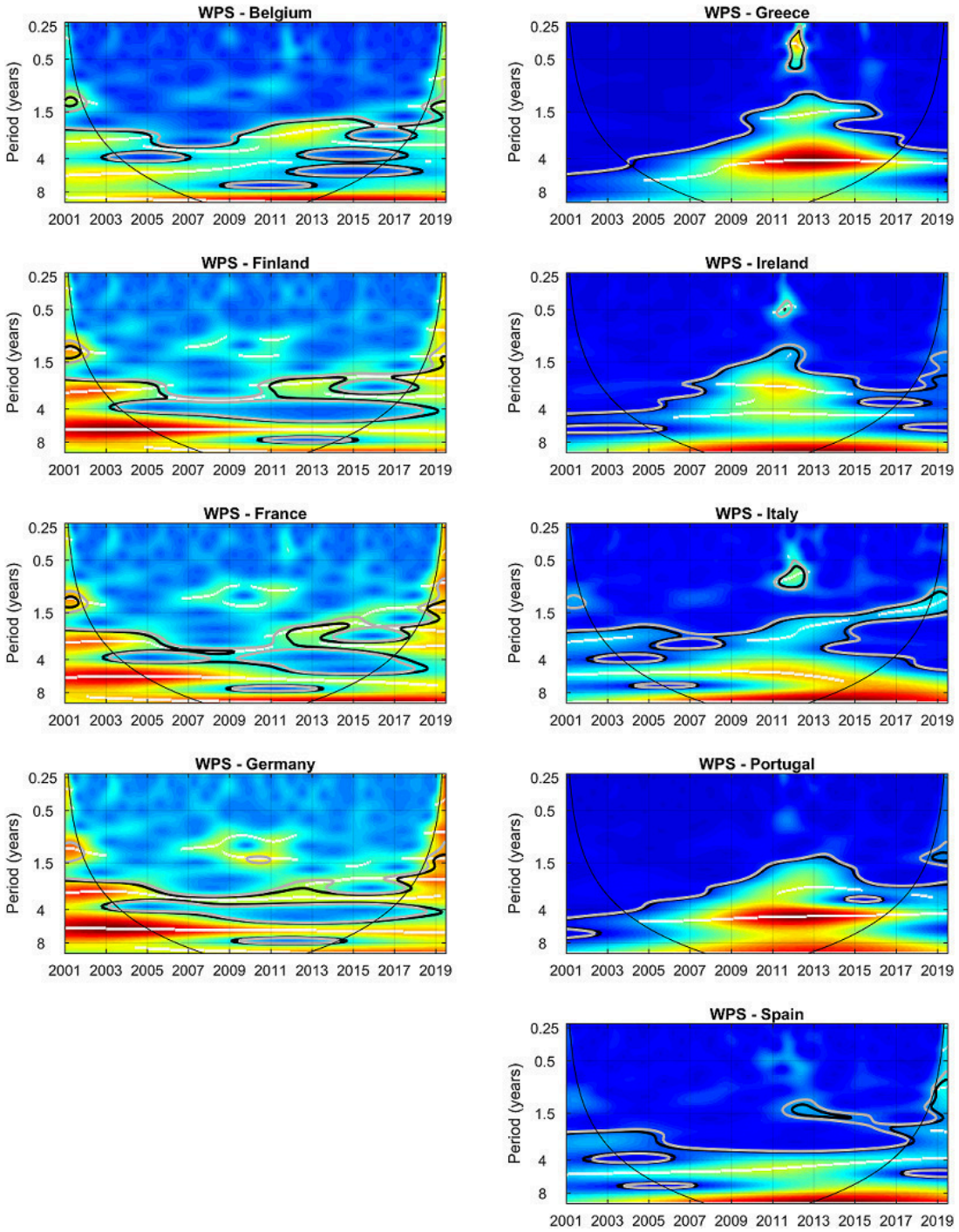

Figure 2.2: The wavelet power spectrum of each country's government yield. The black/grey contour designates 5%/10% significance level. The cone of influence, which indicates the region affected by edge effects, is shown with a parabola-like black line. The colour codes range from blue (low power) to red (high power). The white lines show the local maxima of the wavelet power spectrum.

Figure 2.2 shows the wavelet power spectrum of bond yields for nine countries. In the power spectra, the colours reflect the degree of volatility, with the blue colour depicting low variability and the red colour signifying high volatility. A thick black/grey contour identifies the 5/10% significance regions against the null of a flat power spectrum. The

white stripes identify local maxima and are, therefore, estimates of periods of most relevant cycles.

For the four countries on the left (Belgium, Finland, France and Germany), it is apparent that the dominant cycles are at the lower end of business cycle frequencies: frequencies between four and eight years. However, the dynamic is different for the five countries on the right (Greece, Ireland, Italy, Portugal and Spain). In general, the power spectrum for these countries is much higher after 2008 and, mainly, after 2010. This applies to both the upper and the lower end of business cycle frequencies, but it is mostly visible at the $4 \sim 8$-year frequency band.

Among these five countries, Spain's power spectrum is closest to the power spectrum of the four countries on the left of Figure 2.2. However, the power spectrum at 1.5-year frequency becomes statistically significant around 2012. On the other hand, Greece exhibited the most peculiar characteristics. We observed a predominant five-year cycle starting in 2009 and extending to the end of the sample. Similarly, a shorter cycle is experienced between 2010 and 2015 at the frequency of about 1.5 years, while high frequencies can be seen around 2012. For Italy and Ireland, a (smaller) spike was observed at high frequencies in 2012. While the power spectrum for Ireland is not statistically significant, Ireland is peculiar as it exhibited high volatility at all business cycle frequencies between 2008 and 2015. Portugal, like Greece, has a salient cycle at frequencies slightly below four years while volatility also increased at higher frequencies, but with some delay, when compared to Greece and Ireland.

2.2.2 Core Countries

In Table 2.1, we showed the pairwise dissimilarity index between the countries in our sample. It is based on comparing the wavelet transform of yields of all countries. It is noteworthy that this is not the same as comparing the wavelet power spectra of Figure 2.2. In the computation of the wavelet power spectrum, the absolute value is taken, and this implies that complex numbers disappear. By focusing on the wavelet transform, the information provided by complex numbers is preserved. Precisely, one retains the information about the phase of the cycle. A dissimilarity index between two countries close to zero means that the two countries have a similar wavelet transform. Similarly, this implies that both countries share the same high-power regions and have aligned phases. Therefore, (1) the contribution of cycles at each frequency to the total variance is similar between both countries, (2) this contribution happens at the same time, and finally, (3) the wiggling of each cycle coincides in both countries.

	Belgium	Finland	France	Germany	Greece	Ireland	Italy	Portugal	Spain
Belgium		0.115	0.064	0.103	0.323	0.212	0.245	0.338	0.183
Finland	0.115		0.061	0.031	0.298	0.246	0.278	0.344	0.241
France	0.064	0.061		0.053	0.311	0.248	0.262	0.354	0.208
Germany	0.103	0.031	0.053		0.301	0.252	0.285	0.344	0.237
Greece	0.323	0.298	0.311	0.301		0.207	0.248	0.120	0.225
Ireland	0.212	0.246	0.248	0.252	0.207		0.196	0.193	0.139
Italy	0.245	0.278	0.262	0.285	0.248	0.196		0.210	0.098
Portugal	0.338	0.344	0.354	0.344	0.120	0.193	0.210		0.204
Spain	0.183	0.241	0.208	0.237	0.225	0.139	0.098	0.204	
Color code:				p < 0.005		p < 0.05		p < 0.10	

Table 2.1: Pairwise dissimilarities. p-values obtained by Monte Carlo simulation (10,000 replications) against the null that the cycles are not synchronised.

As we intend to consider all range of high frequencies to business cycle frequencies, the wavelet transform was computed for frequencies from two week-period to eight years. With our weekly data, the highest frequency that we can adopt is bi-weekly. The lower end, eight years, is just the typical lower end of business cycle frequencies[1].

The results are entirely in line with our observation in Figure 2.1. Precisely, there is a set of countries that have well-aligned cycles with one another (Belgium, Finland, France, and Germany), and a group of countries that are autonomous (Greece, Ireland, Italy Portugal, and Spain). The inclusion of Spain and Italy in the second group removes the earlier doubt of where they belong when one looks at Figure 2.2.

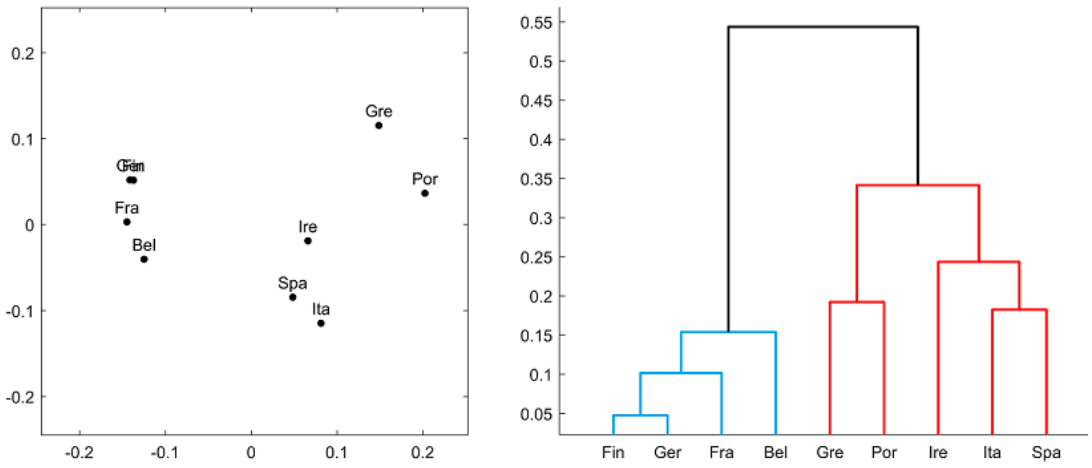

Figure 2.3: Multidimensional Scaling Map

To visualise Table 2.1, we reduced the dissimilarity matrix to a two-column matrix called the configuration matrix, which contains the position of each country in two orthogonal

[1]Given that, traditionally, we associate the frequency band of 1.5 to 8 years to business cycles, in our analysis, we separated business cycle frequencies from short-run frequencies (frequencies higher than 1.5 years).

axes. This, of course, cannot be performed with perfect accuracy because the dissimilarity matrix does not represent Euclidean distances. Figure 2.3 is generated from the configuration matrix, with a multidimensional scaling map (on the left), and a dendrogram (on the right). With their highly synchronised cycles, Germany, Finland, France and Belgium are in the same group. Thus, they are referred to as core countries while Greece, Ireland, Italy, Portugal and Spain are periphery countries.

2.2.3 Wavelet Coherency and Phase-Differences between the Core Countries and the Peripheral Countries

The interpretation of our econometric results proceeds as follows. We evaluated the statistically significant regions for coherency between two variables. These regions imply that, in those episodes, we can affirm that there is a significant co-movement of variables for cycles at the indicated period. For the statistically significant time-frequency regions, we analysed phase-differences to determine the type of co-movement and identified the leading and lagging variables. However, a low and statistically non-significant coherency will provide a limited meaningful explanation as the phase-differences will be erratic given the absence of a meaningful relationship.

Figure 2.5 presents the wavelet coherency and the wavelet phase-difference between the yield of the Core and each periphery countries[2]. We equally presented the same computations for two core countries - Belgium and France - in Figure 2.4 to enable us to make comparisons.

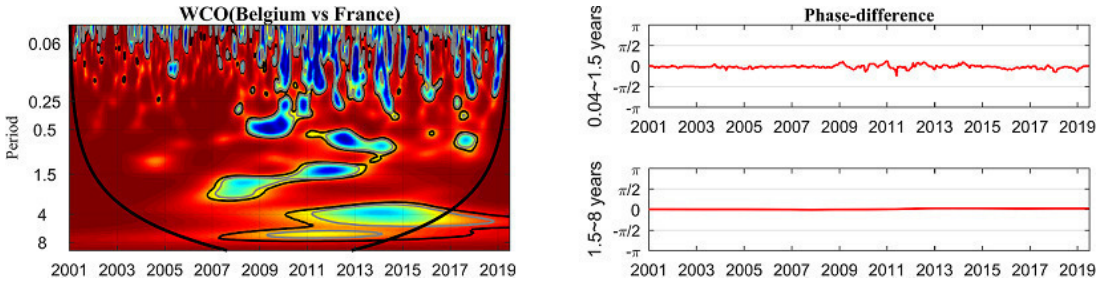

Figure 2.4: **On the left** - wavelet coherency between the yield of Belgium and France. The black contour designates 5% significance. The colour codes for coherency range from blue (low coherency - close to zero) to red (high coherency - close to one). **On the right** - phase-differences between Belgium and France.

We observed that the wavelet coherency between two core countries is red and statistically significant almost everywhere. Kindly note that the phase-differences are almost zero for the whole sample period, implying that the yields are positively correlated at all frequencies and co-move. In such instances, there is no leading or lagging country.

[2]The yield of the Core is the average yield of Belgium, France, Finland, and Germany.

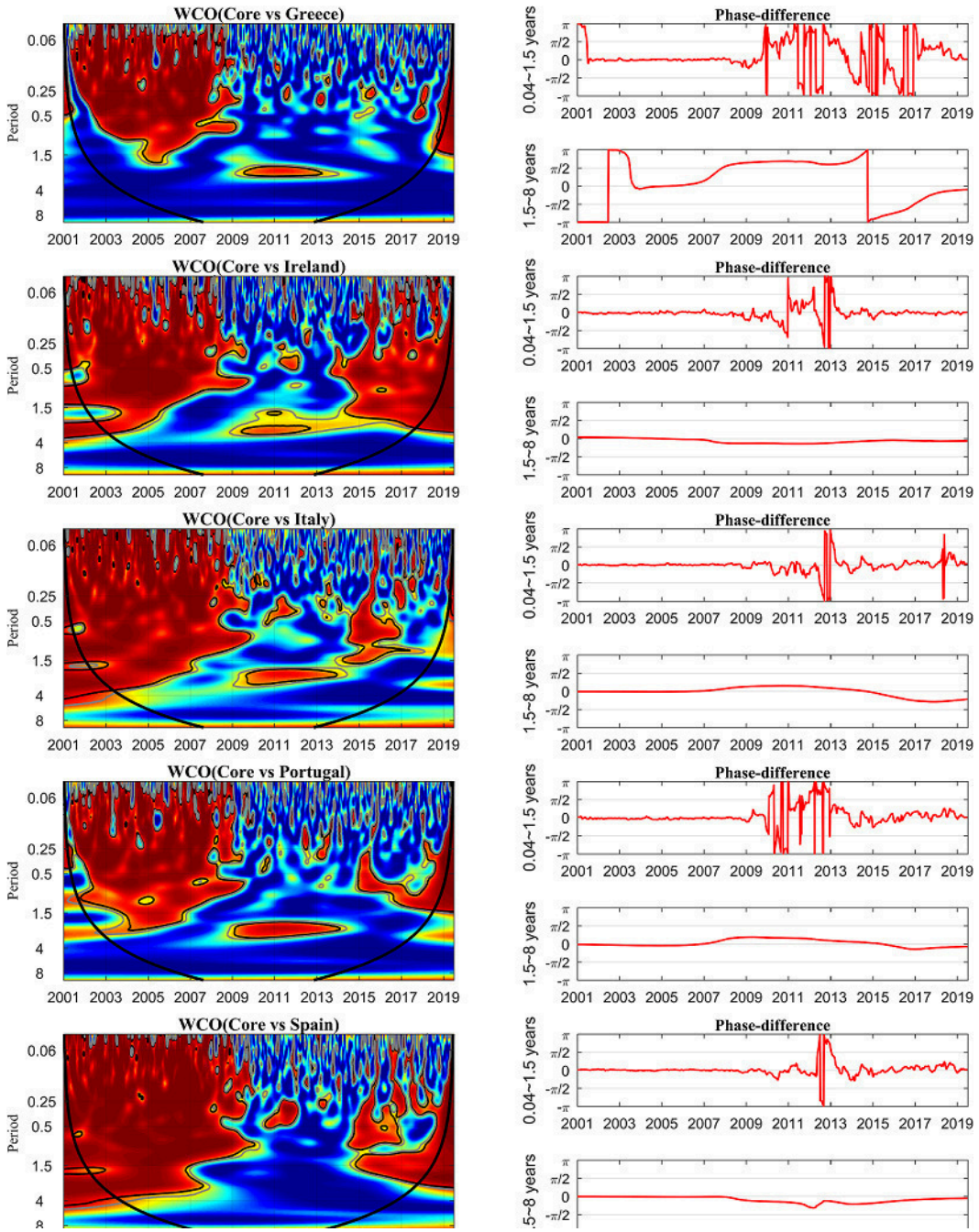

Figure 2.5: **On the left** - wavelet coherency between the yield of the core countries and each of the periphery countries. The black contour designates 5% significance. The colour codes for coherency range from blue (low coherency - close to zero) to red (high coherency - close to one). **On the right** - phase-differences between the core countries and each periphery country.

However, the scenario differs when evaluating the link between the Core and periphery countries. Greece presented the most peculiar case, with its high coherency at higher frequencies until 2008. Thereafter, the picture turns blue, indicating low coherencies and maintained this until the end of the sample period. At higher frequencies, the phase-difference became erratic in 2009. This signifies that the Greek bond yields detached from others as from this period. In contrast to other countries, the coherency

is mostly blue at low frequencies at the beginning of the sample period. This suggests that the long-run co-movement between Greece and core countries has always been weak. The most notable exception occurs between 2009 and 2013. During this period, we observed an island of high coherency at the frequency band of about 2-3 years. The phase-difference lies between $\pi/2$ and π, signifying an anti-phase (or negative) relation, with Greece leading. We do not observe this with any other countries. It suggests that in this period, there was a flight-to-quality flow, with investors taking refuge in core countries.

For other periphery countries, except Spain, we observed the same region of high coherency. However, the phase-difference is close to zero. This suggests that these countries remained tied to the core countries at business cycle frequencies during the crisis period. Ireland, Italy, and Spain were highly coherent for a longer period at both lower and higher frequencies. However, Portugal is somewhat between Greece and the other periphery countries. Regarding shorter-run phase differences, Portugal and Ireland experienced an erratic phase-difference around 2010. Similarly, this was experienced in Spain and Italy between 2012 and 2013. However, Ireland became synchronised with the core countries in 2014. While Spain and Italy were the only periphery countries whose governments did not seek external assistance, Ireland was the first to re-align with the core countries. After Ireland, there was evidence that Portugal and Spain experienced the same scenario. Regarding Italy, we observed high coherency at several frequencies between 2015 and 2017, but this vanished thereafter.

2.2.4 Wavelet Partial Coherency and contagion between Greece, Ireland and Portugal

In the previous subsection, we established that Greece, Ireland, and Portugal were the first countries to show signs of stress in their sovereign bond markets. In this subsection, we explored those results further. We investigated evidence of contagion by estimating the partial wavelet coherency and phase-differences between the yields of these countries after controlling for the yields of Spain, Italy, and the Core. We interpreted the existence of leftover (significant) coherency at high frequencies as evidence of contagion, while the partial phase-difference informs the source of such contagion.

Regarding this, we observed that Portugal consistently lagged both Greece and Ireland between 2008 and 2014 at higher frequencies. i.e. at the 0.25 to the 1.5-year frequency band. Similarly, the partial phase-differences between Greece and Portugal, and Ireland and Portugal are consistently between 0 and $\pi/2$. Thus, Portugal is not the source of contagion. Regarding Greece and Ireland, we observed a switch in 2010. Prior to that period, Greece lagged Ireland while Greece became the leading country afterwards. This

evidence suggests that until 2010, the primary source of contagion was Ireland while Greece became the originating country afterwards. The Irish banking crisis forced its government to issue a broad state guarantee of Irish domestic banks in September 2008, and the subsequent public finance crisis in Greece, which led to a bailout programme in 2010 are the most obvious culprits.

At business cycle frequencies, phase relations are much more stable. Ireland consistently leads both Portugal and Greece. The phase relation between Portugal and Greece is also stable, with Portuguese yields slightly leading Greek yields for most parts of the sample period. However, the phase-difference becomes zero between 2009 and 2011, suggesting that the yields were highly synchronised in the peak of the crisis at business cycle frequencies.

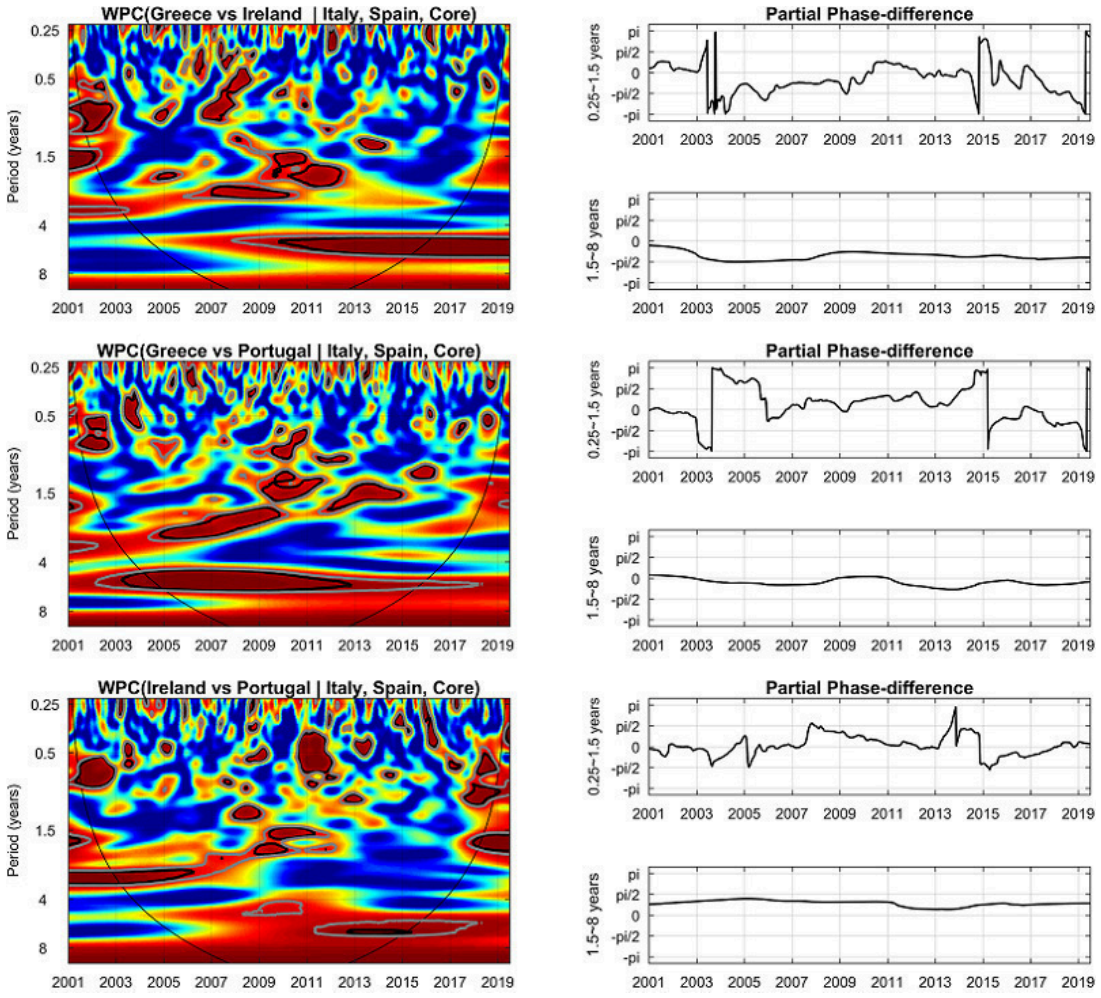

Figure 2.6: **On the left** - wavelet partial coherency between the Greece, Ireland and Portugal, after controlling for Italy, Spain and the Core countries. The black/grey contour designates the 5/10% significance. The colour codes for coherency range from blue (low coherency - close to zero) to red (high coherency - close to one). **On the right** - the partial phase-differences.

2.3 Conclusions

We applied the Continuous Wavelet Transform to study the sovereign debt yields in nine Eurozone countries. We used weekly data from 2001 to June 2019. We first applied the dissimilarity index to demarcate core countries (Belgium, Finland, France and Germany) from the periphery countries, also known as GIIPS (Greece, Ireland, Italy, Portugal and Spain). We estimated the wavelet coherency and the wavelet phase-difference between the core and peripheral countries.

We established that Greece had a significant coherency with the core countries until 2008 and became erratic as from 2009. For other periphery countries, their detachment from the core occurred later (in the case of Ireland and Portugal) and even much later in the case of Spain and Italy. In the case of Ireland, we also observed that it re-aligned with the core countries in 2014. An interesting result that we established was the evidence of the flight-to-quality flow, with investors taking refuge in core countries due to the instability in Greece.

We equally investigated evidence of contagion between the first three countries that detached from the core: Greece, Ireland, and Portugal. We concluded that until 2010, Ireland was the main source of contagion while Greece took over later. We can connect these timings to the Irish banking crises, which started in September 2008, and the Greek public finance crisis, which led to a bailout programme in 2010.

Chapter 3

A Time-Frequency Analysis of the Canadian Macroeconomy and the Yield Curve

Abstract

We used wavelet analysis to study the relationship between the yield curve and macroeconomic indicators in Canada. We relied on the Nelson-Siegel approach to model the zero-coupon yield curve and used the Kalman filter to estimate its time-varying factors: the level, the slope and the curvature. Apart from establishing a bidirectional yield-macro relation, the paper broadened the existing literature by exploring the link between the monetary policy and the yield curve. We reached several conclusions. First, the monetary policy variable, the bank rate, affects mainly short-run interest rates. Arguably, the main driver for economic activity is the long-run interest rate (instead of the short-run), suggesting that monetary policy is mostly ineffective. Second, we concluded that concerning the inflation rate, the Bank of Canada is very proactive. Third, regarding the unemployment rate, we found that both the slope and the curvature are leading indicators for the long-run evolution of unemployment. Finally, our results suggested that the industrial production index leads the yield curve factors and not the other way.

Keywords*: Term Structure; Yield Curve; Macroeconomic Variables; Wavelet Power Spectrum; Wavelet Coherency; Wavelet Phase-Difference*

3.1 Introduction

"The ability of monetary policy to affect aggregate expenditures rests on the premise to influence market expectations regarding the future path of short-term interest rates" - (Geiger, 2011, p.1). However, the impact of any central bank on macroeconomic dynamics depends on its influence on financial market prices, particularly its grip on the long-term interest rate, which governs the level of credit demand and consequently expenditures. The typical hypothesis is that expectations connect the short- and long-run interest rates, with the yield curve representing the pivot between the aggregate demand and monetary policy, offering the central bank valuable information on private market expectations (Geiger, 2011). Such a vital influence has fuelled a proliferation of yield curve models.

While the modelling of the yield curve is evolving (see Diebold and Rudebusch (2013) for a review), efforts have been made to explore unidirectional and bidirectional links between macroeconomic variables and the yield curve. Such efforts deployed mostly traditional econometrics techniques (see Ang and Piazzesi, 2003; Wu, 2001; Estrella and Hardouvelis, 1991; Benati and Goodhart, 2008), with few novel approaches (see Aguiar-Conraria et al., 2012a,b). However, there is a paucity of literature on the role of the yield curve in monetary policy space. Such investigation is crucial for countries like Canada since its central bank uses an interest rate measure - Target for the Overnight Rate - as a monetary transmission mechanism. This paper fills the void by, not only exploring the bidirectional macro-yield link, but also evaluating the link between the Canadian yield curve and its monetary policy. The paper equally deepens the literature by adopting the wavelet approach. The ability of wavelet tools to capture the high irregularity in the financial data through its decomposition into both time and frequency domains influences its choice for this study.

A wide range of empirical studies has explored the relationship between the yield curve and the macroeconomic variables. Diebold et al. (2006b) used Nelson-Siegel model to explore the macroeconomic-yield link and found that inflation rate and real economic activity highly correlated with level and slope factors, respectively, but the curvature factor had no underlying relationship with any of the main macroeconomic variables. Evans and Marshall (2007) established that inflation and economic activity are responsible for the huge variability in short- and medium-term yields, respectively. The explanatory power of these two variables is commonly attributed to the role of monetary policy as a transmission channel of macroeconomic dynamics (Kozicki and Tinsley, 2001). Rudebusch and Wu (2008) obtained a similar result, but with a more structural interpretation: level factor reflected the underlying market view about the central bank's medium-term inflation targeting while slope factor captured the central bank's cyclical response. Empirical studies by Kozicki and Tinsley (2001) and Dewachter and

Lyrio (2006) explored the feedback from an implicit inflation target generated from the yield curve to explain the yield curve dynamics. Similarly, Taylor (1993) found that the short end of the yield curve evolves at par with the central bank's policy instrument, which responds to changes in inflation and economic activity. Furthermore, Moneta (2005) hypothesised that a positive yield curve is associated with the future expected economic growth by investors while a negative yield curve is associated with an expected impairment in economic growth.

To our knowledge, two papers used wavelets to explore this relation for the USA. Gallegati et al. (2014) relied on the Discrete Wavelet Transform to perform a scale-by-scale decomposition of several indicators that measure the stance of monetary policy variables, including the yield curve slope and GDP. Similarly, Aguiar-Conraria et al. (2012a) relied on the continuous wavelet transform to explore the link between the yield curve and the macroeconomy in the USA. The main advantage of using wavelets lies in its ability to estimate relations that are not only time-varying but also frequency-varying, providing a thorough vision of the relationship between the yield curve components and the macroeconomic variables that is almost impossible to obtain with purely time-domain or frequency-domain analysis.

The literature on the Canadian yield curve is scarce, and limited available studies have widespread focus. For instance, Lange (2013) explored the link between the Canadian yield curve and its macroeconomic variables using a dynamic latent approach and found bidirectional causality between them. Garcia and Luger (2007) equally explored this relationship using the equilibrium-based approach and incorporated a vector autoregression description of Canada's key macroeconomic dynamics. They found that in-sample average pricing errors from the equilibrium-based model are slightly larger than those from a relatively flexible no-arbitrage model. However, Hao and Ng (2011) investigated the ability of Canadian financial and macroeconomic variables in predicting recessions and found that government bond yield spread (akin to the yield slope) among others is a powerful predictor of recession. The study by Booth et al. (2007) focused on the drivers of provincial-Canada yield spreads and found a strong correlation between provincial yield spreads and provincial debt and deficit levels. Hejazi et al. (2000) examined the implicit determinants of the Canadian term premia and found that the conditional variances of Canadian macroeconomic variables are not significant predictors of the T-bill term structure. This finding is contrary to the evidence from the USA.

While a strand of literature on the yield curve focused on the link between the yield curve and macroeconomic variables and its predictive power, there is paltry literature on the yield curve and the monetary policy. Cook and Hahn (1989) examined the market's reaction to monetary policy actions and found a positive response to the federal funds

rate target increases at all maturities. Edelberg et al. (1996) found a marginal significance response of bond rates to policy shocks, but a highly significant response regarding treasury bill rates.

The paper proceeds as follows. In section 3.2, we describe our modelling and estimation choices for the yield curve factors. We also present the data. In section 3.3, we present our main results and section 3.4 concludes.

3.2 Methodology and Data

3.2.1 Yield Curve Model Specification and Estimation

Despite a growing body of literature on yield curve modelling, three distinct approaches are popular: no-arbitrage models, equilibrium models and parsimonious model. While the no-arbitrage approach perfectly fixes the yield curve at a point in time and ensures no arbitrage opportunity exist, the equilibrium approach typically uses affine models to model the dynamics of the instantaneous rates and subsequently derive yields of other maturities under various assumptions about the risk premium. The parsimonious model, popularised by Nelson and Siegel (1987), distils the yield curve into a three-dimensional parameter: level, slope and curvature.

This study uses the parsimonious model to explore the relationship between the Canadian yield curve and the macroeconomic variables. The model is represented by:

$$y(\tau) = \beta_1 + \beta_2 \left(\frac{1 - e^{-\lambda\tau}}{\lambda\tau} \right) + \beta_3 \left(\frac{1 - e^{-\lambda\tau}}{\lambda\tau} - e^{-\lambda\tau} \right),$$

where $y(\tau)$ and τ denote the zero-coupon yields and maturity, respectively, while β_1, β_2 and β_3 are time-varying parameters. Based on Diebold and Li (2006), the time-varying parameters capture the level, slope and curvature of the yield curve at each period t. The yield can be estimated from the equation:

$$y_t(\tau) = L_t + S_t \left(\frac{1 - e^{-\lambda\tau}}{\lambda\tau} \right) + C_t \left(\frac{1 - e^{-\lambda\tau}}{\lambda\tau} - e^{-\lambda\tau} \right). \tag{3.1}$$

The role of the three components L_t, S_t and C_t becomes clear when we consider their limiting behaviours with respect to time to maturity τ. L_t may be viewed as the long-term factor with a loading of 1 and does not decay to zero in the limit; S_t may be interpreted as a short-term factor with a loading that starts at 1 and monotonically decays fast to zero; finally, C_t may be viewed as a medium-term factor with a loading that starts at zero, increases and then decays to zero.

Note that long-run interest rates are usually higher than short-run, as an investor is expected to be compensated for funds invested for longer periods. That means that, for most of the periods, y_t is an increasing function of maturity τ. Given that the factor loading $\left(\frac{1-e^{-\lambda\tau}}{\lambda\tau}\right)$ is decreasing with τ, then S_t will actually be negative most of the times, and an increase in S_t is to be interpreted as a flattening of the curve (with short-run interest rates becoming closer to long-run rates). This definition of the slope may seem counter-intuitive, but it is a convention in the yield curve literature [1].

To estimate these components, we considered a state-space representation of the model, with a measurement system of equations, in which one relates the yields of different maturities to the three factors:

$$\begin{bmatrix} y_t(\tau_1) \\ y_t(\tau_2) \\ \vdots \\ y_t(\tau_N) \end{bmatrix} = \begin{bmatrix} 1 & \left(\frac{1-e^{-\lambda\tau_1}}{\lambda\tau_1}\right) & \left(\frac{1-e^{-\lambda\tau_1}}{\lambda\tau_1} - e^{-\lambda\tau_1}\right) \\ 1 & \left(\frac{1-e^{-\lambda_2}}{\lambda\tau_2}\right) & \left(\frac{1-e^{-\lambda\tau_2}}{\lambda\tau_2} - e^{-\lambda\tau_2}\right) \\ \vdots & \vdots & \vdots \\ 1 & \left(\frac{1-e^{-\lambda\tau_N}}{\lambda\tau_N}\right) & \left(\frac{1-e^{-\lambda\tau_N}}{\lambda\tau_N} - e^{-\lambda\tau_N}\right) \end{bmatrix} \begin{bmatrix} L_t \\ S_t \\ \vdots \\ C_t \end{bmatrix} + \begin{bmatrix} \varepsilon_t(\tau_1) \\ \varepsilon_t(\tau_2) \\ \vdots \\ \varepsilon_t(\tau_N) \end{bmatrix}, \quad (3.2)$$

The factors are modelled as latent factors with the following transition system of equations:

$$\begin{bmatrix} L_t - \bar{L} \\ S_t - \bar{S} \\ C_t - \bar{C} \end{bmatrix} = \begin{bmatrix} a_{11} & a_{12} & a_{13} \\ a_{21} & a_{22} & a_{23} \\ a_{31} & a_{32} & a_{33} \end{bmatrix} \begin{bmatrix} L_{t-1} - \bar{L} \\ S_{t-1} - \bar{S} \\ C_{t-1} - \bar{C} \end{bmatrix} + \begin{bmatrix} \eta_{L,t} \\ \eta_{S,t} \\ \eta_{C,t} \end{bmatrix}, \quad (3.3)$$

where $t = 1, \ldots, T$ is the sample period, $\bar{L}$, $\bar{S}$ and $\bar{C}$ are estimates of the mean values of the three latent factors, and $\eta_{L,t}$, $\eta_{S,t}$ and $\eta_{C,t}$ are innovations to the autoregressive processes of the latent factors. We used the Kalman filter to estimate this set of equations (see Aguiar-Conraria et al. (2012b) for further details).

3.2.2 Data

The daily zero-coupon bond yields for Canada for various maturities - 3, 6, 9, 12, 15, 18, 21, 24, 30, 36, 48, 60, 72, 84, 96, 108 and 120 months - were extracted from the Bank of Canada's website[2]; these yields were converted to monthly yields by a simple average method. Our choice of macroeconomic variables includes the unemployment rate and CPI Inflation. A business cycle index complements the unemployment rate. While indexes such as GDP growth or output gap are notional measures of the business cycle, their availability in either quarterly or yearly basis makes them inappropriate for our purpose.

[1] Typically, the empirical measure for the slope is: $Slope_t = y_t(3) - y_t(120)$. Therefore, a negative value for the slope means that the interest rate is increasing with maturity

[2] Data downloaded from `http://www.bankofcanada.ca/rates/interest-rates/bond-yield-curves/` on September 22, 2016.

Capacity utilisation is another possible indicator, but its lack of availability for the entire sample period inhibits its consideration. Following Aguiar-Conraria and Soares (2011), we relied on the industrial production index's year-on-year growth data.

The transition of the Bank of Canada from its previous key monetary instrument - Bank Rate - to the current - Target for the Overnight Rate - on February 22, 1996 creates a bit of a challenge for our choice of the monetary policy instrument. Our sample covers the period, January 1986 - May 2016. While the data for the Target for the Overnight Rate is unavailable for the entire sample period, the data for Bank Rate is available. Despite this, the correlation between the two rates - Target for the Overnight Rate and Bank Rate - is very strong, and this strong association undergirds the choice of Bank Rate as our monetary policy instrument. The data for Bank Rate was extracted from the Bank of Canada's website while the data for CPI inflation and industrial production index was downloaded from Statistic Canada's website and IMF, respectively.

The estimated factors, which are plotted as time plots, and the corresponding wavelet power spectra are given in Fig. 3.1. In Fig. 3.2, we have the plots and the wavelet power spectra for macroeconomic activity indicators[3]. In the plots of wavelet power, the black conical line identifies the region, referred to as the cone of influence (COI), where edge effects - unavoidable artefacts appearing when computing the continuous wavelet transform for a finite series - are important; outside this line, the results should be interpreted with caution (see, e.g. Aguiar-Conraria and Soares (2014) for more details). The degree of variability is distinguished by a colour spectrum, ranging from dark blue (low variability) to red (high variability). The white lines in the power spectra indicate local maxima. The black contours signify 5% significance level, while the grey contours represent 1% significance level. These were computed using a known theoretical distribution for the power, assuming a flat spectrum as the null (see Torrence and Compo (1998) for more details).

[3]There is a well-known bias regarding the estimation of the wavelet coefficients at the lowest scale levels. For that reason, we implement the correction proposed by the Liu et al. (2007).

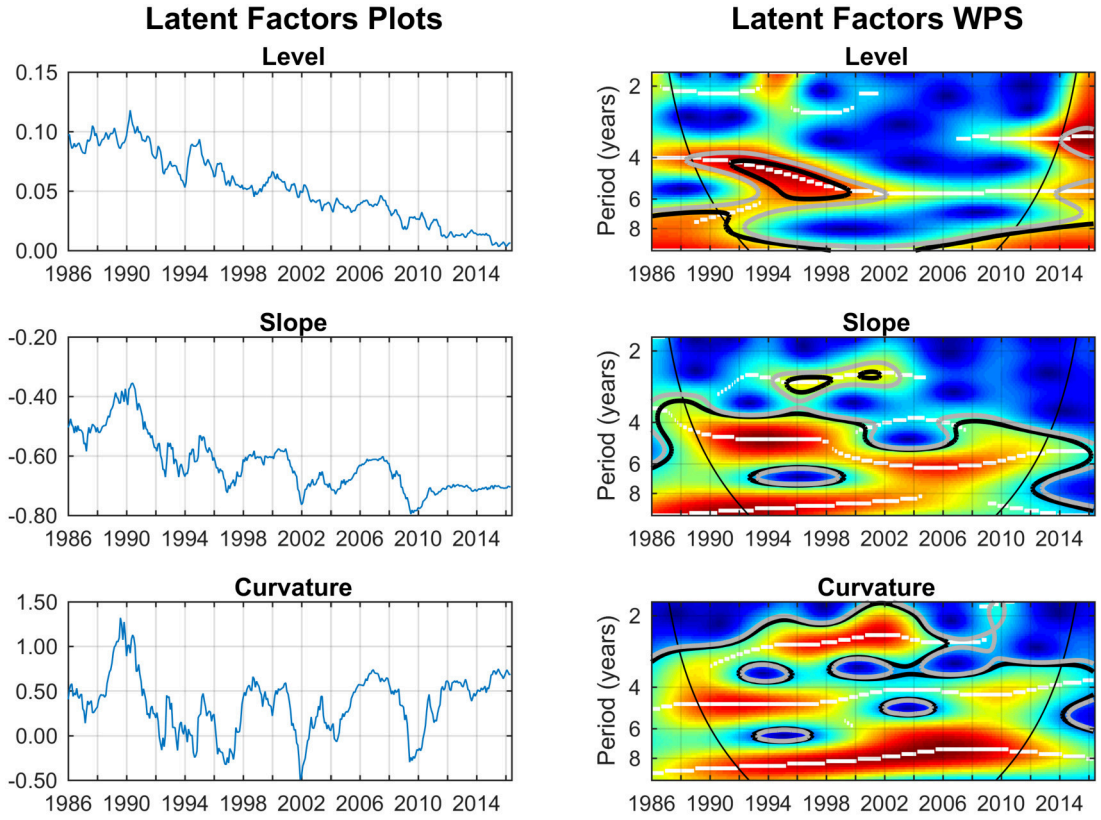

Figure 3.1: Level, slope and curvature of the Canadian yield curve (left panel) and corresponding wavelet power spectra (right panel). The colour code for power ranges from dark blue (low power) to red (high power); the black (grey) contours designate the 5% (1%) significance levels; the cone of influence, which indicates the region affected by edge effects, is delimited with a black conic line; the white lines show the local maxima of the wavelet power spectra.

For the level factor, one can see that the series was most volatile in the 1990s, in particular for cycles at the lower business cycle frequencies ($4 \sim 8$-year periodic cycle). To be more precise, the volatility is significant at 5% for the $4 \sim 8$-year frequency band between 1992 and 2000. If one considers 1% significance level, then there are almost no significant regions. In the case of the slope, if we focus on the $4 \sim 8$-year frequency band, the wavelet power spectrum is significant almost across the entire sample. At higher frequencies ($2 \sim 4$-year periodic cycle), it is also significant in the second half of the 1990s and early 2000s. For the curvature, the high volatility occurs at various frequency bands and across the entire sample, with several cycles occurring simultaneously, as we can observe a white stripe at a frequency slightly lower than 2 years, another slightly lower than 4, and the 8-year period cycle. One also observed this multiplicity of cycles for other factors, but they are not as evident as in the case of the curvature.

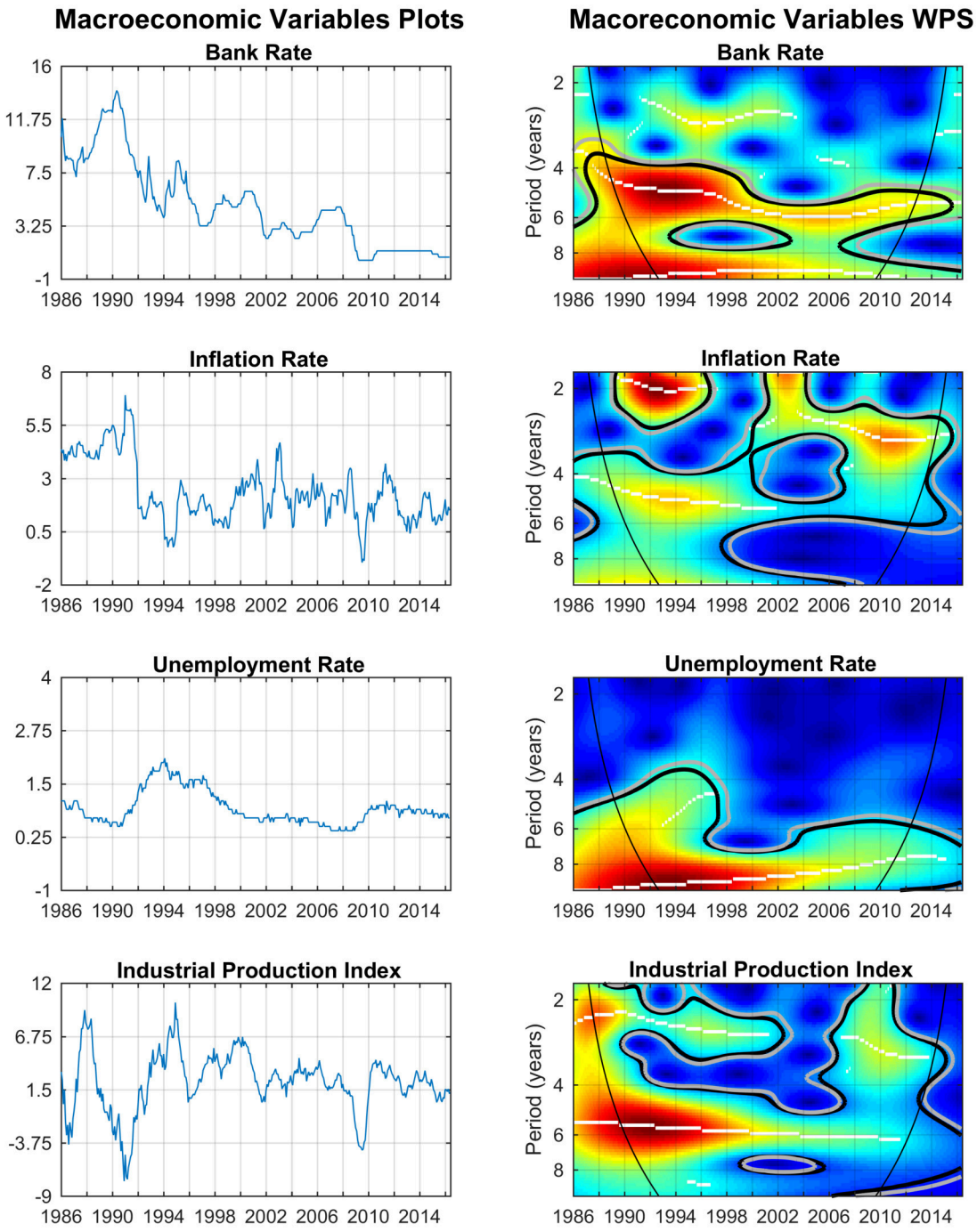

Figure 3.2: Macroeconomic variables (left panel) and corresponding wavelet power spectra (right panel). The colour code for power ranges from dark blue (low power) to red (high power); the black (grey) contours designate the 5% (1%) significance levels; the cone of influence, which indicates the region affected by edge effects, is delimited with a black conic line; the white lines show the local maxima of the wavelet power spectra.

It is interesting to note that the bank rate's power spectrum is very similar to the power spectrum of the slope (Fig. 3.1). The wavelet power spectrum is significant almost across the entire sample, especially in the $4 \sim 8$-year frequency band. In the case of the inflation rate, the wavelet power spectrum is quite heterogeneous. One can see a significant island at the 2-year frequency during the first half of the 1990s and later in

the early 2000s. In the first part of the sample, we can also observe some white stripes suggesting that there was an important cycle of $4 \sim 6$-year period, and approaching the end of the sample, 3-year cycle. For unemployment, the power spectrum is statistically significant for all the sample period for lower frequencies. Finally, for the industrial production index, one observed a persistent 6-year cycle, although much more important before than after 2000. At higher frequencies, the wavelet power spectrum is also quite high until the year 2000 and subsequently around the year 2010.

3.3 Empirical Results

In this section, we present the wavelet coherency and wavelet phase difference between each of the macroeconomic variables and each latent factor of the yield curve and discuss their main implications. Significance tests for the coherency were conducted based on Monte Carlo simulations: we fitted an ARMA model to each of the series and constructed new samples with the same basic properties. For each pair of series, we performed the exercise 5000 times and then extracted the critical values at 1% and 5% significance levels. As for the power, the 5% significance levels are indicated in the coherency plots with black contours and the 1% significance levels with grey contours. Because of the possibility of having false positives, in the sense of rejecting the null too often, (see Maraun et al. (2007)), we focussed on the regions which are significant at 1%. The colour code for the coherency ranges from dark blue (low coherency) to red (high coherency).

To facilitate the presentation, we displayed the mean phase difference for two frequency bands (cycles of period 2-4 years and cycles of 4-8 years). Because the phase differences are measured on a circular scale, the mean is computed as a circular mean (see Zar (1996) for details). These (mean) phase differences are indicated in the corresponding plots with a solid black line. Confidence intervals for the circular mean at each point in time were also computed - we used the formulas proposed by Zar (1996); see also Berens et al. (2009) - and the interpretation of the mean phase at each point is done considering values as extreme as the two endpoints of the corresponding interval. The limits of the confidence intervals for the mean phases are indicated in the pictures with red dashed lines.

3.3.1 Bank Rate and the Yield Curve

Figure 3.3 shows the level of coherency between the bank rate and latent factors (left panel), as well as the phase differences between them (right panel). The most striking feature of Figure 3.3 is the high coherency, across most of the times and frequencies, between the bank rate and the slope of the yield curve. Similarly, the phase difference

is basically zero, implying that these two variables are well synchronised. Much more synchronised than, for example, the level of the yield curve and the bank rate, which are very synchronised only between the early 1990s and early 2000s in the $4 \sim 6$-year frequency band.

This implies that when the Bank of Canada changes the bank rate, its main impact is felt at short-term interest rates. If it were felt simultaneously for all maturities, then one would expect much larger statistically significant coherent regions between the bank rate and the yield curve level. For example, an increase in the bank rate will lead to a stronger increase in shorter maturities, resulting in the flattening of the yield curve. The relation between the curvature and the bank rate is also interesting, as it has a very large region of strong coherency, although this disappears completely after 2010. The phase difference, slightly negative in several periods of significant coherency tells us that the curvature served as a leading indicator of the bank rate, meaning that changes in the curvature preceded changes in the bank rate in the same direction.

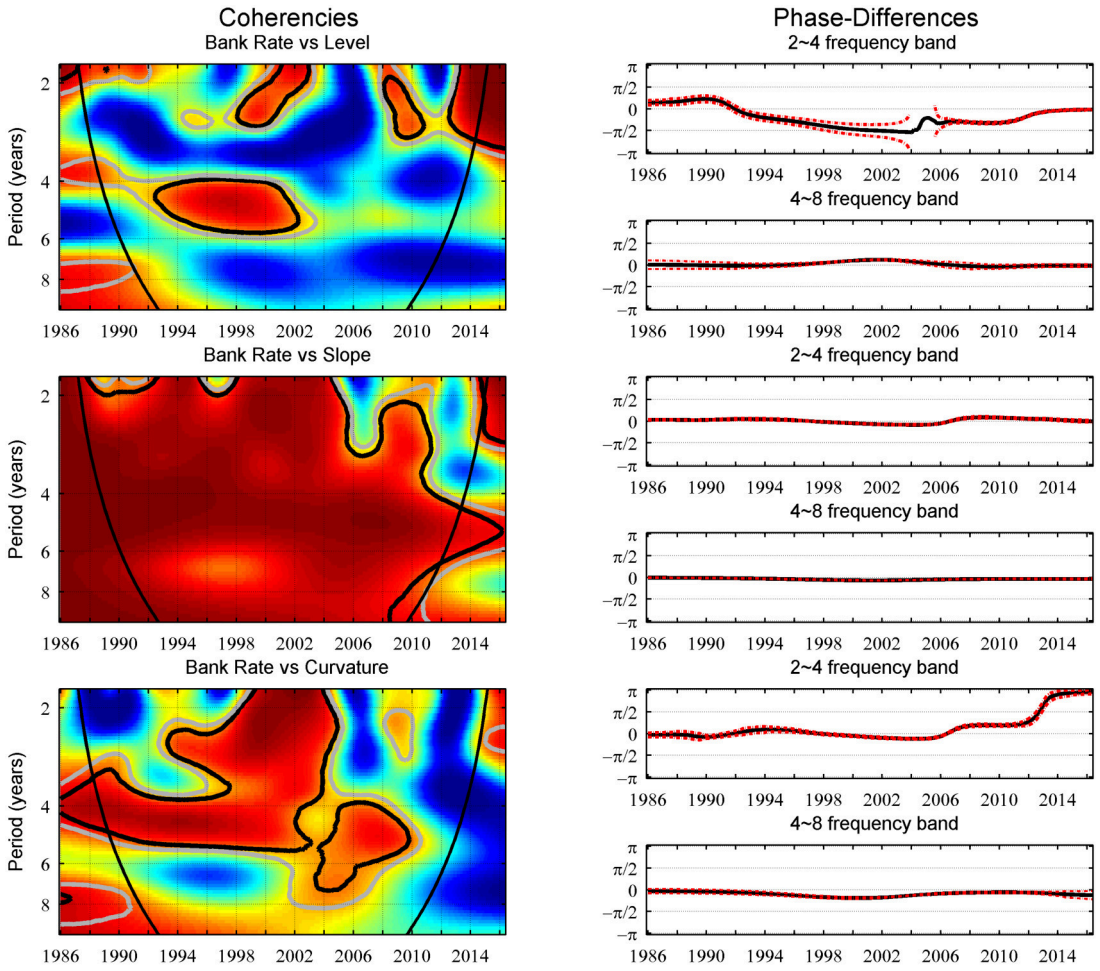

Figure 3.3: Bank rate and latent factors of the yield curve: coherency (left panel) and phase differences (right panel). The colour code for coherency ranges from dark blue (low coherency) to red (high coherency); the black (grey) contours designate the 5% (1%); the cone of influence, which indicates the region affected by edge effects, is delimited with a black conic line. Phase differences are indicated with a solid black line and confidence intervals with a red dashed line.

3.3.2 Inflation Rate and the Yield Curve

Figure 3.4 presents the wavelet coherency and the phase difference between the inflation rate and the yield curve. At $4 \sim 6$-year frequencies, and until the early 2000s, there is high coherence between the yield curve factors and inflation. The phase difference (in areas where coherency is statistically significant), lies consistently between $-\frac{\pi}{2}$ and zero, implying that the variables are in-phase with the yield curve factor leading. If one takes into consideration our results for the bank rate, these results suggest that the Bank of Canada had a very proactive monetary policy. Changes in the slope of the yield curve (and the level between the early 1990s and early 2000s) anticipated changes in the same direction of inflation. This suggests that when the central bank predicts a rise (or fall) in inflation, it would immediately adjust its monetary policy and increase (or decrease) the

bank rate. After that, regions of high coherency are no longer dominant, and sometimes the phase difference is between zero and $\frac{\pi}{2}$, suggesting that monetary policy became more reactive.

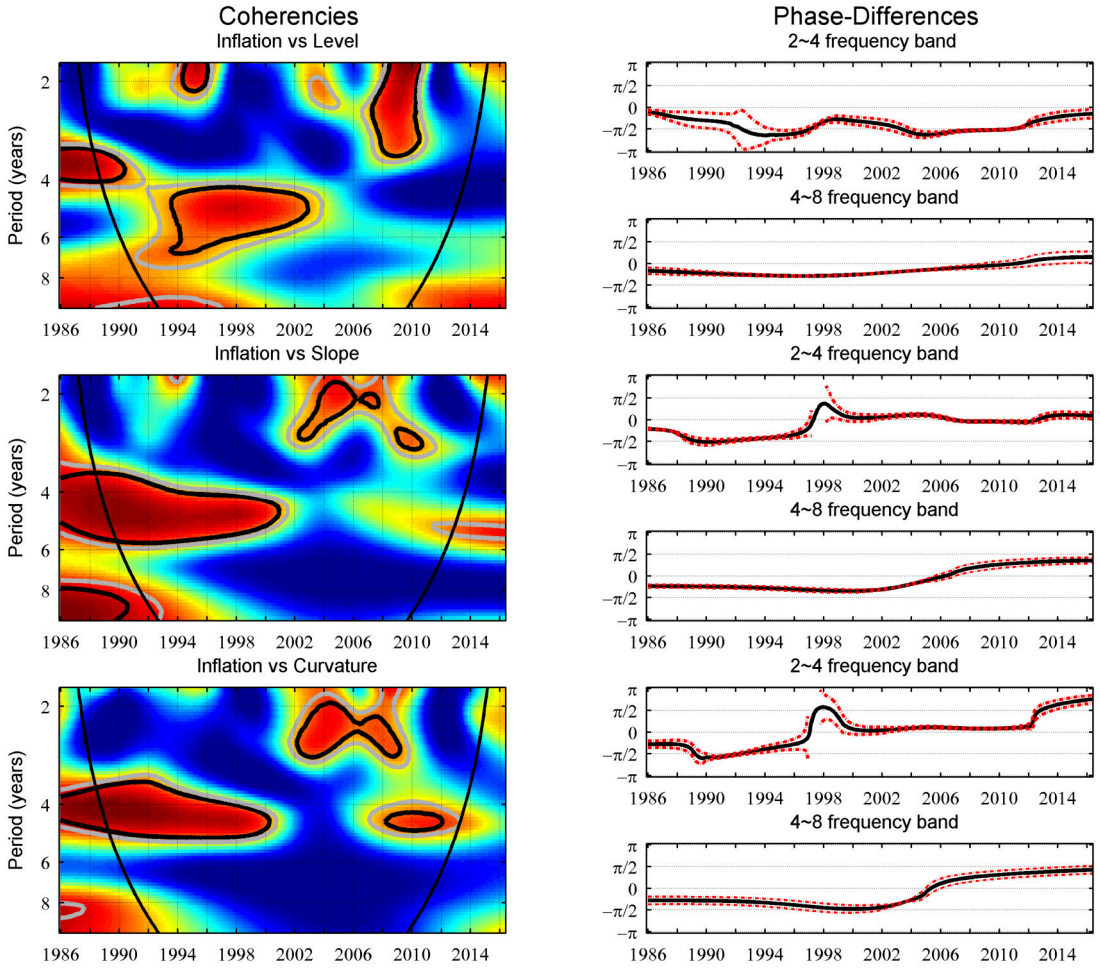

Figure 3.4: Inflation rate and latent factors of the yield curve: coherency (left panel) and phase differences (right panel). The colour code for coherency ranges from dark blue (low coherency) to red (high coherency); the black (grey) contours designate the 5% (1%); the cone of influence, which indicates the region affected by edge effects, is delimited with a black conic line. Phase differences are indicated with a solid black line and confidence intervals with a red dashed line.

3.3.3 Unemployment Rate and the Yield Curve

Regarding the unemployment rate, one can observe from Figure 3.5 that the unemployment rate seems to be largely independent of the level factor of the yield curve. This perspective somewhat changes once one looks at the relationship with the slope and the curvature, where some regions of statistical significant coherencies can be observed. While this is valid for medium and low frequencies until 2010 in the case of the slope, the curvature reflected this in the second half of the sample. In this scenario, the phase difference indicates an anti-phase relation with the yield curve factor leading. This implies that

both the slope and the curvature are viewed as leading indicators for the long-run evolution of unemployment. Note that the wavelet power spectrum for the unemployment rate (Figure 3.2) suggests that the cyclical behaviour of unemployment occurs mainly at the lower frequencies, adding significance to this result.

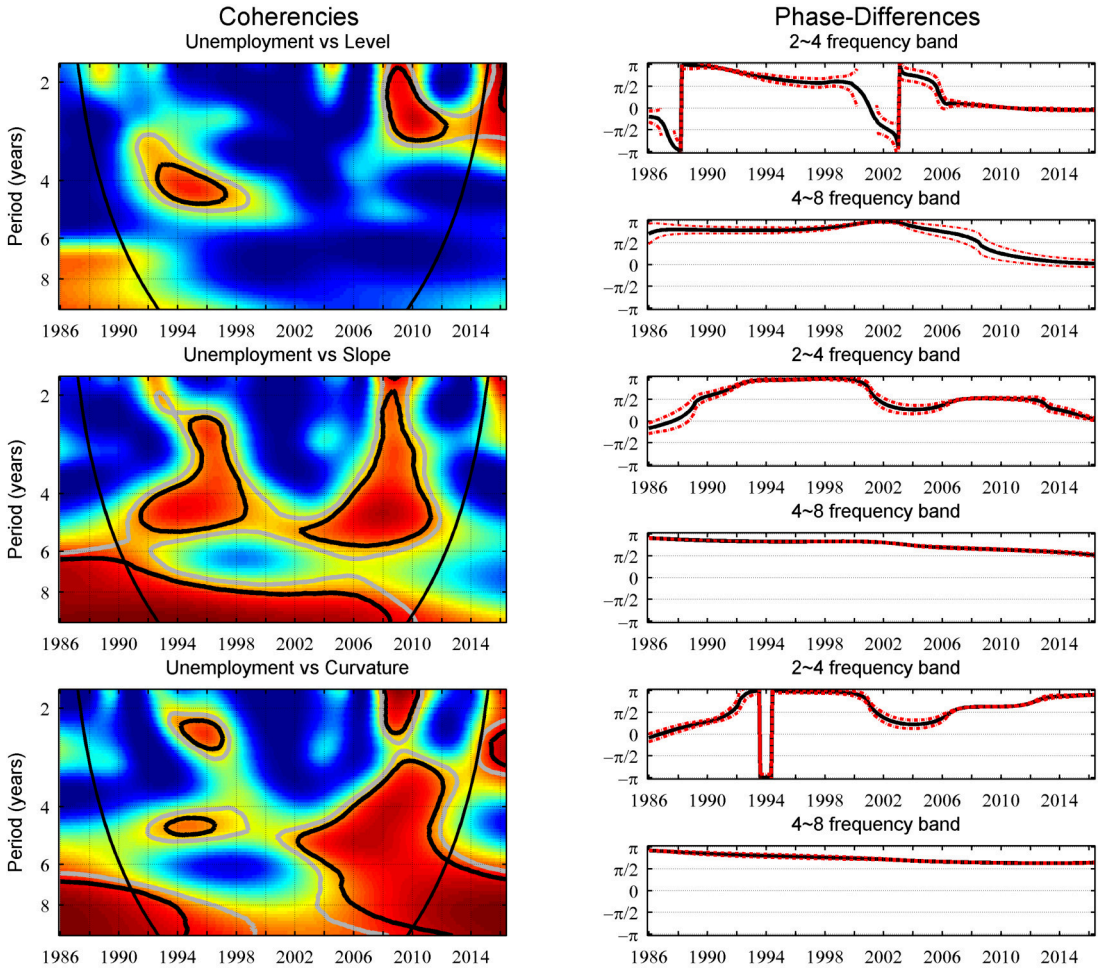

Figure 3.5: Unemployment rate and latent factors of the yield curve: coherency (left panel) and phase differences (right panel). The colour code for coherency ranges from dark blue (low coherency) to red (high coherency); the black (grey) contours designate the 5%(1%); the cone of influence, which indicates the region affected by edge effects, is delimited with a black conic line. Phase differences are indicated with a solid black line and the confidence intervals with a red dashed line

3.3.4 Industrial Production and the Yield Curve

We estimated the coherency and phase difference between the industrial production and each of the yield curve factors. In Figure 3.6, we observed several islands of statistically significant coherency. In the case of the level, the most important region of statistical significance occurred in the $4 \sim 8$-year frequency band between the second half of the 1990s and first half of the 2000s (it is the only 5% significant region that included a 1% sub-region). Interestingly, the phase difference is between $\frac{\pi}{2}$ and π, suggesting an

anti-phase relation with the level of the yield curve leading. In the case of the slope and the curvature, there are several statistically significant islands, mainly in the $2 \sim 4$-year frequency band, but also in the $4 \sim 6$-years band (towards the end of the sample). For these cases, the phase difference is between $\frac{\pi}{2}$ and π, before 1998, and between 0 and $\frac{\pi}{2}$ after that. Therefore, these variables are out of phase until 1998, with the yield curve leading, and in-phase after that, with the yield curve factors lagging.

Recall that Figure 3.3 showed that the slope and curvature are closely related to the variable representing the monetary policy, the bank rate. Similarly, note that the level of the yield curve and the bank rate were synchronised between the mid-1990s and early 2000s in the $4 \sim 6$-year frequency band. In that sense, if we interpret the yield curve factors as proxies for the monetary policy, the fact that, in Figure 3.6, the phase difference in the second half of the sample indicated that the industrial production index is in-phase and leading the slope and the curvature, suggesting that the Bank of Canada's monetary policy is lagging the evolution of the industrial production. Given the mandate of the Bank of Canada (2% inflation target), this interpretation is consistent only if the industrial production index is a leading indicator of inflation in the second half of the sample. In the first half, given the anti-phase relation of industrial production and the yield curve factors, one would also expect the same relation between industrial production and inflation.

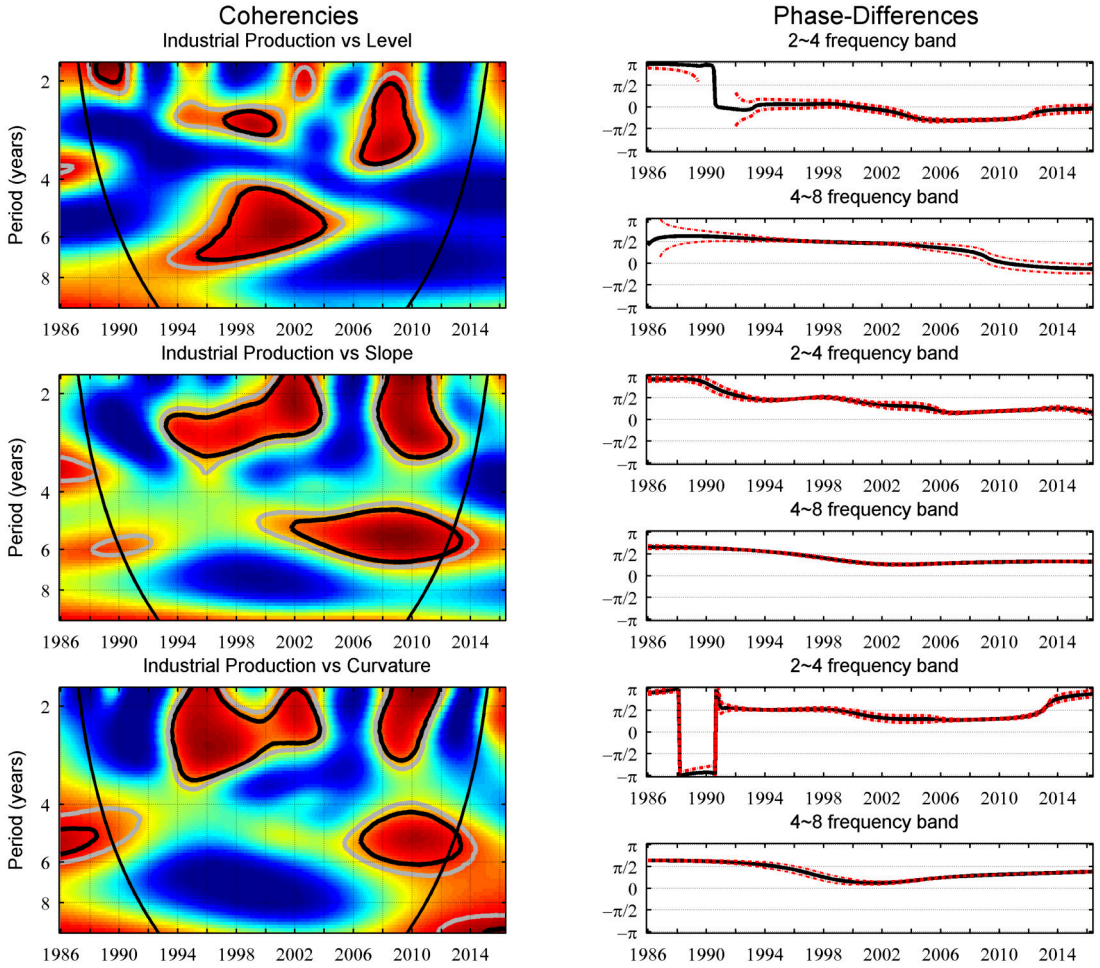

Figure 3.6: Industrial production index and latent factors of the yield curve: coherency (left panel) and phase differences (right panel). The colour code for coherency ranges from dark blue (low coherency) to red (high coherency); the black (grey) contours designate the 5% (1%); the cone of influence, which indicates the region affected by edge effects, is delimited with a black conic line. Phase differences are indicated with a solid black line and the confidence intervals with a red dashed line

With the aim of testing the predictions in the last paragraphs, we estimated the coherency and phase difference between industrial production and the inflation rate. In Figure 3.7, we observed two main regions of high coherency: at lower frequencies in the 1990s (only at 5%), and at higher frequencies towards the last third of the sample (in this case also at 1% significance). As expected, the phase difference associated with the first region is between $\frac{\pi}{2}$ and π, implying an anti-phase relation with inflation leading. The associated phase difference is between 0 and $\frac{\pi}{2}$ at higher frequencies (between 2 and 4 year periods).

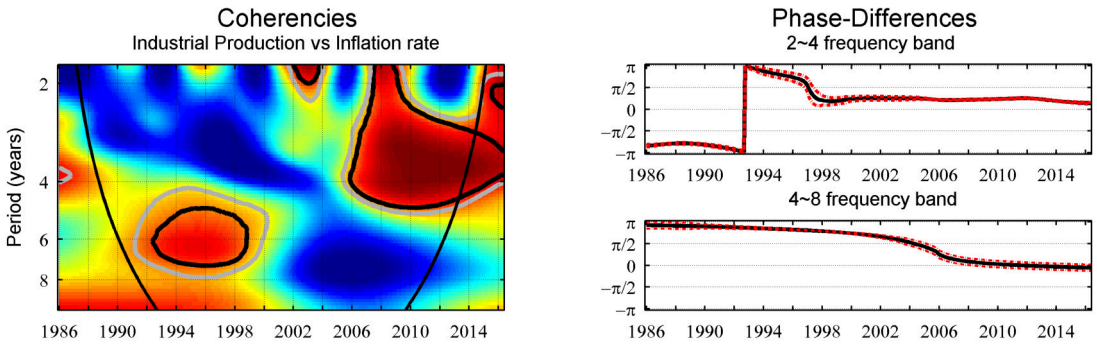

Figure 3.7: Industrial production index and the inflation: coherency (left panel) and phase differences (right panel). The colour code for coherency ranges from dark blue (low coherency) to red (high coherency); the black (grey) contours designate the 5% (1%); the cone of influence, which indicates the region affected by edge effects, is delimited with a black conic line. Phase differences are indicated with a solid black line and the confidence intervals with a red dashed line.

3.4 Conclusion

In this paper, we used wavelets to study the yield curve and some key macroeconomic indicators, namely the inflation rate, the unemployment rate, the industrial production index and the bank rate (an important monetary policy instrument). With the continuous wavelet transform, we used two important tools - the wavelet coherency and the wavelet phase-difference - to study the relationship between each of the three-dimensional latent factors of the yield curve and the four macroeconomic indicators.

We reached several conclusions. One, the monetary policy variable - the bank rate - does not have a uniform impact across time horizons. Changes in the bank rate affect mainly short-run interest rates. If one believes that the main driver for economic activity is the long-run interest rate (instead of the short-run rate), then it is not difficult to argue that monetary policy is quite ineffective. Two, we concluded that concerning the inflation rate, the Bank of Canada is very proactive, in the sense of trying to act on inflation before it happens. This reiterates the information on its website: "monetary policy is always forward-looking and the policy rate setting is based on the Bank's judgement of where inflation is likely to be in the future, not what it is today[4]".

Three, regarding the unemployment rate, we found that both the slope and the curvature are leading indicators for the long-run evolution of unemployment. Finally, our results suggest that the industrial production index leads the yield curve factors and not the other way. Therefore, nominal interest rates do not seem to be a very important determinant of economic activity. The main difference between our results and the results of a similar study obtained by Aguiar-Conraria et al. (2012b) for the USA is that

[4] http://www.bankofcanada.ca/core-functions/monetary-policy/

Fed interest rates impacted on the three factors of the US yield curve, showing that monetary policy impacted both short-term and long-run interest rates. It is also interesting to note that the relationships between the yield curve and real macroeconomic activity are stronger in the USA than in Canada.

Our results are not directly comparable with previous studies on the Canadian yield curve because wavelet analysis provides a fundamentally different way of looking at the data. However, it is fair to say that our conclusions align with the existing studies on the Canadian yield curve in certain aspects. For instance, our findings on the proactiveness of the Canadian monetary policy are consistent with Lange (2013) that highlighted the forward-looking, monetary policy stance on future inflation. Similarly, our result on the link between latent factors and monetary policy rate partly aligns with the existing studies. For example, our result on the high coherency between the monetary policy rate and the slope factor shares some semblance with the findings of Lange (2013) on the large positive links between the monetary policy rate and the slope factor (although our results are not as strong as Lange's regarding level factor).

To be more precise, our findings showed an in-phase relation between the monetary policy rate and the level factor, which is consistent with Lange (2013), but there appears to be a moderate coherency between them in the early 1990s and 2000s. Our results regarding the relationship between the yield curve and real activity differed from Lange's, who found a very strong relation between them; even stronger than in the USA.

Chapter 4

The Performance of OECD's Composite Leading Indicator

Abstract

This paper evaluated the performance of OECD's composite leading indicator using the Continuous Wavelet Transform. We used two wavelet tools - wavelet coherency and wavelet phase-difference - to assess the co-movement between the composite leading indicator and three macroeconomic variables – industrial production index, unemployment rate and real GDP growth – at different timescales. We also explored the lead-lag relation between each pair of variables across time and frequency. We concluded that OECD's composite leading indicator is a useful leading indicator of the Industrial Production Index. Although it can be suited for forecasting the unemployment rate, it exhibits poor performance regarding GDP growth.

Keywords*: Composite Leading Indicator; Business Cycle Indicator; Wavelet Power Spectrum; Wavelet Coherency; Wavelet Phase-Difference*

4.1 Introduction

The business cycle fluctuation and the counteracting effects of fiscal and monetary policies are of utmost importance to policymakers and market participants. With the enormous influence of the business cycle fluctuation on the dynamics of macroeconomic variables, renewed efforts are geared towards exploring common characteristics of business cycles. Such exploration is vital as decisions on monetary policy affect the economy with long and varying lags, and it is essential to have an educated judgement about the prevailing economic conditions and outlook (Fichtner et al., 2009).

Although a single data series, such as real GDP, is often used as a proxy for the business cycle, Boehm and Summers (1999) argued that such a decision is fraught with two problems: the shift in GDP's turning points over time and varying experience of at least one cycle in the real GDP which often does not correspond to growth cycle chronology at any chosen period. These dual problems broaden the search for suitable business cycle indicators. In particular, these problems galvanise interest in a system of indicators that could provide an advanced signal on the economy.

Diebold and Rudebusch (1991) noted that the prospect of such indicators is fascinating to economic agents suffering through cycles of prosperity and depression. This system of indicators is expected to offer advanced information that could assist policymakers in gauging the market expectation, anticipating macroeconomic conditions, and fashioning policy tools to counteract any adverse economic effects. Consequently, such information influences other key macroeconomic variables, such as expected future inflation, expected term interest rates, and the shape of the yield curve.

The possibility of such advanced signal has resulted in a proliferation of leading indicators. While the notion of leading indicators first came to light in 1919, it has evolved from its application to the business cycle to its utilisation for inflation (Bikker and Kennedy, 1999). Granger (2001) opined that the proliferation of leading indicators signifies their policy significance and operational relevance in economic statistics. However, the index of leading indicators is criticised for being 'measurement without theory' (Koopmans, 1947).

Similarly, Neftci (1979) argued that the property to lead does not imply a causal relationship between two variables, as the link is not based on the choices of the decision-makers. While Fichtner et al. (2009) explored the performance of leading indicators, he found a declining ability of country-specific leading indicators. Specifically, they are unable to address the significant structural changes occasioned by the rapid advances in globalisation, which has deepened the international financial and

trade linkages. These limitations stimulated the search for other leading indicators, particularly composite leading indicators.

A composite leading indicator (CLI) is constructed from various series, notably producer's price changes, hours worked, profitability changes, stock prices, building approvals, and price-cost ratios containing information on the anticipatory movement of the coincident index (Boehm and Summers, 1999). The selected series has the following properties: a significant economic indicator; statistically adequate; not subjected to substantial revisions; reveals a consistent relationship with peaks and troughs of the business cycle; conforms to the general cyclical movements between peaks and troughs; not dominated by erratic, irregular, and non-cyclical influences; promptly and regularly available at various periods, such as monthly or quarterly (see Boehm (1987) and Zarnowitz and Boschan (1975) for details).

While the OECD's CLI is revered, it seeks to improve on the drawbacks of country-specific leading indicators. Although the OECD's CLI is evolving with periodic reviews, it is designed to serve as a bellwether of fluctuations in economic activity around its potential long-term level. It is constructed to predict cycles in a proxy series for economic activity. The fluctuation in the economic activity is measured as the variance of the economic output relative to its long-term potential. The OECD's system of leading indicator utilises univariate analysis to estimate individual trends and cycles for each component series, while the resultant de-trended series is aggregated to obtain a composite indicator (Nilsson et al., 2006).

The indicator is constructed from a limited economic time series with cyclical fluctuation similar to the business cycle and tends to turn earlier than the business cycle. OECD previously adopted monthly series of industrial production index, but has migrated to a quarterly GDP-based business cycle target in April 2012 (Fulop and Gyomai, 2012). While such a switch decreases the timeliness of the referenced series by approximately two months, it enhances the clarity and interpretation of the composite leading indicators. The CLIs are under constant scrutiny and drawing both criticism and accolades. For instance, Diebold and Rudebusch (1991) found a considerable decline in the real-time forecasting performance of CLIs.

Similarly, Artis et al. (1995) did not consider OECD's CLI as a wholesome predictor of the business cycle's turning points. Emerson and Hendry (1996) also argued that the weighting scheme utilised in the aggregated series before scaled CLI is suboptimal. Additionally, McGuckin et al. (2007) argued that CLIs are fraught with the inability to deploy current information in their procedure. Such information lag adds to its uncertainty and forecasting errors. Furthermore, Estrella and Mishkin (1998) opined that the CLI is a bad predictor of industry activity in real-time and advocated for its

replacement with financial variables, such as bond and stock prices, and interest rate spread. Additionally, Fichtner et al. (2009) found a decline in the predictive power of CLIs for many countries.

However, Weale (1996) established that OECD's CLIs have a longer lead over those of the UK's leading indicators. Similarly, CLIs eliminated individual variable's noise and reduced the risk of false signals (Fichtner et al., 2009). Also, Zarnowitz and Braun (1990) posited that incorporating the CLI in a vector-autoregressive model reduces in-sample residual variance. Equally, several attempts have been made to explore the bivariate and multivariate causality between CLIs and business cycle indicators. Koch and Rasche (1988) and Alan (1981) found strong evidence of the CLI linearly predicting the industrial production, even with conditional production values and in- and out-of-sample forecast.

Despite a lack of consensus on the performance of CLIs, a survey of extant literature reveals the dominance of time-domain analysis. This is somewhat puzzling considering the heterogeneity of economic agents and their varying operations at different timescales. Similarly, the impact of low- and high-frequency shocks on any economic phenomenon varies. Furthermore, the dominance of time-domain analysis in the extant literature places the unit root at the core of a fundamental issue relating to business cycles. While the first-difference filter is used to remove non-stationary components from a time series, Baxter (1994) established that the filter has an unintended attribute of removing most cyclical variations in the series. This limits the effectiveness of time-domain analysis in the exploration of business cycle fluctuation.

Additionally, the assessment of business cycle dynamics and the construction of CLIs are more complicated than what the traditional time-domain analysis can explain. We pursued an alternative approach to capture this complexity. We utilised wavelet analysis to explore the forecasting power of OECD's CLI at different business-cycle frequencies and separates its performance between shorter ($2 \sim 4$ years) and longer-run ($4 \sim 8$ years) business-cycle periods. The wavelet analysis is chosen based on its ability to provide insight into economic phenomena, operating contemporaneously at multiple timescales (Gallegati and Semmler, 2014). It offers utility to decompose economic dynamics into multiple timescales and analyse them at each scale.

Although business cycles are low-frequency phenomena and difficult to identify in the data (Dalsgaard et al., 2002), the wavelet approach decomposes the CLI series, regardless of their frequencies, into both time and frequency domains and offer an atomistic view of its hidden dynamics. We relied on two continuous wavelet tools - wavelet coherency and phase-difference - to assess the performance of OECD's CLI. For sixteen countries, we estimated the wavelet coherency between their respective CLIs and

three macroeconomic variables: real GDP growth, unemployment and Industrial Production Index.

4.2 Data and Exploratory Analysis

We used quarterly data of four indicators for 16 countries: Australia, Canada, Denmark, Finland, France, Germany, Ireland, Italy, Japan, Mexico, New Zealand, Portugal, Spain, Sweden, UK and the US. While the data covers the period 1991Q1 to 2019Q2, sampled countries are spread across different regions and have varying economy sizes with heterogeneous cyclical fluctuations. The data used comprises OECD's CLIs and three business cycle indicators. With CLIs providing early signals about changes in economic activity, we considered either the real GDP or industrial production index as a measure of real economic activity. However, dual problems associated with the real GDP (see Boehm and Summers, 1999) nullifies its consideration and places industrial production index as our chosen variable.

Similarly, we considered the GDP growth. Its choice is premised on the business cycle focusing on alternating periods of expansion and contraction of macroeconomic activity, regarding deviations of the GDP growth from an appropriately defined trend growth rate (Altavilla, 2004). Furthermore, we complemented the industrial production index with the unemployment rate. While all the data were obtained from the OECD's website, we extracted the quarterly data of industrial production index, unemployment rate and GDP growth. However, monthly data of CLI was obtained and converted to quarterly data by a simple average method.

Table 4.1 presents the descriptive statistics of our data. The industrial production index indicated higher volatility compared to other variables, as shown by the standard deviation of all the variables. While the CLI is negatively skewed for all countries, GDP growth is equally negatively skewed for all countries except for Australia, Denmark and Ireland. Additionally, the industrial production index is negatively skewed for all countries except for Germany, Ireland, Japan, Portugal and Spain. However, the unemployment rate is positively skewed except for Germany, Italy, Japan and Sweden. The skewness and kurtosis measures for all variables indicated evidence against normal distribution (skewness $\neq 0$ and kurtosis $\neq 3$). The GDP growth is leptokurtic for most countries, as their kurtosis is greater than 3. However, Australia, Denmark, New Zealand and Portugal have kurtosis values that are less than 3.

Table 4.1: Descriptive Statistics

	Australia	Canada	Denmark	Finland	France	Germany	Ireland	Italy	Japan	Mexico	New Zealand	Portugal	Spain	Sweden	UK	USA
CLI																
Mean	99.9966	99.8237	99.9877	100.164	99.8566	100.026	99.9197	99.9969	99.9113	99.8839	100.0914	99.9145	99.979	99.5668	100.053	99.8176
Std. Dev	0.6771	0.9195	0.9800	2.0957	0.9435	1.4277	2.6368	1.0946	1.1075	1.8695	1.1898	1.4341	1.2179	1.4021	1.1965	1.1882
Skewness	-0.1295	-0.8349	-0.4816	-0.5278	-0.0932	-1.0142	0.4831	-0.4403	-0.6438	-2.4806	-1.2943	-0.5529	-0.3794	-0.4067	-1.4856	-1.467
Kurtosis	1.7024	1.6647	0.3429	-0.2003	-0.1731	2.1476	0.7827	0.1831	0.2499	11.4314	2.5750	0.0255	-0.3589	0.5204	4.3131	3.6958
Ind. Prod																
Mean	98.8168	98.1442	93.3865	94.9109	102.438	86.5671	52.2529	114.897	103.309	83.3252	95.0251	113.616	111.935	99.1115	99.8143	91.1336
Std. Dev	8.7547	12.3951	11.9914	19.6869	7.6437	12.0617	26.6914	10.683	6.1059	13.9334	9.9812	12.7628	13.4628	15.2131	3.6100	13.2974
Skewness	-0.6835	-0.6292	-0.3717	-0.6848	-0.1065	0.0905	0.3603	-0.1416	0.0567	-0.2565	-0.5145	0.0954	0.3372	-0.7117	-0.8287	-1.0512
Kurtosis	-0.3941	-0.4509	-0.5753	-0.4699	-0.9767	-1.4291	-0.5483	-1.4271	1.8955	-0.7493	-0.4307	-1.4764	-1.3206	0.0641	-0.0346	-0.1126
GDP Growth																
Mean	0.7621	0.5838	0.4441	0.4553	0.3881	0.3578	1.3780	0.1814	0.2446	0.6017	0.7058	0.3391	0.4880	0.5477	0.5104	0.6301
Std. Dev	0.5830	0.6171	0.9444	1.2200	0.4584	0.8511	2.9684	0.6835	0.9171	1.2608	0.7436	0.8382	0.7063	0.8839	0.5606	0.5744
Skewness	0.3628	-1.3548	0.1479	-1.6326	-1.2655	-1.5854	3.7047	-1.0017	-1.6074	-2.5222	-0.6400	-0.8054	-1.7411	-1.0898	-1.706	-1.2373
Kurtosis	2.3031	4.2465	0.9113	9.0085	4.2524	10.4037	26.2604	4.2715	7.4915	10.9187	2.1641	1.1830	3.8510	5.4941	6.3828	4.6750
Unemployment																
Mean	6.5978	7.8287	6.0468	9.7076	9.2997	7.2997	9.4310	9.6722	3.8371	3.9219	6.0246	8.8129	16.6287	7.2895	6.4772	6.8886
Std. Dev	1.8699	1.5681	1.5530	2.8537	1.4135	2.1496	4.2772	1.7927	0.9799	1.0262	1.9220	3.2127	5.1917	1.4836	1.7785	1.6094
Skewness	0.9987	0.8925	0.3548	1.2210	0.4383	-0.2728	0.1990	-0.2488	-0.1705	0.6803	1.0712	0.8963	0.0099	-0.4774	0.5003	0.8907
Kurtosis	-0.0617	-0.0994	-0.6822	0.6608	-0.8419	-0.963	-1.594	-1.0487	-1.0709	-0.0996	0.6707	0.0182	-1.097	0.91107	-0.8947	-0.0307

Figure 4.1 shows OECD's CLIs for all countries in our sample (left panel) and their corresponding wavelet power spectra (right panel). The power intensity is differentiated by a colour spectrum, evolving from low power (dark blue) to high power (red). In the power-spectra plots, the white lines signify the local maxima. On the other hand, the black and grey contours denote the 5% and 10% significance levels, respectively[1]. The black conical line in the power plots identifies the cone of influence (COI), which is the regions where unavoidable border distortions occur while computing the continuous wavelet transform of a finite series. The results must be interpreted cautiously beyond this region (see, e.g. Aguiar-Conraria and Soares (2014) for more details).

As expected, CLIs function at business cycle frequencies for most countries, with most of the volatility concentrated in the $4 \sim 8$-year frequency band. However, Mexico and New Zealand are notable exceptions, as they experienced volatility within the $2 \sim 4$-year frequency band. While Mexico exhibited strong coherency between 1994 and 1995 due to the Tequila crisis, the crisis was caused by the currency devaluation and evolved into both currency and banking crisis. On the other hand, New Zealand exhibited strong coherency in the 1990s due to the adoption of inflation targeting policy regime during that period. While other countries experienced high volatility in the 1990s, Germany, Ireland and Portugal did not exhibit high volatility during this period. However, the UK was somewhat immune from any volatility during this period.

All countries, except Japan, experienced high volatility during the global financial crisis of 2007/2008. While Japan seemed immune from the global financial crisis of 2007, it was less resistant to the Asian financial crisis that occurred ten years earlier. The non-synchronisation of Japan's power spectrum with other countries is contrary to expectation in an era dominated by increased global economic integration. However, this is partly explained by the lack of co-movement in the international business cycle. Specifically, the synchronisation level of Japan's business cycle with other G7 countries has been declining since the 1960s, with the business cycle fluctuation in Japan mostly explained by domestic shocks rather than by global shocks (Stock and Watson, 2005).

[1]The computation is done with a known theoretical distribution for the power and the null is assumed to be a flat spectrum; see Torrence and Compo (1998) for details.

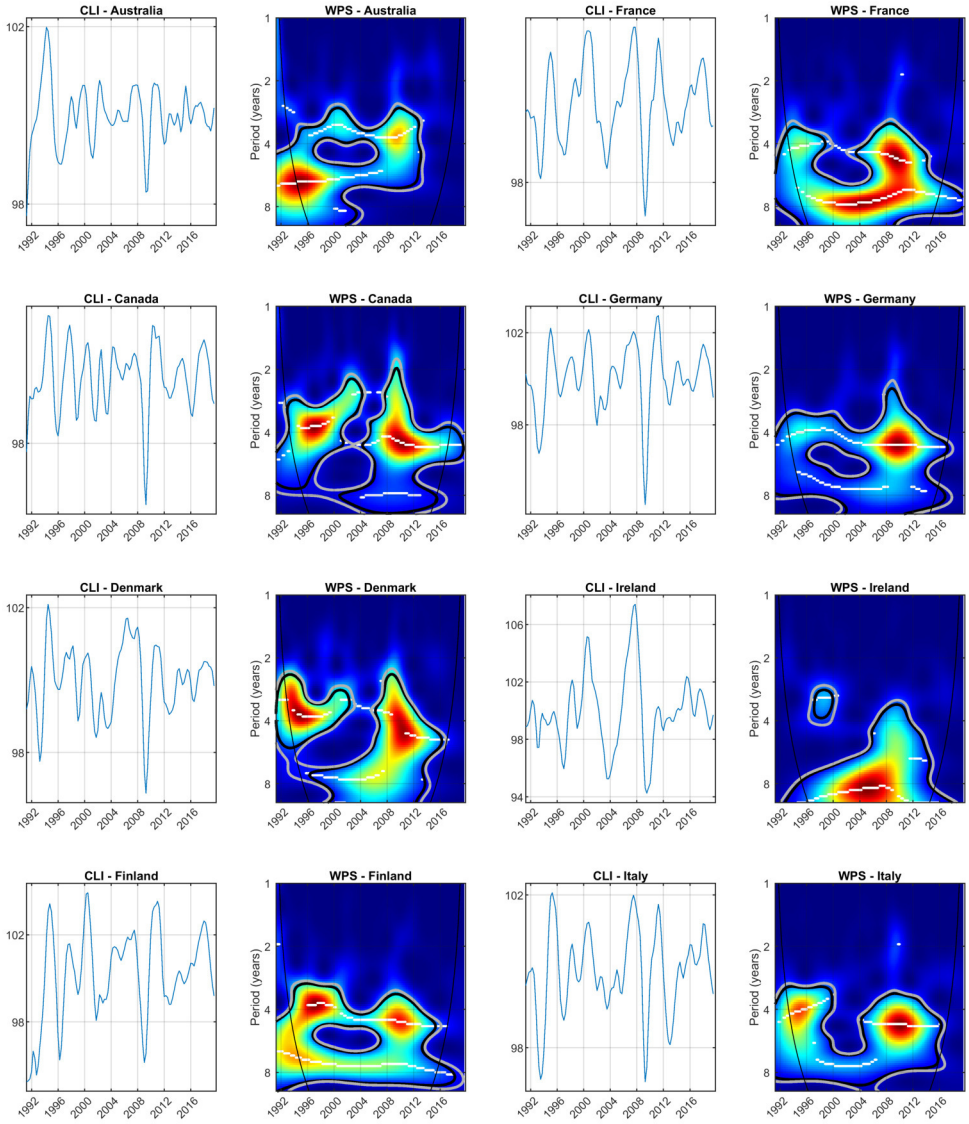
CLI - Australia
WPS - Australia
CLI - France
WPS - France
CLI - Canada
WPS - Canada
CLI - Germany
WPS - Germany
CLI - Denmark
WPS - Denmark
CLI - Ireland
WPS - Ireland
CLI - Finland
WPS - Finland
CLI - Italy
WPS - Italy
Period (years)
1992
1996
2000
2004
2008
2012
2016

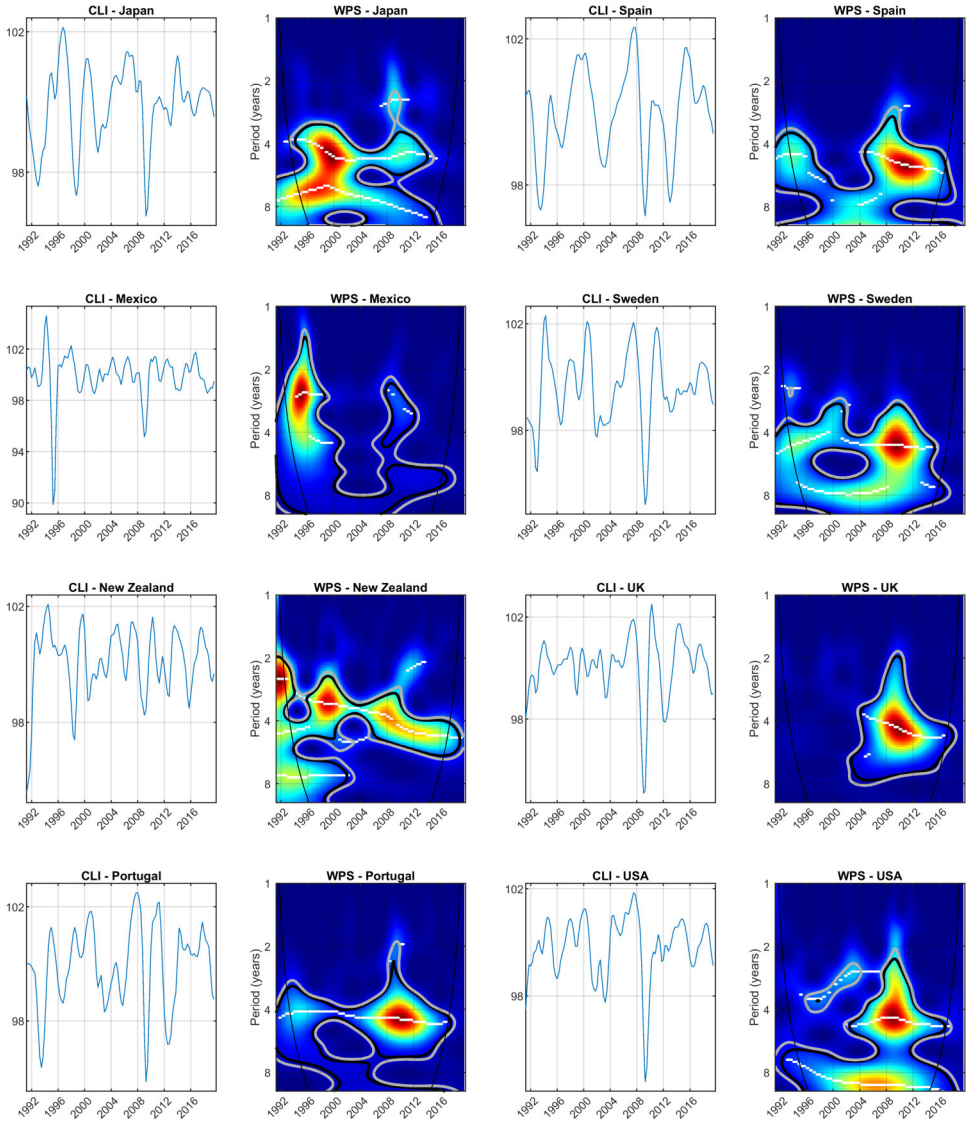

Figure 4.1: Composite Leading Indicators and their Wavelet Power Spectra. The colour spectrum depicts the extent of variability and evolves from low power (blue colour) to high power (red colour). The white lines within the power spectra represent the local maxima. The black contour denotes 5%, while the grey contour represents the 10% significant level. The cone of influence, represented by the black conic line, indicates that the results are unreliable outside this line and should be interpreted with special care.

4.3 Results

The interpretation of our findings follows the standard approach used in related studies (see Aguiar-Conraria et al., 2012b), and this is summarised as follows: we explored the

statistically significant coherency regions for the time-frequency domain. These regions indicate a significant co-movement between two series at a specified timescale[2]. We analysed the phase differences for statistically significant regions to determine the direction of the co-movement, as well as identified the leading and lagging variables. We analysed the following pairs of variables – Industrial Production Index vs CLI, Unemployment vs CLI, and GDP growth vs CLI - sequentially. This procedure evaluated the predictive performance of the CLI on the evolution of each macroeconomic variable and identified business-cycle frequencies such prediction occurs.

4.3.1 Industrial Production and Composite Leading Indicator

Figure 4.2 shows the wavelet coherency between the industrial production index and CLI (left panel), and their corresponding phase-difference computed for two frequency bands - $2 \sim 4$ years and $4 \sim 8$ years (right panel). The interpretation of the colours and contours in the coherency plots are identical to the power spectral. We observed a region of high coherency for all the countries between 2002 and 2012, with the region generally covering both frequency bands. Similarly, we observed regions of high coherency for some countries during the 1990s, but these regions occurred mainly in the $2 \sim 4$-year frequency band. However, Ireland and New Zealand are notable exceptions.

While New Zealand exhibited high coherency during the period of global financial crisis within the $2 \sim 4$-year frequency band, CLI led the industrial production index in a phase relation. For Ireland, there is a weak coherency between these two variables. While such weak coherency corroborates the established weak link between industrial production and the CLI for smaller open economies, such as Ireland (Fichtner et al., 2009), our study identified Portugal as an exception to such a claim with a strong coherency between the two variables.

Overall, the CLI led the industrial production index in a phase relation for all the sixteen countries at both frequency bands. This is evident with the phase-difference consistently lying between $-\frac{\pi}{2}$ and 0. The result is consistent with the OECD's claim that CLIs have the property of moving in the same direction with the business cycle. Similarly, such relationship conforms with the expected co-movement of the CLI and a pro-cyclical industrial production index. However, some countries did not conform to this relationship within a certain period. For instance, industrial production led the CLI within the $4 \sim 8$-year frequency band between 2004 and 2010 for Australia and Finland.

[2]Significant regions are found by using Monte-Carlo simulations: an ARMA model is fitted for each series, and new samples were constructed with the same basic properties. For each pair of series, we simulate the process 5000 times and then extract the critical values at 5% and 10% significance levels.

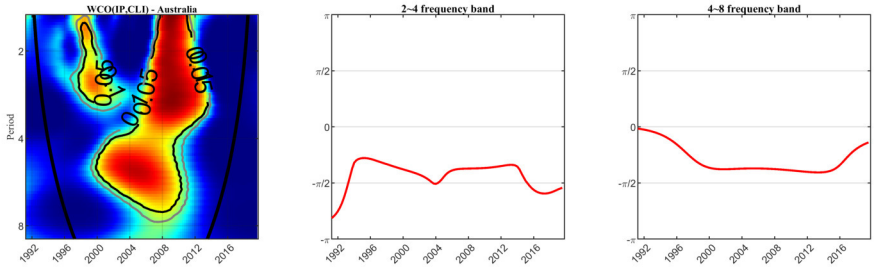
WCO(IP,CLI) - Australia
2~4 frequency band
4~8 frequency band
Period
2
4
8
0.05
0.1
1992
1996
2000
2004
2008
2012
2016
π
π/2
0
-π/2
-π

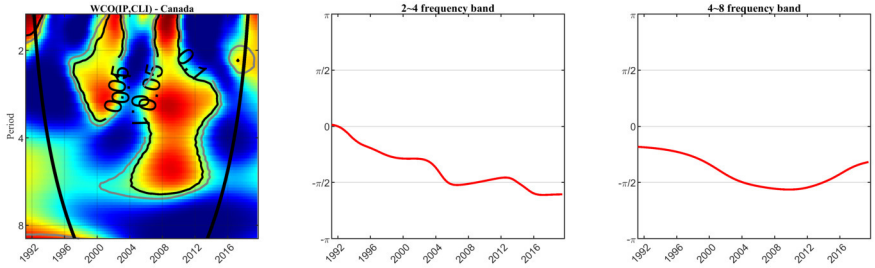
WCO(IP,CLI) - Canada
2~4 frequency band
4~8 frequency band
Period
2
4
8
0.05
0.1
1992
1996
2000
2004
2008
2012
2016
π
π/2
0
-π/2
-π

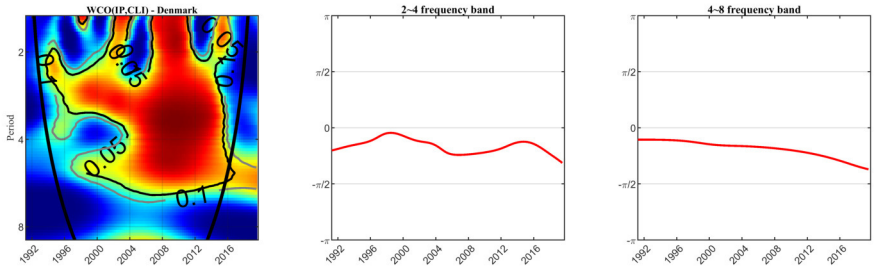
WCO(IP,CLI) - Denmark
2~4 frequency band
4~8 frequency band
Period
2
4
8
0.05
0.1
1992
1996
2000
2004
2008
2012
2016
π
π/2
0
-π/2
-π

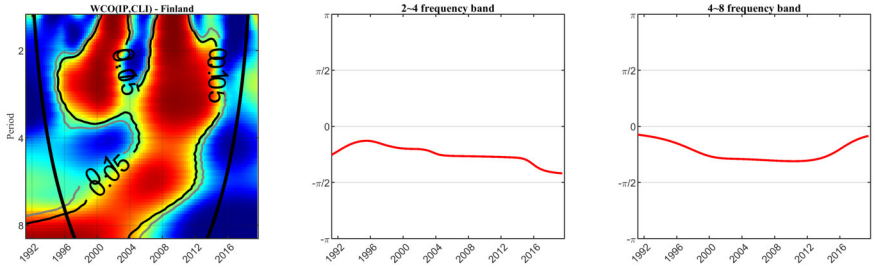
WCO(IP,CLI) - Finland
2~4 frequency band
4~8 frequency band
Period
2
4
8
0.05
1992
1996
2000
2004
2008
2012
2016
π
π/2
0
-π/2
-π

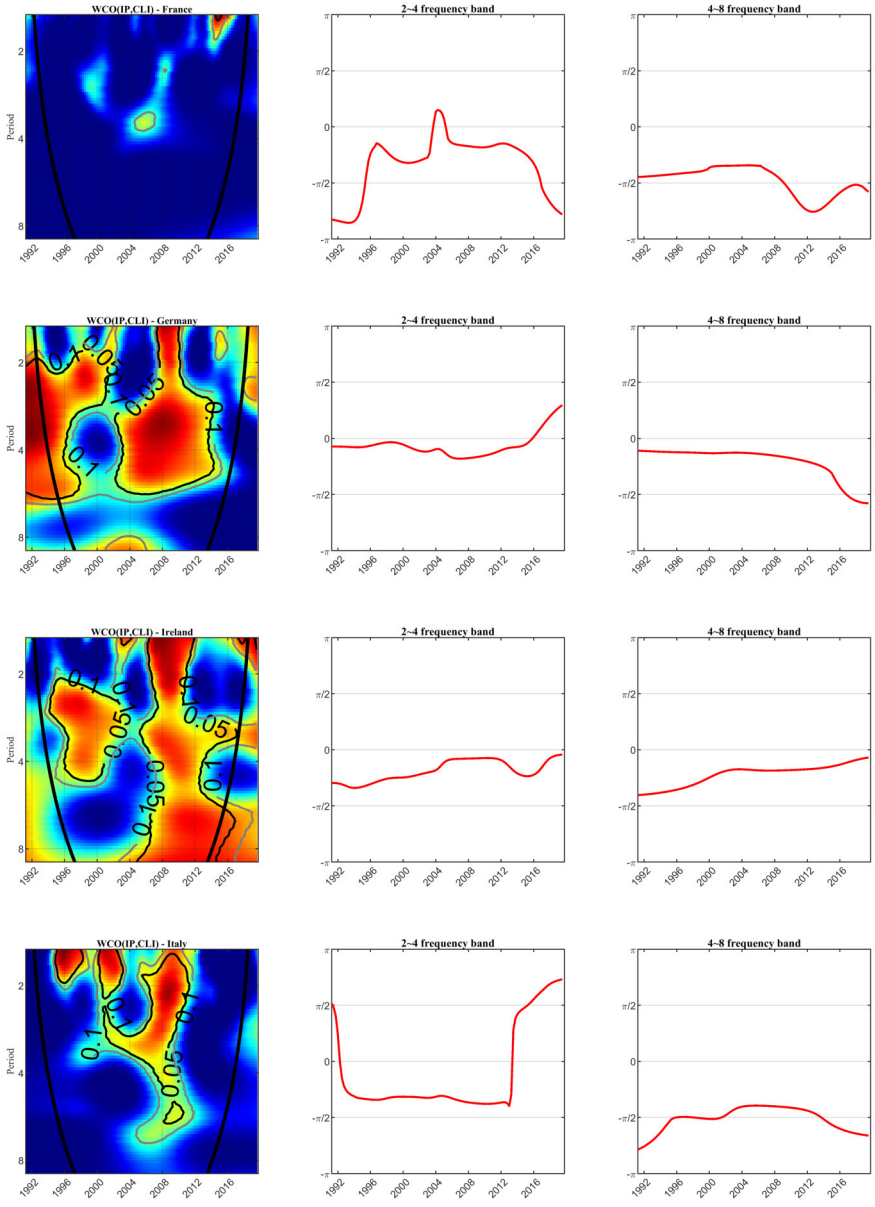
WCO(IP,CLI) - France
2~4 frequency band
4~8 frequency band
WCO(IP,CLI) - Germany
2~4 frequency band
4~8 frequency band
WCO(IP,CLI) - Ireland
2~4 frequency band
4~8 frequency band
WCO(IP,CLI) - Italy
2~4 frequency band
4~8 frequency band
Period
1992
1996
2000
2004
2008
2012
2016

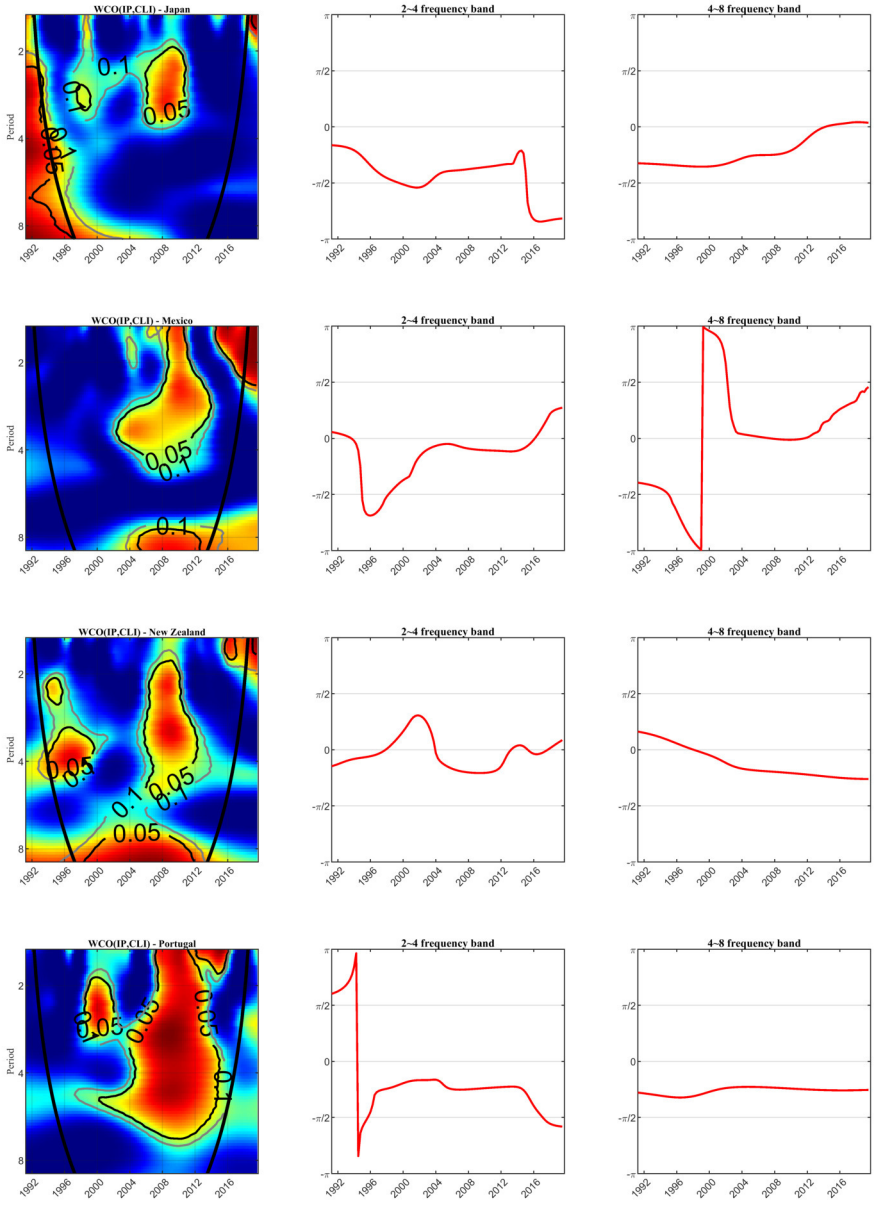
WCO(IP,CLI) - Japan
2~4 frequency band
4~8 frequency band
WCO(IP,CLI) - Mexico
2~4 frequency band
4~8 frequency band
WCO(IP,CLI) - New Zealand
2~4 frequency band
4~8 frequency band
WCO(IP,CLI) - Portugal
2~4 frequency band
4~8 frequency band
Period
1992
1996
2000
2004
2008
2012
2016

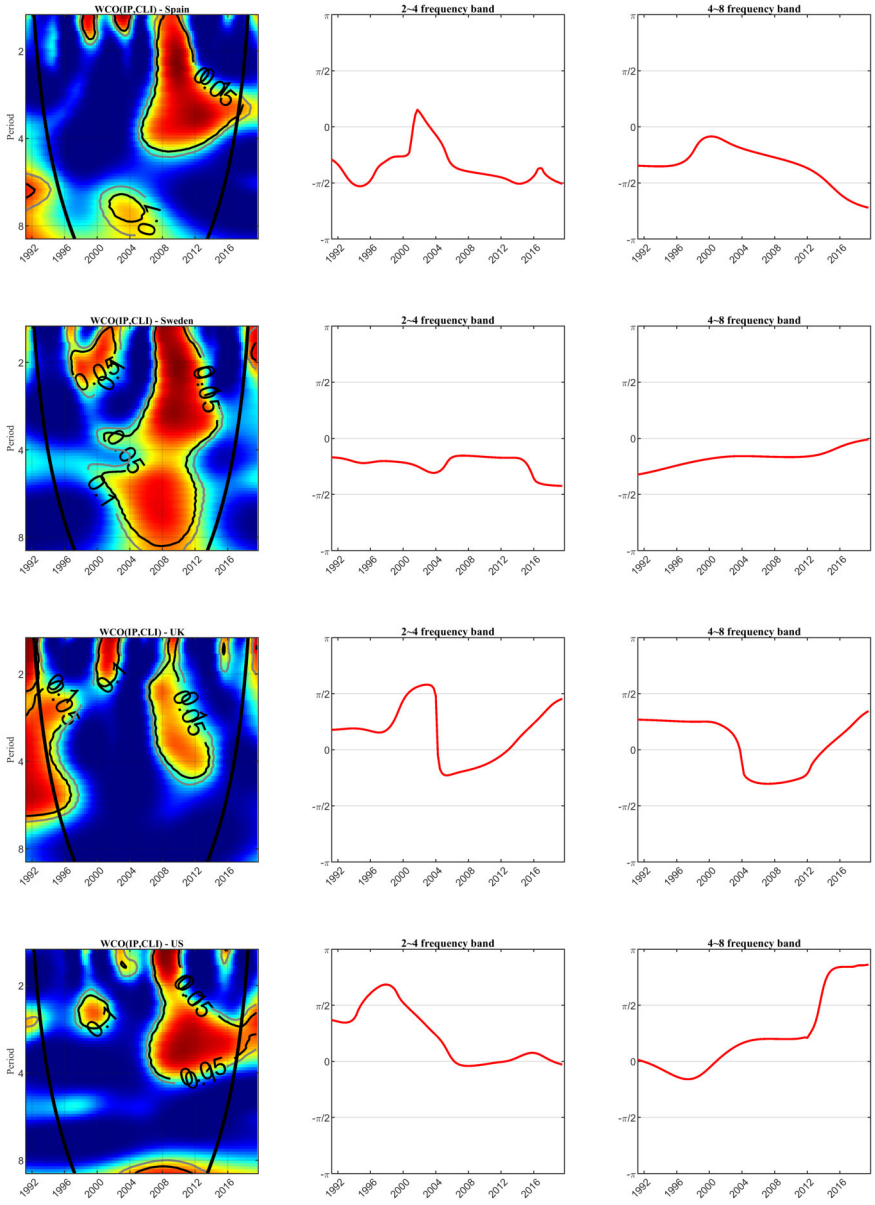

Figure 4.2: On the left - the wavelet coherency between the Industrial Production Index and CLI. The black and the grey contours denote the 5% and 10% significance level, respectively. The colour codes for coherency evolve from blue (low coherency) to red (high coherency). While the low coherency has a value close to zero, high coherency has a value closed to one. At the centre and on the right - phase-differences between IP and CLI for the frequency bands of $2 \sim 4$ and $4 \sim 8$ years, respectively.

4.3.2 Unemployment and Composite Leading Indicator

Figure 4.3 shows the wavelet coherency between the unemployment rate and CLIs, as well as their respective phase-differences. The results showed that the forecasting power of the CLI on the employment rate is somewhat mixed. For instance, regions of high coherency are scarce for Germany, Ireland, Italy, Mexico, New Zealand, Portugal and the UK. However, there are large statistically significant coherency regions for other countries, especially for France, Spain, and the US. It should be noted that the phase difference of the statistically significant coherency lies in any of these two quadrants: 0 and $\frac{\pi}{2}$ or $\frac{\pi}{2}$ and π.

However, for most countries, the coherency lies between $\frac{\pi}{2}$ and π, implying that CLI led in an anti-phase relation as expected. However, this mostly reflected the CLI performance after the global financial crisis. Prior to this period, CLI often lagged the unemployment rate. For France, Ireland, Japan, Portugal, Spain and the USA, CLI led throughout the statistically coherent regions for both frequency bands: $2 \sim 4$ years and $4 \sim 8$ years. Overall, the forecasting dynamics of CLI on the unemployment rate is reasonable, but it is not as effective as its performance with the industrial production index, especially before the global financial crisis.

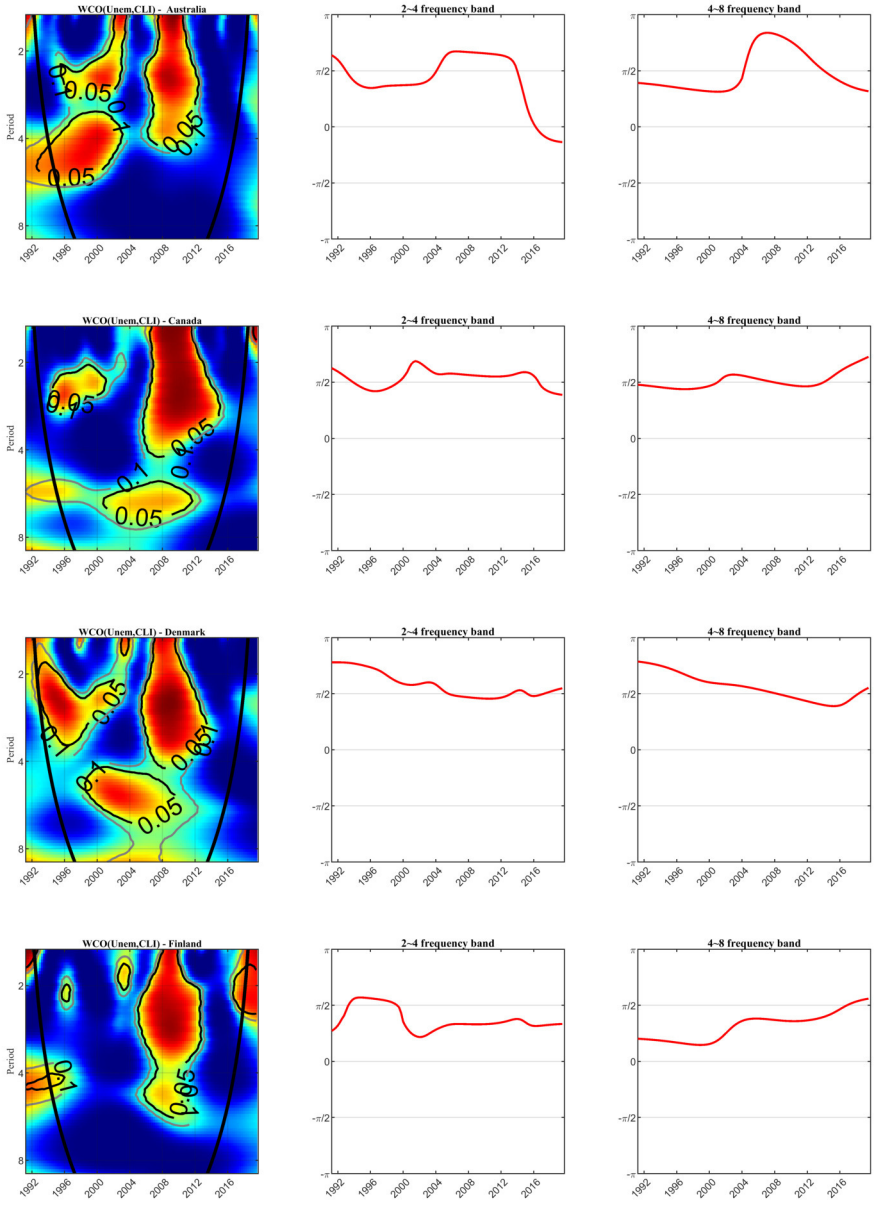
WCO(Unem,CLI) - Australia
2~4 frequency band
4~8 frequency band
WCO(Unem,CLI) - Canada
2~4 frequency band
4~8 frequency band
WCO(Unem,CLI) - Denmark
2~4 frequency band
4~8 frequency band
WCO(Unem,CLI) - Finland
2~4 frequency band
4~8 frequency band
Period
1992
1996
2000
2004
2008
2012
2016

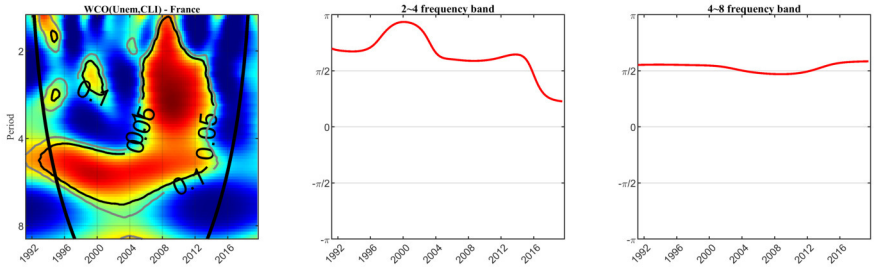
WCO(Unem,CLI) - France
2~4 frequency band
4~8 frequency band
Period
2
4
8
0.1
0.05
1992
1996
2000
2004
2008
2012
2016
π
π/2
0
-π/2
-π

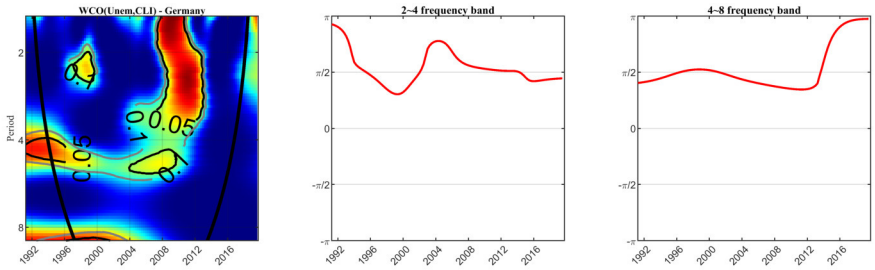
WCO(Unem,CLI) - Germany
2~4 frequency band
4~8 frequency band
Period
2
4
8
0.1
0.05
1992
1996
2000
2004
2008
2012
2016
π
π/2
0
-π/2
-π

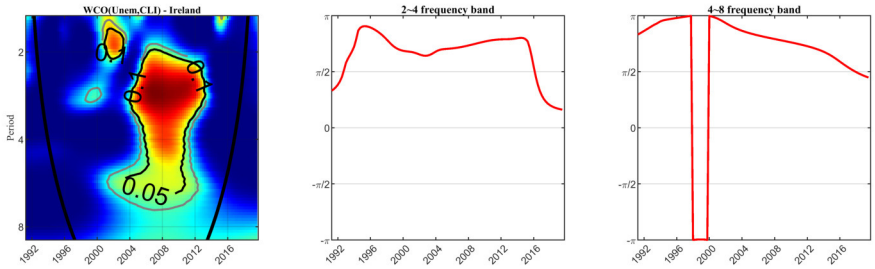
WCO(Unem,CLI) - Ireland
2~4 frequency band
4~8 frequency band
Period
2
4
8
0.1
0.05
1992
1996
2000
2004
2008
2012
2016
π
π/2
0
-π/2
-π

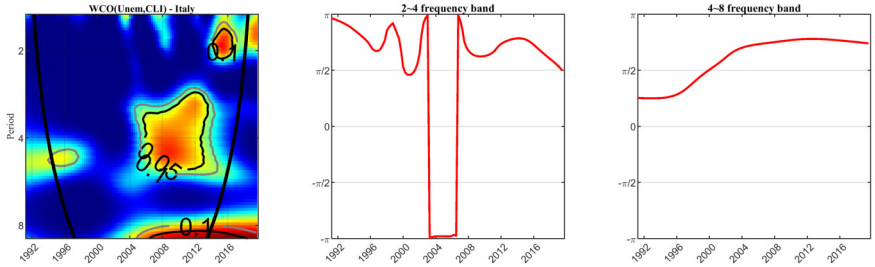
WCO(Unem,CLI) - Italy
2~4 frequency band
4~8 frequency band
Period
2
4
8
0.1
0.05
1992
1996
2000
2004
2008
2012
2016
π
π/2
0
-π/2
-π

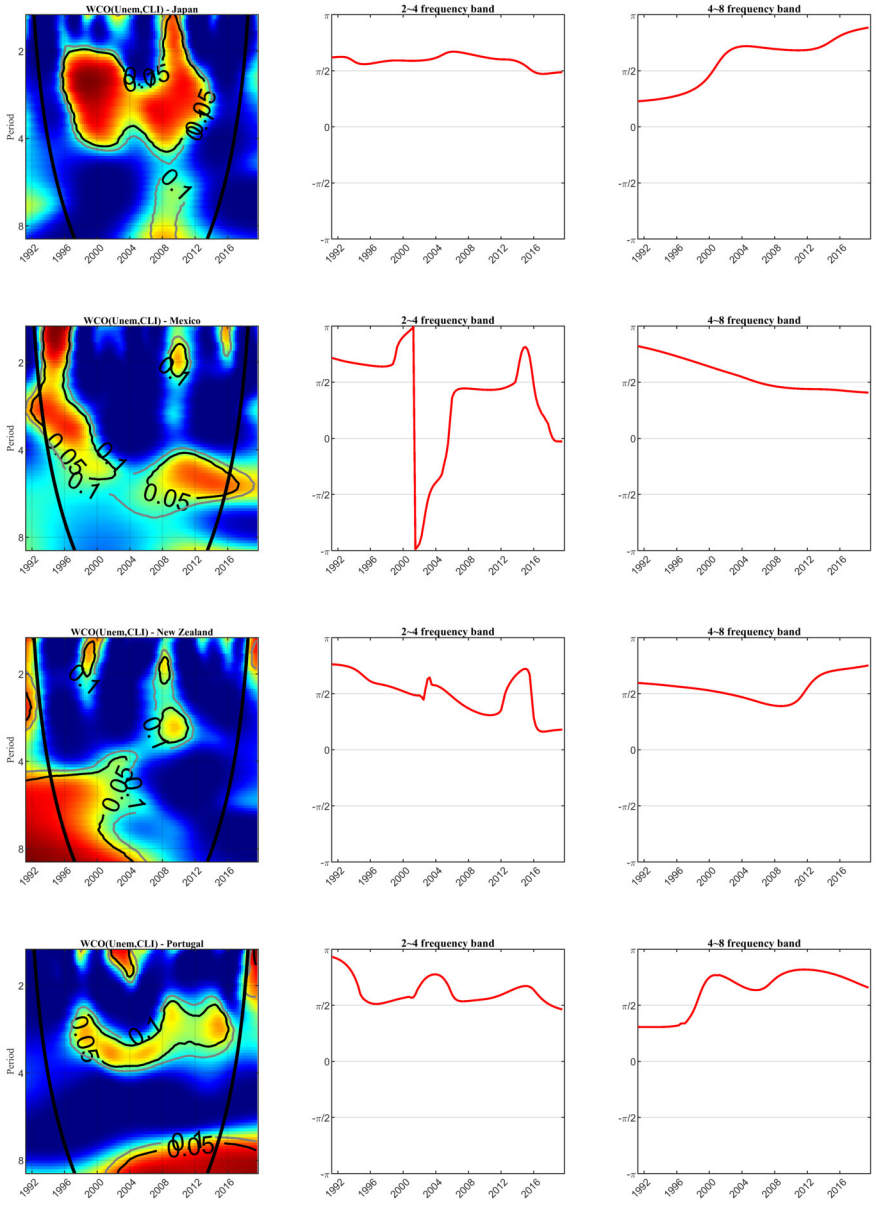
WCO(Unem,CLI) - Japan
2~4 frequency band
4~8 frequency band
WCO(Unem,CLI) - Mexico
2~4 frequency band
4~8 frequency band
WCO(Unem,CLI) - New Zealand
2~4 frequency band
4~8 frequency band
WCO(Unem,CLI) - Portugal
2~4 frequency band
4~8 frequency band
Period
1992
1996
2000
2004
2008
2012
2016

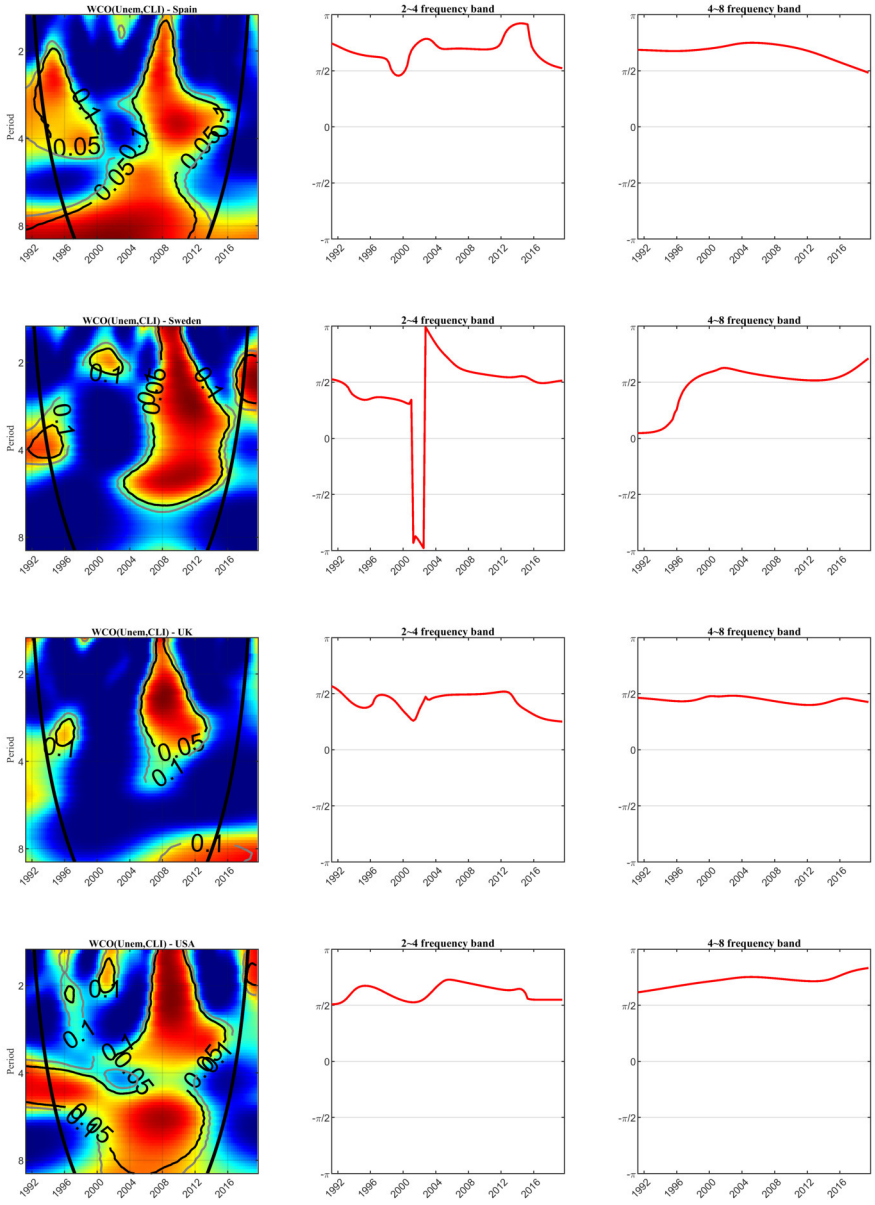

Figure 4.3: On the left - the wavelet coherency between the Unemployment Rate and CLI. The black and the grey contours denote the 5% and 10% significance level, respectively. The colour codes for coherency evolve from blue (low coherency) to red (high coherency). While the low coherency has a value close to zero, high coherency has a value closed to one. At the centre and on the right - phase-differences between Unemployment and CLI for the frequency bands of $2 \sim 4$ and $4 \sim 8$ years, respectively.

4.3.3 GDP Growth and Composite Leading Indicator

The performance of CLI regarding the GDP growth can be seen in Figure 4.4. It should be clear that among all the pair of variables tested, this pair has the most significant regions of high coherency for all countries in our sample. However, the predictive performance of CLI is suboptimal. The phase-difference consistently lies between 0 and $\frac{\pi}{2}$, implying that the OECD's CLI lagged GDP growth. Given that the primary objective of the CLI is to assist in predicting the turning point of macroeconomic conditions, the CLI fails in this mission.

This result is somewhat counterintuitive considering the efficient performance of OECD's CLI on the industrial production index. However, the de-trending and smoothing method utilised for estimating the cycle is at the core of the problem. The OECD's system of CLIs is based on the growth cycle approach, which measures cycle based on the deviation-from-trend approach. Nilsson and Gyomai (2011) opined that the quality of the leading indicator is dependent on the selection of well-behaved de-trending method. While OECD utilises the Phase-Average Trend (PAT) to measure growth cycle, Boschan and Ebanks (1978) argued that the PAT is faced with constant and occasional significant revisions, particularly towards the end of the series.

Although growth cycles are easy to detect in a historical time series with this method, Boschan and Banerji (1990) posited that it faces the problem of accurate real-time measurement. This is due to the unstable PAT estimates of the unknown trend over the latest year or two. As an estimate, the most recent trend measurement is subject to revisions, thereby making it difficult to have a precise measure of growth cycle date in real-time (Dua and Banerji, 2001).

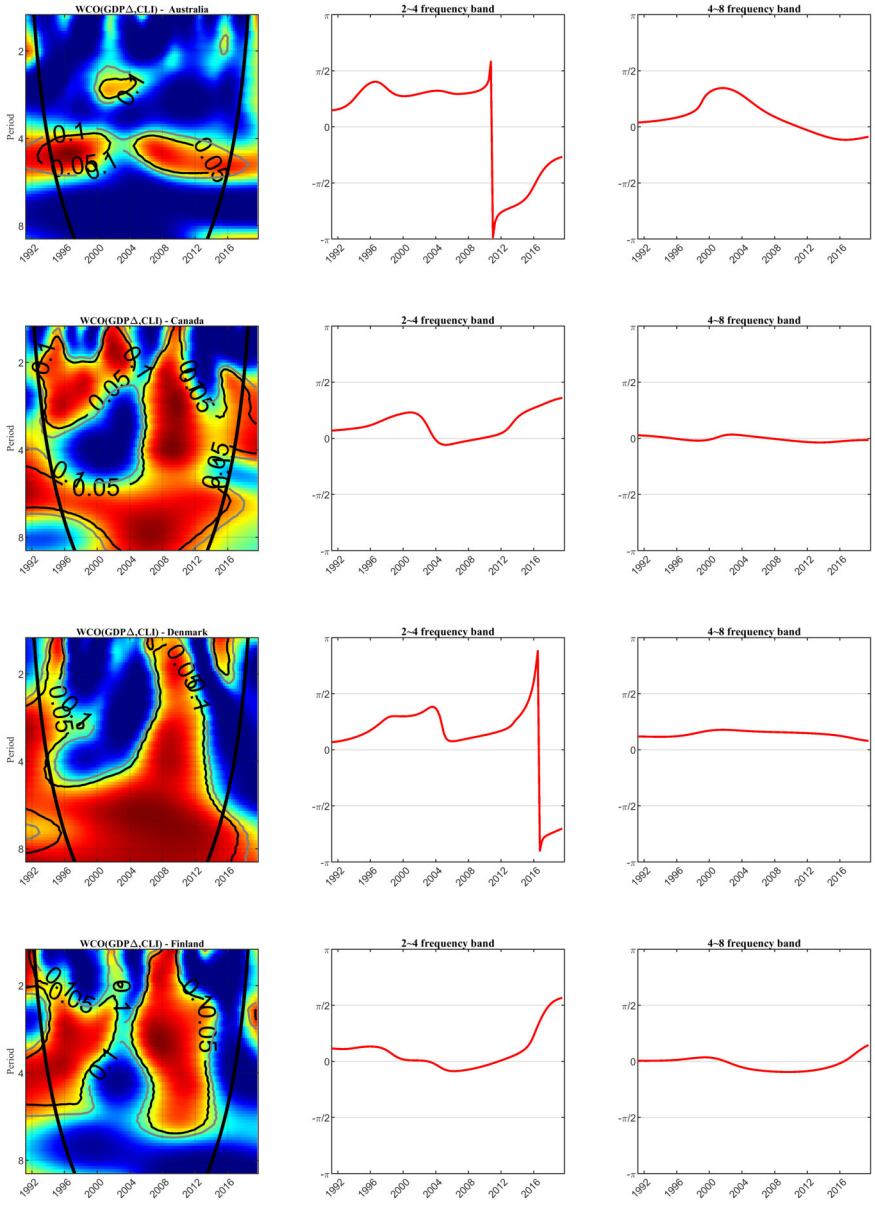
WCO(GDPΔ,CLI) - Australia
2~4 frequency band
4~8 frequency band
WCO(GDPΔ,CLI) - Canada
2~4 frequency band
4~8 frequency band
WCO(GDPΔ,CLI) - Denmark
2~4 frequency band
4~8 frequency band
WCO(GDPΔ,CLI) - Finland
2~4 frequency band
4~8 frequency band
Period
1992
1996
2000
2004
2008
2012
2016

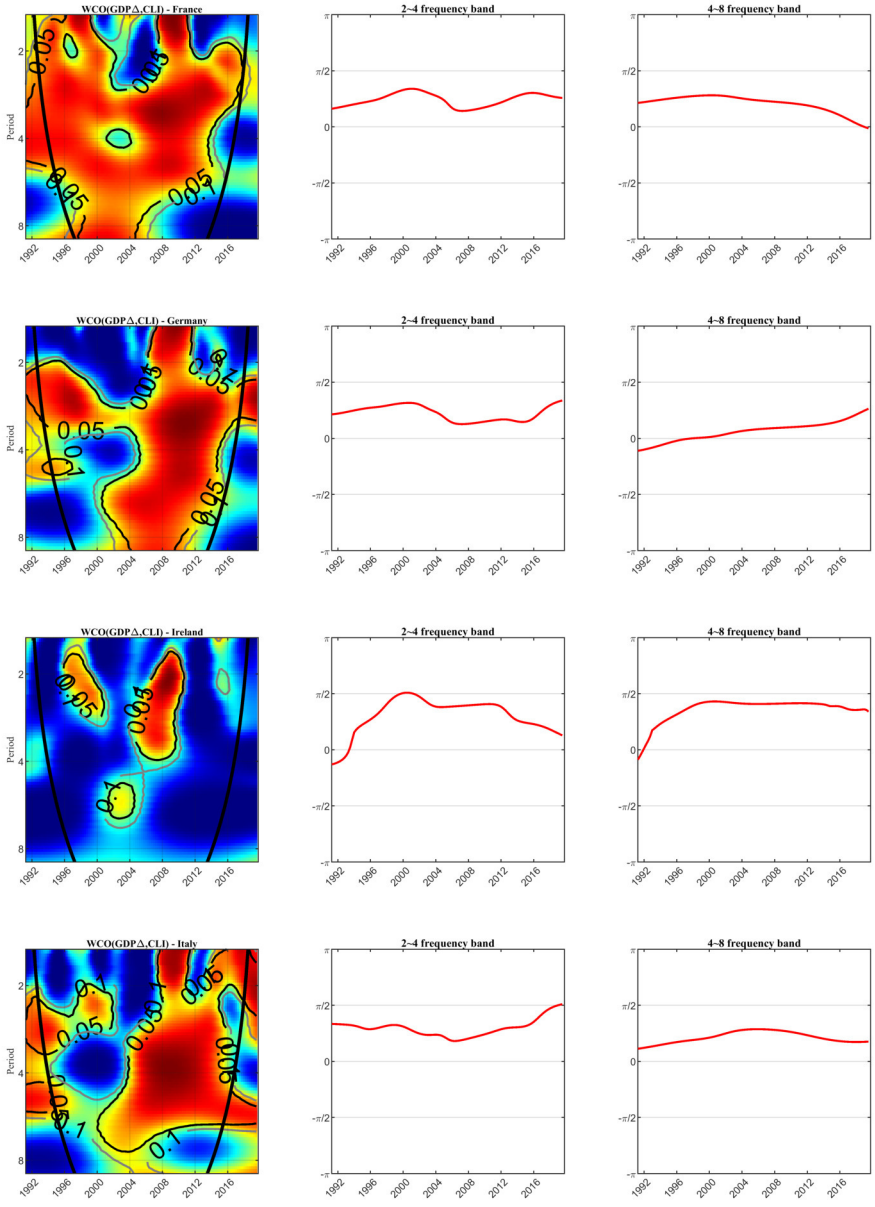
WCO(GDPΔ,CLI) - France
2~4 frequency band
4~8 frequency band
WCO(GDPΔ,CLI) - Germany
2~4 frequency band
4~8 frequency band
WCO(GDPΔ,CLI) - Ireland
2~4 frequency band
4~8 frequency band
WCO(GDPΔ,CLI) - Italy
2~4 frequency band
4~8 frequency band
Period
1992
1996
2000
2004
2008
2012
2016

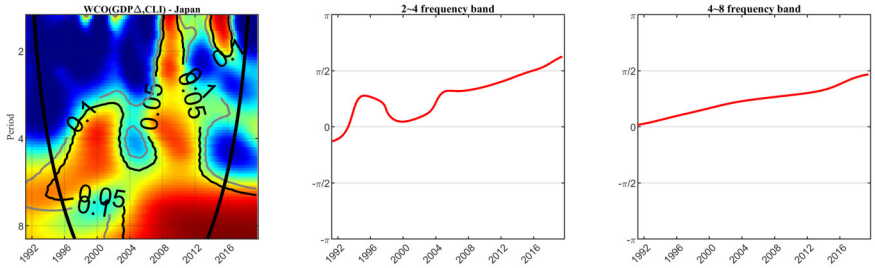
WCO(GDPΔ,CLI) - Japan
2~4 frequency band
4~8 frequency band
Period
2
4
8
0.1
0.05
0.05
0.1
0.05
0.1
0.95
1992
1996
2000
2004
2008
2012
2016
π
π/2
0
-π/2
-π

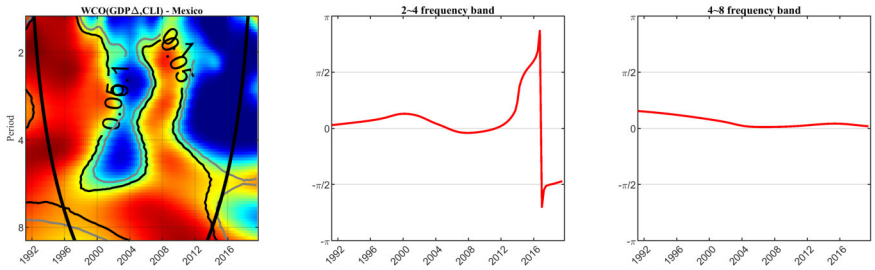
WCO(GDPΔ,CLI) - Mexico
2~4 frequency band
4~8 frequency band
Period
2
4
8
0.1
0.05
0.05
0.1
0.05
1992
1996
2000
2004
2008
2012
2016
π
π/2
0
-π/2
-π

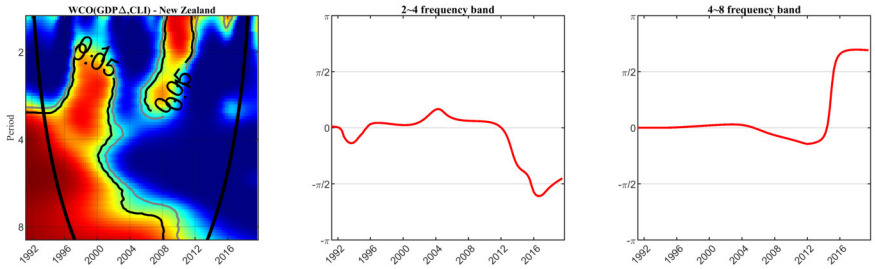
WCO(GDPΔ,CLI) - New Zealand
2~4 frequency band
4~8 frequency band
Period
2
4
8
0.1
0.05
0.05
1992
1996
2000
2004
2008
2012
2016
π
π/2
0
-π/2
-π

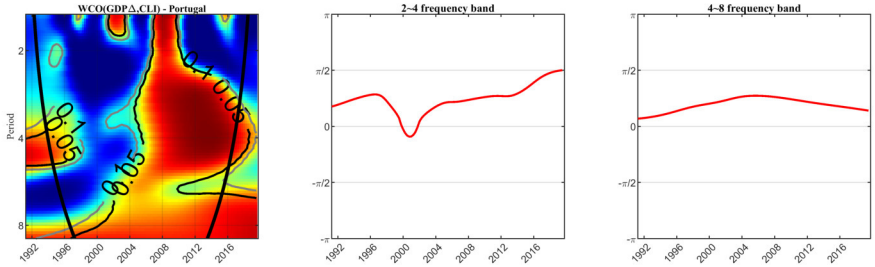
WCO(GDPΔ,CLI) - Portugal
2~4 frequency band
4~8 frequency band
Period
2
4
8
0.1
0.05
0.05
0.4
0.05
1992
1996
2000
2004
2008
2012
2016
π
π/2
0
-π/2
-π

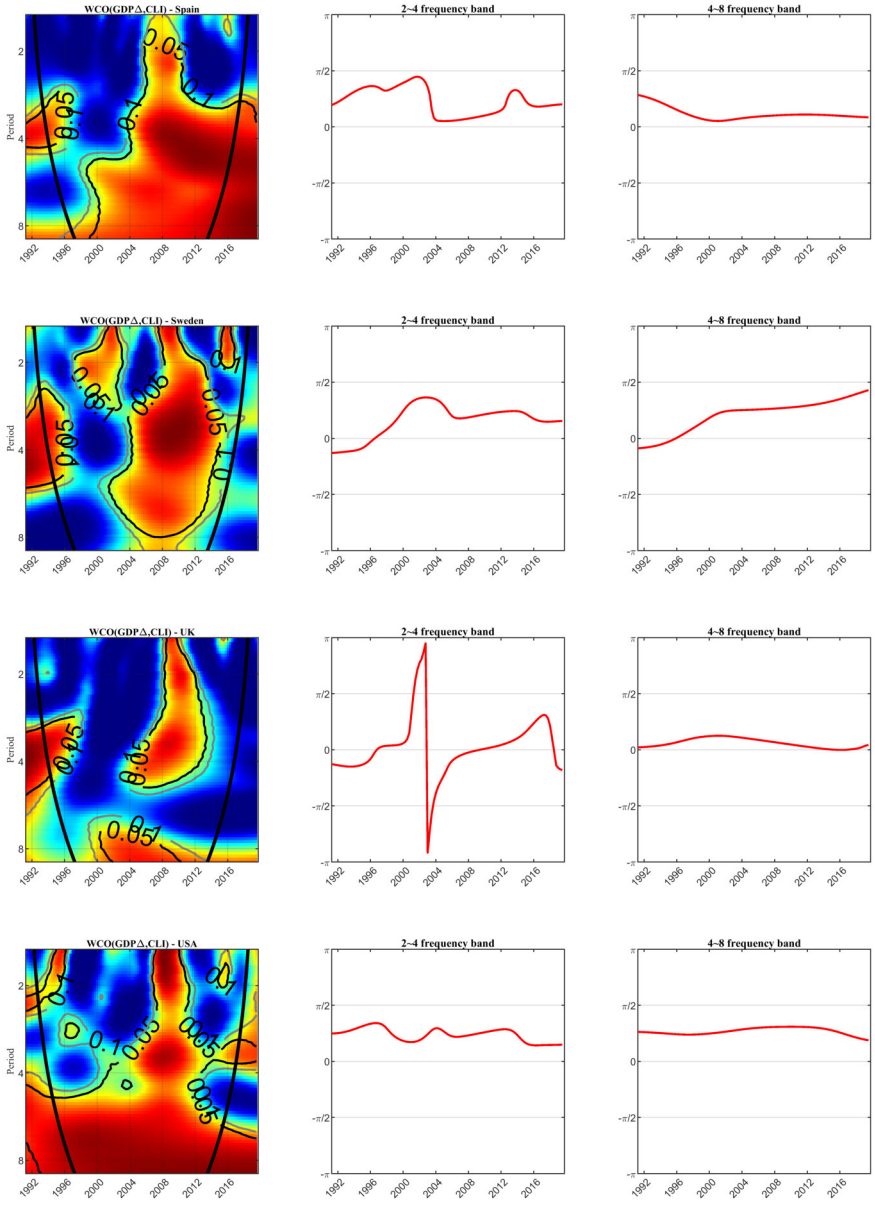

Figure 4.4: On the left - the wavelet coherency between Real GDP growth and CLI. The black and the grey contours denote the 5% and 10% significance level, respectively. The colour codes for coherency evolve from blue (low coherency) to red (high coherency). While the low coherency has a value close to zero, high coherency has a value closed to one. At the centre and on the right - phase-differences between Real GDP growth and CLI for the frequency bands of $2 \sim 4$ and $4 \sim 8$ years, respectively.

4.4 Conclusion

We utilised wavelet analysis to explore the predictive performance of the OECD's composite leading indicator on three macroeconomic indicators: industrial production index, unemployment rate and GDP growth. We used two principal wavelet tools: wavelet coherency and the wavelet phase-difference. While the former reveals the correlation between each macroeconomic variable and the CLI in each moment and frequency, the latter offers information about the lead-lag relationship between the two variables.

While our sample covers 16 countries across various geographical locations and cultures. The evaluation of the forecasting power of OECD's composite leading indicator on the three indicators shows the followings: it is a valid leading indicator for the industrial production index; its forecasting effectiveness is less apparent with the unemployment rate; it is consistently ineffective with the GDP growth.

Chapter 5

Conclusion

This thesis extends the application of wavelet analysis to economic phenomena. It addresses limitations of the traditional time-domain analysis and spectral analysis. Specifically, it uses wavelet tools to evaluate the information content and the predictive power of the yield curve, as well as the forecasting ability of the composite leading indicator. In achieving this objective, the thesis is partitioned into two. The first part serves as a primer to wavelet analysis. It introduces the concept of wavelet and highlights the limitation of both time-domain analysis and spectra analysis. Similarly, it enumerates various types of wavelet and provides the rationale for adopting Morlet wavelet for this thesis.

Furthermore, it introduces the notion of wavelet transforms, which involves the translation and dilation of the mother wavelet to generate the daughter wavelet. It focuses on the Continuous Wavelet Transform and provides the rationale for its increasing popularity in various empirical works in economics in the last two decades. On the other hand, the second part of the thesis focuses on the application of various wavelet tools to economic processes. The thesis uses the wavelet power spectrum, cross-wavelet power and coherency, multiple and partial coherencies, wavelet phase-difference, and wavelet spectral dissimilarity matrix for its analysis. While this part focuses on three empirical papers, the papers used wavelet tools to explain economic phenomenon or dynamics in different business cycle frequencies.

The first paper investigated financial contagion in the European debt market during various crisis-ridden periods in Eurozone and evaluated the cross-market co-movement. It also differentiated contagion from interdependence in the Eurozone. The paper used weekly data of 10-year sovereign bond yields for 9 Eurozone countries. The paper found evidence of contagion originating from Ireland at the onset of the sovereign debt crisis until around 2010, while Greece led the wave of contagion afterwards. The paper also established the spread of contagion to three periphery countries - Portugal, Greece and Ireland – at higher frequencies. While the contagion did not spread to Italy and Spain,

the Greek crisis triggered a flight-to-quality flow to Belgium, Finland, France and Germany.

The second paper used the Nelson-Siegel model to explore the dynamics of three-dimensional factors of the Canadian yield curve and its co-movement with four macroeconomic variables: Unemployment Rate, Inflation Rate, Bank Rate and Industrial Production Index. The paper utilised wavelet tools to interrogate this relationship, using monthly zero-coupon yields. The paper established a bidirectional relationship between the three yield factors and macroeconomic variables. Similarly, the paper found that the Canadian monetary policy rate affects mainly short-run interest rates while the Bank of Canada is very proactive in its effort to rein in inflation. While the slope and curvature lead in the long-run evolution of the unemployment rate, the industrial production index is a leading indicator of the latent factors of the yield curve.

The third paper evaluated the performance of OECD's Composite Leading Indicators using the Continuous Wavelet Transform. The paper assessed the co-movement between CLI and some macroeconomic variables, such as the Industrial Production Index, Unemployment Rate and real GDP Growth, at different timescales. Similarly, it assessed the lead-lag relation between each pair of variables across time and frequency. The paper established that OECD's composite leading indicator is an efficient leading indicator of industrial production index. While it can be suited for forecasting the unemployment rate, it exhibited poor performance regarding GDP growth. Thus, OECD's composite leading indicator has limited predictive power.

Overall, this thesis deepens the application of wavelet analysis in the economics literature and shows that exploring the dynamics of economic processes and phenomena across different timescales could reveal hidden information about these processes and phenomena. Apart from wavelet analysis providing perfect fitting for the financial time series, it prevents the unanticipated removal of cyclical components experienced with the first-differencing of the time series. Similarly, it prevents the loss of time information related to spectral analysis. Specifically, the thesis shows the benefits of wavelet, especially the positive compromise between time and frequency domains which limits their inherent drawbacks. Furthermore, wavelet analysis offers various mechanisms to investigate the multiscale structure of economic and financial processes.

References

Aguiar-Conraria, L., Azevedo, N., and Soares, M. J. (2008). Using wavelets to decompose the time–frequency effects of monetary policy. *Physica A: Statistical mechanics and its Applications*, 387(12):2863–2878.

Aguiar-Conraria, L., Brinca, P., Guðjónsson, H. V., and Soares, M. J. (2017). Business cycle synchronization across us states. *The BE Journal of Macroeconomics*, 17(1).

Aguiar-Conraria, L., Magalhães, P. C., and Soares, M. J. (2012a). Cycles in politics: wavelet analysis of political time series. *American Journal of Political Science*, 56(2):500–518.

Aguiar-Conraria, L., Magalhães, P. C., and Soares, M. J. (2013a). The nationalization of electoral cycles in the united states: a wavelet analysis. *Public Choice*, 156(3-4):387–408.

Aguiar-Conraria, L., Martins, M. M., and Soares, M. J. (2012b). The yield curve and the macro-economy across time and frequencies. *Journal of Economic Dynamics and Control*, 36(12):1950–1970.

Aguiar-Conraria, L., Martins, M. M., and Soares, M. J. (2013b). Convergence of the economic sentiment cycles in the eurozone: A time-frequency analysis. *JCMS: Journal of Common Market Studies*, 51(3):377–398.

Aguiar-Conraria, L. and Soares, M. J. (2011). Business cycle synchronization and the euro: A wavelet analysis. *Journal of Macroeconomics*, 33(3):477–489.

Aguiar-Conraria, L. and Soares, M. J. (2014). The continuous wavelet transform: moving beyond uni-and bivariate analysis. *Journal of Economic Surveys*, 28(2):344–375.

Alan, A. (1981). The index of leading indicators: Measurement without theory, twenty-five years later. *NBER Working Papers*.

Altavilla, C. (2004). Do emu members share the same business cycle? *JCMS: Journal of Common Market Studies*, 42(5):869–896.

Alvarez-Ramirez, J., Rodriguez, E., and Espinosa-Paredes, G. (2012). A partisan effect in the efficiency of the us stock market. *Physica A: Statistical Mechanics and its Applications*, 391(20):4923–4932.

Ang, A. and Piazzesi, M. (2003). A no-arbitrage vector autoregression of term structure dynamics with macroeconomic and latent variables. *Journal of Monetary economics*, 50(4):745–787.

Arghyrou, M. G. and Kontonikas, A. (2012). The emu sovereign-debt crisis: Fundamentals, expectations and contagion. *Journal of International Financial Markets, Institutions and Money*, 22(4):658–677.

Artis, M. J., Bladen-Hovell, R., and Zhang, W. (1995). Turning points in the international business cycle: An analysis of the oecd leading indicators for the g-7 countries. *OECD economic studies*, (24):125–166.

Bae, K.-H., Karolyi, G. A., and Stulz, R. M. (2003). A new approach to measuring financial contagion. *The Review of Financial Studies*, 16(3):717–763.

Baubeau, P. and Cazelles, B. (2009). French economic cycles: a wavelet analysis of french retrospective gnp series. *Cliometrica*, 3(3):275–300.

Baxter, M. (1994). Real exchange rates and real interest differentials: Have we missed the business-cycle relationship? *Journal of Monetary Economics*, 33(1):5–37.

Bekaert, G., Ehrmann, M., Fratzscher, M., and Mehl, A. (2014). The global crisis and equity market contagion. *The Journal of Finance*, 69(6):2597–2649.

Bekiros, S., Boubaker, S., Nguyen, D. K., and Uddin, G. S. (2017). Black swan events and safe havens: The role of gold in globally integrated emerging markets. *Journal of International Money and Finance*, 73:317–334.

Benati, L. and Goodhart, C. (2008). Investigating time-variation in the marginal predictive power of the yield spread. *Journal of Economic Dynamics and Control*, 32(4):1236–1272.

Berens, P. et al. (2009). Circstat: a matlab toolbox for circular statistics. *J Stat Softw*, 31(10):1–21.

Bertero, E. and Mayer, C. (1990). Structure and performance: Global interdependence of stock markets around the crash of october 1987∗. *European Economic Review*, 34(6):1155–1180.

Bikker, J. A. and Kennedy, N. O. (1999). Composite leading indicators of underlying inflation for seven eu countries. *Journal of Forecasting*, 18(4):225–258.

Bodart, V. and Candelon, B. (2009). Evidence of interdependence and contagion using a frequency domain framework. *Emerging markets review*, 10(2):140–150.

Boehm, E. A. (1987). *New Economic Indicators for Australia: A Further Report*. Institute of Applied Economic and Social Research.

Boehm, E. A. and Summers, P. M. (1999). Analysing and forecasting business cycles with the aid of economic indicators. *International Journal of Management Reviews*, 1(3):245–277.

Bonser-Neal, C. and Morley, T. R. (1997). Does the yield spread predict real economic activity? a multicountry analysis. *Economic Review-Federal Reserve Bank of Kansas City*, 82(3):37.

Booth, L., Georgopoulos, G., and Hejazi, W. (2007). What drives provincial-canada yield spreads? *Canadian Journal of Economics/Revue canadienne d'économique*, 40(3):1008–1032.

Boschan, C. and Banerji, A. (1990). *A Reassessment of Composite Indexes. Analyzing Modern Business Cycles: Essays Honoring Geoffrey H. Moore. (P. A. Klein, Editor).* Armonk, NY. M. E. Sharpe.

Boschan, C. and Ebanks, W. W. (1978). *The Phase-Average Trend: A New Way of Measuring Economic Growth.*

Boyer, B. H., Gibson, M. S., Loretan, M., et al. (1997). *Pitfalls in tests for changes in correlations*, volume 597. Board of Governors of the Federal Reserve System Washington, DC.

Broto, C. and Perez-Quiros, G. (2015). Disentangling contagion among sovereign cds spreads during the european debt crisis. *Journal of Empirical Finance*, 32:165–179.

Calvo, S. (1999). *Capital flows to Latin America: is there evidence of contagion effects?* The World Bank.

Caraiani, P. (2012). Money and output: New evidence based on wavelet coherence. *Economics Letters*, 116(3):547–550.

Cazelles, B., Chavez, M., Magny, G. C. d., Guégan, J.-F., and Hales, S. (2007). Time-dependent spectral analysis of epidemiological time-series with wavelets. *Journal of the Royal Society Interface*, 4(15):625–636.

Chiang, T. C., Jeon, B. N., and Li, H. (2007). Dynamic correlation analysis of financial contagion: Evidence from asian markets. *Journal of International Money and finance*, 26(7):1206–1228.

Cohen, E. A. and Walden, A. T. (2010). A statistical study of temporally smoothed wavelet coherence. *IEEE Transactions on Signal Processing*, 58(6):2964–2973.

Connor, J. and Rossiter, R. (2005). Wavelet transforms and commodity prices. *Studies in Nonlinear Dynamics & Econometrics*, 9(1).

Cook, T. and Hahn, T. (1989). The effect of changes in the federal funds rate target on market interest rates in the 1970s. *Journal of Monetary Economics*, 24(3):331–351.

Crowley, P. M. and Mayes, D. G. (2009). How fused is the euro area core? *OECD Journal: Journal of Business Cycle Measurement and Analysis*, 2008(1):63–95.

Dalsgaard, T., Elmeskov, J., and Park, C.-Y. (2002). *Ongoing changes in the business cycle-evidence and causes.* Number 20. SUERF Studies.

Daubechies, I. (1992). Ten lectures on wavelets, volume 61 of cbms-nsf regional conference series in applied mathematics (society for industrial and applied mathematics (siam).

Dewachter, H. and Lyrio, M. (2006). Macro factors and the term structure of interest rates. *Journal of Money, Credit, and Banking*, 38(1):119–140.

Diebold, F. X., Ji, L., and Li, C. (2006a). A three-factor yield curve model: non-affine structure, systematic risk sources, and generalized duration. *Macroeconomics, Finance and Econometrics: Essays in Memory of Albert Ando*, 1:240–274.

Diebold, F. X. and Li, C. (2006). Forecasting the term structure of government bond yields. *Journal of econometrics*, 130(2):337–364.

Diebold, F. X. and Rudebusch, G. D. (1991). Forecasting output with the composite leading index: A real-time analysis. *Journal of the American Statistical Association*, 86(415):603–610.

Diebold, F. X. and Rudebusch, G. D. (2013). *Yield curve modeling and forecasting: the dynamic Nelson-Siegel approach*. Princeton University Press.

Diebold, F. X., Rudebusch, G. D., and Aruoba, S. B. (2006b). The macroeconomy and the yield curve: a dynamic latent factor approach. *Journal of econometrics*, 131(1-2):309–338.

Dornbusch, R., Park, Y. C., and Claessens, S. (2000). Contagion: How it spreads and how it can be stopped. *World Bank Research Observer*, 15(2):177–197.

Dua, P. and Banerji, A. (2001). An indicator approach to business and growth rate cycles: The case of india. *Indian Economic Review*, pages 55–78.

Dungey*, M., Fry, R., González-Hermosillo, B., and Martin, V. L. (2005). Empirical modelling of contagion: a review of methodologies. *Quantitative finance*, 5(1):9–24.

Edelberg, W., Marshall, D., et al. (1996). Monetary policy shocks and long-term interest rates. *Economic Perspectives-Federal Reserve Bank of Chicago*, 20:2–17.

Edwards, S. and Susmel, R. (2001). Volatility dependence and contagion in emerging equity markets. *Journal of Development Economics*, 66(2):505–532.

Emerson, R. A. and Hendry, D. F. (1996). An evaluation of forecasting using leading indicators. *Journal of Forecasting*, 15(4):271–291.

Estrella, A. and Hardouvelis, G. A. (1991). The term structure as a predictor of real economic activity. *The journal of Finance*, 46(2):555–576.

Estrella, A. and Mishkin, F. S. (1998). Predicting us recessions: Financial variables as leading indicators. *The Review of Economics and Statistics*, 80(1):45–61.

Evans, C. L. and Marshall, D. A. (2007). Economic determinants of the nominal treasury yield curve. *Journal of Monetary Economics*, 54(7):1986–2003.

Fernandez, V. P. (2005). The international capm and a wavelet-based decomposition of value at risk. *Studies in Nonlinear Dynamics & Econometrics*, 9(4).

Fernández-Macho, J. (2012). Wavelet multiple correlation and cross-correlation: A multiscale analysis of eurozone stock markets. *Physica A: Statistical Mechanics and its Applications*, 391(4):1097–1104.

Fichtner, F., Rüffer, R., and Schnatz, B. (2009). Leading indicators in a globalised world.

Flor, M. A. and Klarl, T. (2017). On the cyclicity of regional house prices: New evidence for us metropolitan statistical areas. *Journal of Economic Dynamics and Control*, 77:134–156.

Forbes, K. J. and Rigobon, R. (2002). No contagion, only interdependence: measuring stock market comovements. *The journal of Finance*, 57(5):2223–2261.

Ftiti, Z., Tiwari, A., Belanès, A., and Guesmi, K. (2015). Tests of financial market contagion: Evolutionary cospectral analysis versus wavelet analysis. *Computational Economics*, 46(4):575–611.

Fulop, G. and Gyomai, G. (2012). Transition of the oecd cli system to a gdp-based business cycle target. *URL: http://www. oecd. org/std/leading-indicators/49985449. pdf (usage date: 10.04. 2015)*.

Gabor, D. (1946). Theory of communication. part 1: The analysis of information. *Journal of the Institution of Electrical Engineers-Part III: Radio and Communication Engineering*, 93(26):429–441.

Gallegati, M. (2008). Wavelet analysis of stock returns and aggregate economic activity. *Computational Statistics & Data Analysis*, 52(6):3061–3074.

Gallegati, M. (2012). A wavelet-based approach to test for financial market contagion. *Computational Statistics & Data Analysis*, 56(11):3491–3497.

Gallegati, M., Gallegati, M., Ramsey, J. B., and Semmler, W. (2011). The us wage phillips curve across frequencies and over time. *Oxford Bulletin of Economics and Statistics*, 73(4):489–508.

Gallegati, M., Ramsey, J. B., and Semmler, W. (2014). Interest rate spreads and output: A time scale decomposition analysis using wavelets. *Computational Statistics & Data Analysis*, 76:283–290.

Gallegati, M. and Semmler, W. (2014). *Wavelet applications in economics and finance*, volume 20. Springer.

Garcia, R. and Luger, R. (2007). The canadian macroeconomy and the yield curve: an equilibrium-based approach. *Canadian Journal of Economics/Revue canadienne d'économique*, 40(2):561–583.

Ge, Z. (2008). Significance tests for the wavelet cross spectrum and wavelet linear coherence. In *Annales geophysicae: atmospheres, hydrospheres and space sciences*, volume 26, page 3819.

Geiger, F. (2011). The theory of the term structure of interest rates. In *The Yield Curve and Financial Risk Premia*, pages 43–82. Springer.

Gençay, R., Selcuk, F., and Whitcher, B. (2005). Multiscale systematic risk. *Journal of International Money and Finance*, 24(1):55–70.

Gençay, R., Selçuk, F., and Whitcher, B. J. (2001). *An introduction to wavelets and other filtering methods in finance and economics*. Elsevier.

Gereffi, G. (2005). The global economy: organization, governance, and development. *The handbook of economic sociology*, 2:160–182.

Giordano, R., Pericoli, M., and Tommasino, P. (2013). Pure or wake-up-call contagion? another look at the emu sovereign debt crisis. *International Finance*, 16(2):131–160.

Goupillaud, P., Grossmann, A., and Morlet, J. (1984). Cycle-octave and related transforms in seismic signal analysis. *Geoexploration*, 23(1):85–102.

Granger, C. W. (1966). The typical spectral shape of an economic variable. *Econometrica: Journal of the Econometric Society*, pages 150–161.

Granger, C. W. (2001). Macroeconometrics–past and future. *Journal of Econometrics*, 100(1):17–19.

Gray, D. (2014). Central european foreign exchange markets: a cross-spectral analysis of the 2007 financial crisis. *The European Journal of Finance*, 20(6):550–567.

Grinsted, A., Moore, J. C., and Jevrejeva, S. (2004). Application of the cross wavelet transform and wavelet coherence to geophysical time series. *Nonlinear processes in geophysics*, 11(5/6):561–566.

Grossmann, A. and Morlet, J. (1984). Decomposition of hardy functions into square integrable wavelets of constant shape. *SIAM journal on mathematical analysis*, 15(4):723–736.

Hao, L. and Ng, E. C. (2011). Predicting canadian recessions using dynamic probit modelling approaches. *Canadian Journal of Economics/Revue canadienne d'économique*, 44(4):1297–1330.

Hejazi, W., Lai, H., and Yang, X. (2000). The expectations hypothesis, term premia, and the canadian term structure of interest rates. *Canadian Journal of Economics/Revue canadienne d'économique*, 33(1):133–148.

Jammazi, R. (2012). Cross dynamics of oil-stock interactions: A redundant wavelet analysis. *Energy*, 44(1):750–777.

Kenc, T. and Dibooglu, S. (2010). The 2007–2009 financial crisis, global imbalances and capital flows: Implications for reform. *Economic Systems*, 34(1):3–21.

King, M. A. and Wadhwani, S. (1990). Transmission of volatility between stock markets. *The Review of Financial Studies*, 3(1):5–33.

King, R. G. and Watson, M. W. (1996). Money, prices, interest rates and the business cycle. *The Review of Economics and statistics*, pages 35–53.

Ko, J.-H. and Funashima, Y. (2019). On the sources of the feldstein–horioka puzzle across time and frequencies. *Oxford Bulletin of Economics and Statistics*, 81(4):889–910.

Koch, P. D. and Rasche, R. H. (1988). An examination of the commerce department leading-lndicator approach. *Journal of Business & Economic Statistics*, 6(2):167–187.

Koopmans, T. C. (1947). Measurement without theory. *The Review of Economics and Statistics*, 29(3):161–172.

Kozicki, S. and Tinsley, P. A. (2001). Shifting endpoints in the term structure of interest rates. *Journal of monetary Economics*, 47(3):613–652.

Lange, R. H. (2013). The canadian macroeconomy and the yield curve: A dynamic latent factor approach. *International Review of Economics & Finance*, 27:261–274.

Liu, Y., San Liang, X., and Weisberg, R. H. (2007). Rectification of the bias in the wavelet power spectrum. *Journal of Atmospheric and Oceanic Technology*, 24(12):2093–2102.

Madaleno, M. and Pinho, C. (2012). International stock market indices comovements: a new look. *International Journal of Finance & Economics*, 17(1):89–102.

Maraun, D., Kurths, J., and Holschneider, M. (2007). Nonstationary gaussian processes in wavelet domain: synthesis, estimation, and significance testing. *Physical Review E*, 75(1):016707.

Martins, S. and Amado, C. (2018). Financial market contagion and the sovereign debt crisis: a smooth transition approach. *NIPE Working Paper*, (NIPE WP 08/2018):1–37.

Masih, A. M. and Masih, R. (1999). Are asian stock market fluctuations due mainly to intra-regional contagion effects? evidence based on asian emerging stock markets. *Pacific-Basin Finance Journal*, 7(3-4):251–282.

McGuckin, R. H., Ozyildirim, A., and Zarnowitz, V. (2007). A more timely and useful index of leading indicators. *Journal of Business & Economic Statistics*, 25(1):110–120.

Meyers, S. D., Kelly, B. G., and O'Brien, J. J. (1993). An introduction to wavelet analysis in oceanography and meteorology: With application to the dispersion of yanai waves. *Monthly weather review*, 121(10):2858–2866.

Mink, M. and De Haan, J. (2013). Contagion during the greek sovereign debt crisis. *Journal of International Money and Finance*, 34:102–113.

Missio, S. and Watzka, S. (2011). Financial contagion and the european debt crisis.

Moneta, F. (2005). Does the yield spread predict recessions in the euro area? *International Finance*, 8(2):263–301.

Neftci, S. N. (1979). Lead-lag relations, exogeneity and prediction of economic time series. *Econometrica: Journal of the Econometric Society*, pages 101–113.

Nelson, C. R. and Siegel, A. F. (1987). Parsimonious modeling of yield curves. *Journal of business*, pages 473–489.

Nerlove, M. (1964). Spectral analysis of seasonal adjustment procedures. *Econometrica: Journal of the Econometric Society*, pages 241–286.

Nilsson, R., Brunet, O., et al. (2006). Composite leading indicators for major oecd non-member economies: Brazil, china, india, indonesia, russian federation, south africa. Technical report, OECD Publishing.

Nilsson, R. and Gyomai, G. (2011). Cycle extraction: A comparison of the phase-average trend method, the hodrick-prescott and christiano-fitzgerald filters.

Orlov, A. G. (2009). A cospectral analysis of exchange rate comovements during asian financial crisis. *Journal of International Financial Markets, Institutions and Money*, 19(5):742–758.

Pericoli, M. and Sbracia, M. (2003). A primer on financial contagion. *Journal of economic surveys*, 17(4):571–608.

Rajan, R. G. (2006). Has finance made the world riskier? *European Financial Management*, 12(4):499–533.

Ramsey, J. B. and Lampart, C. (1998). Decomposition of economic relationships by timescale using wavelets. *Macroeconomic dynamics*, 2(1):49–71.

Rodriguez, J. C. (2007). Measuring financial contagion: A copula approach. *Journal of empirical finance*, 14(3):401–423.

Rua, A. and Nunes, L. C. (2009). International comovement of stock market returns: A wavelet analysis. *Journal of Empirical Finance*, 16(4):632–639.

Rua, A. and Nunes, L. C. (2012). A wavelet-based assessment of market risk: The emerging markets case. *The Quarterly Review of Economics and Finance*, 52(1):84–92.

Rudebusch, G. D. and Wu, T. (2008). A macro-finance model of the term structure, monetary policy and the economy. *The Economic Journal*, 118(530):906–926.

Schwert, G. W. (1990). Stock volatility and the crash of'87. *The review of financial studies*, 3(1):77–102.

Smets, F. (1997). Financial asset prices and monetary policy: theory and evidence.

Stock, J. H. and Watson, M. W. (2005). Understanding changes in international business cycle dynamics. *Journal of the European Economic Association*, 3(5):968–1006.

Taylor, J. B. (1993). Discretion versus policy rules in practice. In *Carnegie-Rochester conference series on public policy*, volume 39, pages 195–214. Elsevier.

Torrence, C. and Compo, G. P. (1998). A practical guide to wavelet analysis. *Bulletin of the American Meteorological society*, 79(1):61–78.

Vacha, L. and Barunik, J. (2012). Co-movement of energy commodities revisited: Evidence from wavelet coherence analysis. *Energy Economics*, 34(1):241–247.

Verona, F. (2016). Time–frequency characterization of the us financial cycle. *Economics Letters*, 144:75–79.

Verona, F. (2019). Investment, tobin's q, and cash flow across time and frequencies. *Oxford Bulletin of Economics and Statistics*.

Weale, M. (1996). An assessment of oecd and uk leading indicators. *National Institute Economic Review*, 156(1):63–71.

Wen, Y. (2002). The business cycle effects of christmas. *Journal of Monetary Economics*, 49(6):1289–1314.

Wen, Y. (2005). Understanding the inventory cycle. *Journal of Monetary Economics*, 52(8):1533–1555.

Wong, H., Ip, W.-C., Xie, Z., and Lui, X. (2003). Modelling and forecasting by wavelets, and the application to exchange rates. *Journal of Applied Statistics*, 30(5):537–553.

Wu, T. (2001). Monetary policy and the slope factor in empirical term structure estimations.

Zar, J. H. (1996). Biostatistical analysis–prentice–hall international. *Inc., London*.

Zarnowitz, V. and Boschan, C. (1975). New composite indexes of coincident and lagging indicators. *Business Conditions Digest*, 20.

Zarnowitz, V. and Braun, P. (1990). Major macroeconomics variables and leading indexes: Some estimates of their interrelations. In *Analyzing Modern Business Cycles: Essays Honoring Geoffrey H. Moore*. ME Sharpe.